Katrin Pansy BSc

The role of nuclear orphan receptor *Nr4a1* in *Myc*-driven lymphomagenesis and normal B-cell development

MASTER'S THESIS

to obtain the university degree of

Master of Science

Master's degree programme: Biochemistry and Molecular Biomedical Sciences

submitted to

Graz University of Technology

conducted at

Medical University of Graz, Department of Hematology

Supervisor

Alexander Deutsch, PhD

Medical University of Graz, Department of Hematology

Graz, December 2017

“All I’ve learned is teaching me more.

All I know is driving me on.”

August Burns Red, Carpe Diem

Affidavit

I declare that I have authored this thesis independently, that I have not used other than the declared sources/resources, and that I have explicitly indicated all material which has been quoted either literally or by content from the sources used. The text document uploaded to TUGRAZonline is identical to the present master‘s thesis.

Graz, December 2017 .....

Acknowledgement

This journey would not have been possible without the support of my family, professors and mentors, and friends.

First, I would first like to thank my thesis advisor Dr. Alexander Deutsch of the Medical University of Graz. The door was always open whenever I ran into trouble spot or had questions about my research or writing. I would like to express my gratitude for the useful comments, remarks and engagement through the learning process of this master thesis. I could not have imagined having a better advisor and mentor for my master thesis.

Besides my advisor, I would also like to thank the expert, Mag. Karoline Fechter, for introducing me to the topics, for the patience as well for the support on the way. Without her passionate participation and input, my master thesis would not have been possible. Millions of thanks for the good moments we had working together, for the continuous support and for all helpful discussions.

I also would like to say thank you to the entire team of our working group for their help during my master thesis and the fun we had together.

Very special thanks go to my friends, especially Bianca Kerschbaumer, Michaela Nimmervoll and Elisabeth Jauk, for their encouragement and moral support throughout my years of study. Thank you for always lending an ear, giving me advice, extending a hand and for just being here. I also appreciate every other friend whose name I may have forgotten to mention.

Finally, I must express my very profound gratitude to my parents, Karin und Manfred Pansy, and to my partner, Philipp Mauerhofer, for providing me with unfailing support and continuous encouragement throughout my years of study and through the process of researching and writing this thesis. This accomplishment would not have been possible without them. Thank you.

Kurzfassung

Hintergrund: Die nukleären Waisen-Rezeptoren (engl. nuclear orphan receptors) NR4A1 und NR4A3 wirken als Tumorsuppressoren in der akuten myeloischen Leukämie (AML). Die Arbeitsgruppe um PD.Dr.Alexander Deutsch konnte in einer Studie über die Expression von NR4A-Rezeptoren zeigen, dass in der Mehrheit von Patienten mit B-CLL, FL and DLBCL eine deutliche reduzierte Expression von *NR4A1* und *NR4A3* vorliegt. *In vitro* Versuche zeigten, dass NR4A1 alleine die Apoptose in aggressiven Lymphomzellen voran antreibt und auch das Tumorwachstum verringert. Zusätzlich konnte gezeigt werden, dass der Nr4a1 Verlust die Myc-bedingten Lymhomagenese *in vivo* beschleunigt. Diese Daten deuten darauf hin, dass Nr4a1 eine tumorsuppressive Funktion in der Entstehung von aggressiven Lymphomen besitzt.

Ziel: Das Ziel meiner Masterarbeit war die Funktion des Nr4a1-Rezeptors in Myc-getriebener Lymphomentstehung als auch in der normalen B-Zell Entwicklung zu untersuchen. Als erstes wurde die Expression von *Nr4a1* und *Nr4a3* in unterschiedlichen Stadien der B-Zell Entwicklung und in der Myc-bedingten Lymphomentwicklung analysiert. Des Weiteren wurde analysiert, ob der Verlust von *Nr4a1* zu einer veränderten Expression von pro- und anti-apotischen Genen im *EμMyc* Mausmodell führt. Zusätzlich wurde die Expression von diversen miRNAs in Proben von aggressiven Lymphomen untersucht und mit *NR4A1* und *NR4A3* Daten korreliert. Unter nicht-malignen Bedingungen war das Ziel herauszufinden, welche potentielle Zielgene von Nr4a1 als Transkriptionsfaktor in *Nr4a1 -/-* und *Nr4a1 +/+* Mäusen beeinflusst werden. Ein weiterer Punkt meiner Masterarbeit war es, den Einfluss von Spermidin auf den inflammatorischen Prozess in der *Nr4a1 -/-* Maus zu untersuchen, als auch den Effekt von Spermidin in der B-Zell Entwicklung zu analysieren.

Ergebnis: Unsere Daten konnten zeigen, dass *Nr4a1* durch die maligne Transformation in der *Myc*-bedingten Lymphomentstehung eine Runterregulierung aufweist. Des Weiteren ist die Entstehung der Lymphome weniger vom Verlust oder der Inaktivierung von p53 abhängig. Wir konnten außerdem zwei potentielle miRNAs identifizieren, die *NR4A1* regulieren könnten, und in aggressiven Lymphomen überexprimiert sind. Unter nicht malignen Bedingungen konnten wir zeigen, dass Nr4a1 Gene reguliert, die in Immunregulierung, in der immunen Zellmigration als auch im NF-KB Signalweg involviert sind. Zu guter Letzt, konnte gezeigt werden, dass es in *Nr4a1 -/-* Mäusen signifikant weniger reife B-Zellsubpopulationen gibt.

Zusammenfassend zeigen unsere Daten, dass NR4A1 als Tumorsuppressor in der Entstehung von aggressiven Lymphomen eine wichtige Rolle spielt und auch in der B-Zellentwicklung beteiligt ist.

Abstract

Background: The nuclear orphan receptors NR4A1 and NR4A3 are known to be tumor suppressors of acute myeloid leukemia (AML). The group of PD Dr. Alexander Deutsch has already published a comprehensive study of the expression levels of NR4A nuclear receptors in lymphoid neoplasms that has shown a reduction of NR4A1 and NR4A3 in most patients with B-cell chronic lymphocytic leukemia, follicular lymphoma and diffuse large B-cell lymphoma. Intriguingly, functional characterization revealed that NR4A1 alone promotes apoptosis in aggressive lymphoma cells *in vitro* and repress the tumor growth in xenograft models. Furthermore, our data have shown that *Nr4a1* loss accelerates *Myc*-driven lymphomagenesis in mice. To sum up, our data indicate a tumor suppressive function of Nr4a1 in the development of aggressive lymphomas.

Aim: The aim of my master thesis was to investigate the function of the nuclear orphan receptor Nr4a1 in *Myc*-driven lymphomagenesis and in normal B-cell development. In detail, I determined the expression of *Nr4a1* and *Nr4a3* in B-cell development and in *EμMyc*-driven lymphomagenesis. Additionally, I characterized the effect of *Nr4a1* loss on pro- and anti-apoptotic genes in the *EμMyc* mouse model. Further, we determined expression levels of several miRNAs in human aggressive lymphomas and set them in correlation to *NR4A1* and *NR4A3* expression. Under non-malignant conditions, I investigated the function of *Nr4a1* in gene regulation as transcription factor in Nr4a1 -/- and Nr4a1 +/+ mice. Additionally, we investigated whether spermidine influences inflammation processes in *Nr4a1 -/-* mice as well the effects of spermidine in normal B-cell development in bone marrow, spleen and thymus.

Results: *Nr4a1* was downregulated by malignant transformation in *Myc*-driven lymphomagenesis and the development of the lymphoma is less dependent on inactivation of the p53 pathway. Additionally, we identified two miRNAs potentially targeting *NR4A1* being overexpressed in human aggressive lymphomas. Furthermore, we clearly demonstrated that Nr4a1 regulate genes involved in immune regulation, immune cell migration and in NF-KB pathway in a context specific manner under non-malignant conditions. Finally, we observed that loss of *Nr4a1* resulted in a significant reduction of mature B cell subpopulations and *Nr4a1* is mandatory for B-cell development.

In conclusion, our data define that NR4A1 functions as novel tumor suppressor involved in aggressive lymphoma development as well in B-cell development.

Table of Contents

List of Tables

List of Figures

Abbreviations

ABC	activated B-cell type
acetyl-CoA	acetyl coenzyme A
ADP	adenosine diphosphate
AF	activation function
AID	activation-induced cytidine deaminase
AIDS	acquired immunodeficiency syndrome
AML	acute myeloid leukemia
APS	ammonium persulfate
Atg5	autophagy-related protein 5
BAD	BCL-2 associated agonist of cell death
BAK	BCL-2 antagonist/killer 1
BAX	BCL-2 associated X protein
BCL-2	B-cell lymphoma 2
BCL-6	B-cell lymphoma 6
BCL-W	BCL-2 like 2
BCL-XL	BCL-2 like 1
BCR	B-cell receptor
BFL-1	BCL-2 related protein A1
BH	BCL-2 homology
BID	BH3 interacting domain death agonist
BIM	Bcl-2 interacting protein Bim
BL	Burkitt’s lymphoma
BLIMP-1	B-lymphocyte-induced maturation protein 1
BM	bone marrow
BMF	BCL-2 modifying factor
BMF	Bcl-2 modifying factor
CARD11	caspase recruitment domain family member 11
CB	centroblast
CC	centrocyte
CCDN2	cyclin D2
CCDN3	cyclin D3
CD10	class of IgM
CD79	cluster of differentiation 79
CDKN2A	cyclin dependent kinase inhibitor 2A
cDNA	complementary DNA
CFU	colony corming unit
CKS1	cyclin-dependent kinase subunit 1
CLL	chronic lymphocytic leukemia
CLP	common lymphoid precursor
CR	caloric restricition
CREBBP	CREB-binding protein
CRM	caloric restriction mimetics
CSR	class switch recombination
CTD	C-terminal region
CUL	Cullin 1
CXCL1	C-X-C motif chemokine ligand 1
DBD	DNA binding domain
DFMO	OCD suicide inhibitor 2-difluoromethylornithine
DGCR8	DGCR8, microprocessor complex subunit
DLBCL	diffuse large B-cell lymphoma

DNA	deoxyribonucleic acid
DNAse	deoxyribonuclease
DR5	death receptor 5
Drosha	Drosha ribonuclease III
EBF-1	early B-cell factor 1
EBV	Epstein-Barr virus
ECL	electrochemiluminescence
EF-1	elongation factor 1
EP300	E1A-binding protein 1
EZH2	enhancer of zeste homolog 2
FACS	fluorescence-activated cell scanning
FBS	fetal bovine serum
FBXO11	F-box protein 11
FDH	fasten-mimicking diet
FL	follicular lymphoma
FO	follicular zone
GAPDH	glyceraldehyde 3-phosphate dehydrogenase
GC	germinal center
GCB	germinal center B-cell type
GL	germline
GSK3B	glycogen synthase kinase 3 beta
GTP	guanosine-5'-triphosphate
HAT	histone acetyltransferase
HBSS	“Hank's Balanced Salt Solution”
HGBL	high grade B-cell lymphoma
HL	Hodgkin’s lymphoma
HPSC	hematopoietic stem cell
HRP	horseradish peroxidase
ID3	inhibitor of DNA binding 3
Ig	immunoglobulin
IL-1β	tumor necrosis factor 1β
IL-5	interleukin 5
IL-6	interleukin 6
IRF-4	interferon-regulatory factor 4
IRF-8	interferon-regulatory factor 8
LBD	ligand binding domain
LPS	lipopolysaccharide
MAX	MYC associated factor X
MCL	mantle cell lymphoma
MCL-1	myeloid cell leukemia sequence 1 (BCL-2-related)
MDM2	Murine double minute 2, a p53-associated oncogene
MDS	myelodysplastic neoplasm
MEF2B	myocyte-specific enhancer factor 2B
MHC	major histocompatibility complex
miRNA	microRNA
MLL2	histone methyltransferase
MPN	myeloproliferative neoplasm
mRNA	messenger RNA
mRNA	messenger RNA
MYC	Myelocytomatosis oncogene cellular homolog
MYD88	myeloid differentiation primary response protein 88

MZ	marginal zone
NAD	nicotinamide adenine dinucleotide
NF-KB	nuclear factor KB
NHL	non-Hodgkin lymphoma
NK	neutral killer cell
NOXA	immediate-early-response protein APR
NRBE	NGFI-B responsible element
NTD	N-terminal region
NurRE	Nur-response element
ODC	ornithine decarboxylase
p19Arf	p19 alternative reading frame
p19Arf	p19 alternative reading frame protein
p53	tumor suppressor protein p53
PARG	poly(ADP-ribose) glycohydrolase
PARP	poly(ADP-ribose) polymerase
PARP	poly(ADP-ribose)polymerase
Pasha	DGCR8, microprocessor complex subunit
PAX5	paired box 5
PCR	polymerase chain reaction
PI3K	phosphoinositide-3-kinase
PPIA	cyclophilin A or peptidylprolyl isomerase A
PRDM1	positive regulatory domain I-binding factor 1
pri-mRNA	primary microRNA
PTEN	phosphatase and tensin homolog
PU.1	hematopoietic transcription factor PU.1
PUMA	p53 up-regulated modulator of apoptosis
PVDF	polyvinylidene fluoride
RAG1/2	recombination activating gene 1/2
Ran	RAs-related nuclear protein
RBX1	ring-box 1
RIPA	radio-immuno-precipitation assay
RISC	RNA-induced silencing complex
RNA	ribonucleic acid
RNAse	ribonuclease
RPMI	“Roswell Park Memorial Institute”
RXR	retinoid X receptor
SDS	sodium dodecyl sulfate
SHM	somatic hypermutation
SKP1	S pase kinase associated protein 1
SKP2	S phase kinase-associated protein 2
Sp1	specificity protein 1
SPL	Spleen
SRM	spermidine synthase
TAD	transcriptional activation domain
TBS	Tris-buffered saline
TCF3	transcription factor 3
TEMED	tetramethylethylendiamin
TF	transcription factor
TGS	Tris/Glycine/SDS
TIL	tumor-infiltrating lymphocyte
TNFAIP3	tumor necrosis factor inducible protein A20

TNF-α	tumor necrosis factor α
TPA	tetradecanoylphorbol acetate
Trail	TNF-related apoptosis inducing ligand
TXNDC5	thioredoxin domain containing 5
UTR	untranslated regions
VDJ	variable, diversity, joining
WHO	world health organization

1. Introduction

1.1. B-cell development

B-cells and their antibodies belong to humoral immunity. As part of the adaptive immune system B-cells protect against more than $5x10^{13}$ different antigens. Malfunction in B-cell development, B-cell selection as well as B-cell function leads to malignancy, autoimmunity, allergy and immunodeficiencies [1].

1.1.1. Different stages in the bone marrow

Immature B-cells are produced at the prenatal stage in the fetal liver and then constantly in the bone marrow (primary lymphoid tissue) throughout lifetime from hematopoietic stem cells (HPSC). HPSCs are dependent on different transcription factors and cross regulation to develop in different pathways [1]. Transcription factors (TF) Ikarus, PU.1 and EA2 trigger the development of common lymphoid precursors (CLP) from HPSCs to Pro-Pre-B-cells (Figure 1) [2]. CLPs are responsible for the production of B-cells, T cells, natural killer (NK) cells and dendritic cells [3]. Transcription factor EA2 activates TF early B-cell factor (EBF) and TF paired box 5 (Pax5), which are important for the activation of B-cell specific genes such as those involved in pre-BCR signaling [2].

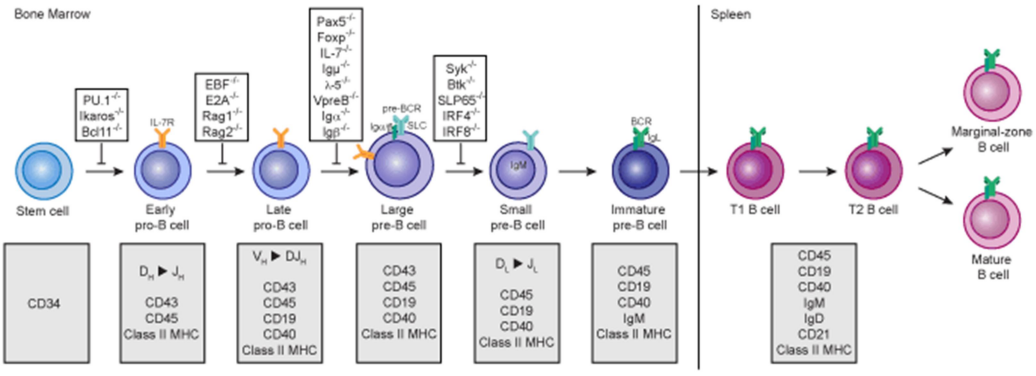

Figure 1: B-cell development
B-cells are produced in bone marrow from HPSC. Immature B-cells, expressing Immunoglobulin M (IgM), migrate to spleen where they develop into marginal zone B-cells or follicular B-cells. – adapted from http://mutagenetix.utsouthwestern.edu/phenotypic/pfile.cfm/599/Bcells.gif

B-cell development is characterized by distinct differentiation steps, during which different changing cell surface markers are expressed. To produce a functional immunoglobulin, the B-cells undergo rearrangement of DNA

segments, which encode the heavy- and the light-chain regions called VDJ-recombination: V (variable), D (diversity) and J (joining) (Figure 2a) [4]. In the early pre-pro B-cell stage, the expression of EBF-1 is increased. EF-1 and EA2 bind to the Ig gene from germline (GL) promoting the D-J_H rearrangement in the heavy chain gene segment. Recombination activating gene 1/2 (RAG 1/2) catalyzes the D-J_H rearrangement within the Ig variable heavy chain gene loci in pro-B-cells and the recombination is completed. RAG affects double-strand DNA breaks and Pax5 starts to promote the V_H to D recombination. In the late pro-B-cell stage, most cells have initiated V_H to DJ_H Ig gene segment recombination. In pre-B-cells VDJ recombination is completed. The Ig heavy chain is expressed on the surface while the light chain complex is surrogated resulting in a pre-B-cell receptor (BCR). If the pre-BCR cannot be displayed on the cell surface because of incorrected VHDJH rearrangement, the B-cell maturation stops and cells undergo apoptosis [5, 6].

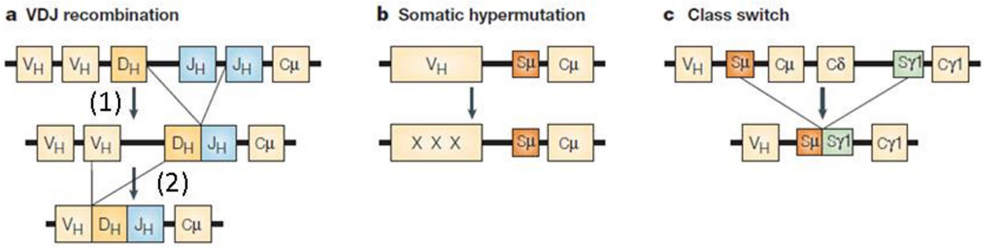

Figure 2: VDJ recombination/ somatic hypermutation and class switch recombination
a. VDJ recombination of the variable heavy chain occurs in 2 steps. First, D-JH rearrangement is done in pro-B-cells. (1). In pro-B-cells the DJ-sequence is added to one of the VH-segments (2). b. Variable regions of BCR are modified by somatic hypermutation (SHM) in the dark zone of the germinal center. c. The class switch recombination (CSR) takes place in the light zone of the germinal center and creates different classes of immunoglobulins (IgM, IgG, IgE, IgA) - adapted from Kuppers, 2005 [4].

Pre-BCR-induced signals reduce RAG expression to avoid a rearrangement of the second heavy chain and proliferation is induced. Subsequently, RAG expression is started again to initiate the V-J rearrangement of light κ and λ chain loci and the pre-BCR is lost in the surface. After a successfully completed light chain rearrangement ($V_κJ_κ$ or $V_λ$ $J_λ$) the intact BCR (V_HDJ_H/ $V_κJ_κ$ or V_HDJ_H/ $V_λ$ $J_λ$) can be expressed on the cell surface [1].

1.1.2. Secondary lymphoid tissue

Immature cells expressing IgM (IgM^{Low}), leave the bone marrow and migrate as transitional B-cells (T1 or T2) to the spleen (secondary lymphoid tissue). There they evolve into marginal zone B-cells or follicular B-cells, depending on their BCR. Marginal zone B-cells develop to short-lives plasma cells after

antigen contact. Antigen-mediated-activated follicular B-cells, supported by T cells, migrate to centroblasts (CB) in the dark zone of the germinal center (GC), where they proliferate and the variable regions of BCR are modified by somatic hypermutation (SHM) (Figure 2b, Figure 3) [7]. Point mutations, deletions and duplications in the rearranged variable regions of heavy and light chains occur during SHM, which is important for the structural basis of clonal selection by antigen, for higher antigen mutants and the affinity maturation of the antibody response. This results in generation of different B-cell clones with a large variety of affinity to the antigen that initiated this response. After proliferation and SHM in the dark zone, cells with modified antigen receptor move to the centrocytes (CC) in the light zone of the germinal center and undergo the class switch recombination (CSR) to generate different classes of immunoglobulins (IgM, IgG, IgE, IgA). The residual B-cells re-enter the dark zone to undergo more cycles of proliferation. Class switch recombination alters the antibody effector functions for a better adapted antibody response. Class switch recombination and somatic hypermutation are caused by activation-induced cytidine deaminase (AID). AID plays a key role for antigen-driven clonal expansion, selection and differentiation of the B-cells. AID deaminates cytocines in S regions to uracil generating a U-G mismatch. Mismatches are removed by DNA repair pathways, resulting in single-strand DNA breaks as well as double-strand DNA breaks and mutations. Class switch recombination occurs by a deletional recombination between two different switch (S) regions located upstream of the heavy chain constant (C_H) region gene expect from Cδ and Cμ. It replaces the μ and δ heavy chain constant (C_H) regions of the expressed immunoglobin with γ, ε or α C_H region downstream (Figure 2c). This results in a change of IgM and IgD expression to IgG, IgE, or IgA. [8] Unused germinal center B-cells die by apoptosis if they are not rescued through antigen contact. The GC B-cells evolve into memory B-cells or plasma cells and leave the microenvironment [9].

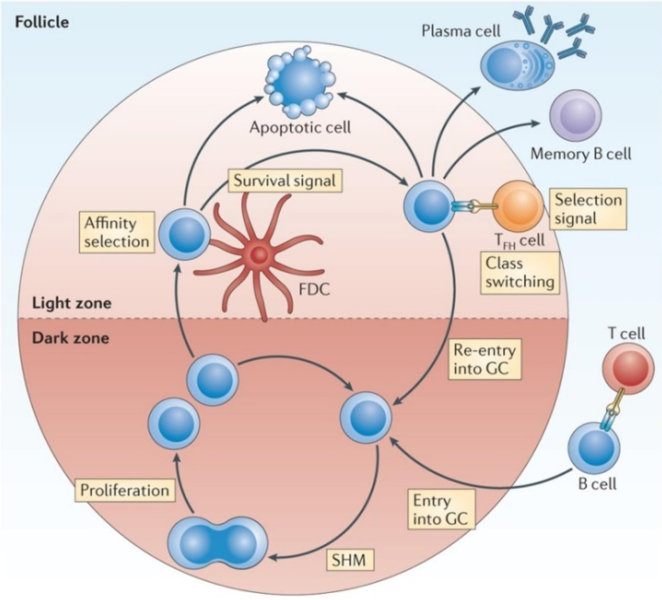

Figure 3: Germinal center with dark zones and light zones
B-cells undergo somatic hypermutation and class switch recombination to develop into memory B-cells or plasma cells. – adapted from Heesters et.al, 2014 [7]

1.1.3. Molecular mechanism of germinal center initiation

Multiple transcription factors and modulators are needed to regulate the germinal center initiation, expansion and exit of B-cells. Pax5 is expressed during the entire life of a B-cell, since mature B-cells depend on Pax5 with regard to their differentiation and function. B-cell lymphoma 6 (BCL-6) expression is a master regulator for the initiation of the GC reaction and maintenance. It controls a transcriptional program for migration towards to the center of the follicle. Nuclear factor-κB (NF-κB) is involved in GC initiation and activates interferon-regulatory factor 4 (IRF-4). In dark zone B-cells, NF-κB and IRF-4 are absent and reappear in light zone B-cells. IRF-4 has multiple functions and regulates the formation of GC. Myocyte-specific enhancer factor 2B (MEF2B) and IRF-4 induce BCL-6 expression during GC initiation. In light zone B-cells, NF-κB transactivates IRF-4 and represses the expression of BCL-6 at the GC exit stage, which induces B lymphocyte-induced-maturation protein 1 (PRDM1 or BLIMP1). BLIMP1 is involved in differentiation to plasma cells. Myelocytomatosis oncogene cellular homolog (MYC) has an important role in almost all proliferating cells. It is required for proliferation, metabolism and telomere maintenance. MYC is needed during GC initiation and re-entry into the dark zone from light zone, but is lacking in most GC B-cells. BCL-6 represses MYC transcription in the dark zone [10].

VDJ recombination, somatic hypermutation and class switch recombination cause double-strand DNA breaks, single-strand DNA breaks, mismatches and mutations. These genetic alterations are essential for a normal B-cell development and the maturation process, but translocations in lymphoid malignancies involves the Ig gene locus and plays a crucial role of molecular mechanisms in lymphomagenesis [11].

1.2. Lymphomagenesis

About 100 different variants of lymphoid malignancies are registered by the World Health Organization (WHO). WHO classification defines lymphoma as neoplasms of the hematopoietic and lymphoid tissues. There are two main forms of lymphomas: Hodgkin lymphomas (HL) and non-Hodgkin lymphomas (NHL). Additionally, two other forms are known: Post-transplant lymphoproliferate disorders and histiocytic and dendritic cell neoplasms. NHLs can be divided into B- and T-/NK-cell neoplasms. Nowadays, more than 30 different B-cell lymphomas are classified containing more than 50 subtypes in total by WHO - updated 2016. Aggressive B-cell lymphomas show a large diversity, clinical as well as pathological, and there exist multiple pathways of transformation. Aggressive B-cell lymphomas include, among others, Burkitt's lymphoma (BL), diffuse large B-cell lymphoma (DLBCL), follicular lymphoma grade 3 (FL III) and mantle cell lymphoma (MCL). These are the most common types comprising almost 50% of all lymphomas – most types are derived from GC B-cells. DLBCL is the most common type of non-non-Hodgkin lymphomas. Some B-cell lymphoma subtypes can be distinguished by clinical and pathological methods, but indistinguishable ones require gene expression profiling (Figure 4) [12].

In the western world, approximately 20 out of 100000 are identified as new cases per year. 95% of lymphomas, which are diagnosed, are B-cell lymphomas, the rest originates from T-/NK-cells [4]. In Austria about 6% of all malignant tumors are hematological neoplasms and around 3000 patients were affected in 2012 (Statistik Austria) [13]. The number of NHL cases increased substantially from a number of 492 (1983) to 1272 (2014). In 2014, 637 patients died from their disease, representing 3 % of cancer deaths reported in Austria. Men have shown an increased mortality rate compared to women (1.3 - 1.6 times higher) [13].

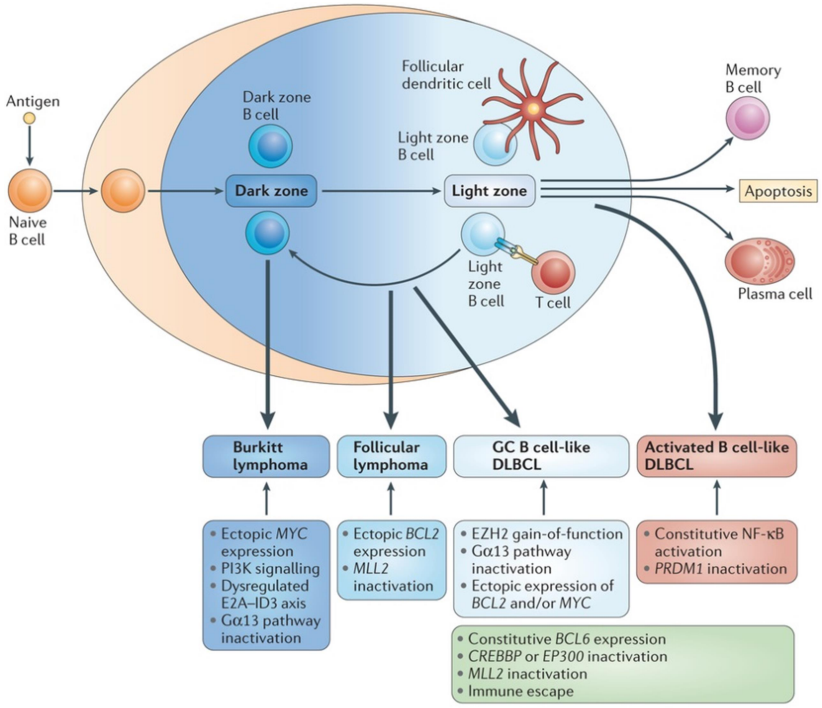

Figure 4: Lymphomas derived from germinal center (GC) and the engaged oncogenic pathways
Aggressive B-cell lymphomas include Burkitt's lymphoma (BL), diffuse large B-cell lymphoma (DLBCL) and follicular lymphoma (FL). BL originate from dark zone B-cells, whereas FL and GCB-DLBCL arise from light zone B-cells. ACB DLBCL is related to a BCR activated cell or a plasmapastic B-cell originates from a later stage of GC differentiation. – adapted from Kuppers, 2005 [4].

1.2.1. Diffuse Large B-cell lymphomas (DLBCL)

Diffuse large B-cell lymphomas are the most aggressive type of B-cell lymphomas, which are derived from GC B-cells, and the most common type of lymphomas worldwide. Gene expression analysis showed that DLBCL can be subdivided into two subtypes: germinal center B-cell type (GCB) and activated B-cell type (ABC). GCB-cells originate from a GC centroblast in the light zone and express high levels of BCL-6. ABC cells are related to a BCR activated cell or a plasmablastic B-cell originating from a later stage of GC differentiation. GCB- and ABC-DLBCL subclasses show chromosomal alterations, disordered transcriptional regulation, different intracellular signaling pathways and different clinical outcome. GCB DLBCL has a much better clinical prognosis compared to the more aggressive ABC DLBCL. Both subtypes show partially the same genetic aberrations, including chromatin modifiers, BCL-6 dysregulation and immune recognition. Chromatin remodeling proteins like *CREB-binding-protein* (*CREBBP*), *histone methyltransferase* (*MLL2*) and/or *E1A-binding protein p300* (*EP300*) are genetically inactivated and result in inhibition of tumor suppressor p53 and inactivation of the proto-oncogene *BCL-6*, which is translocated and is

subsequently dysregulated. BCL-6 regulation can be also affected by multiple indirect mechanism, containing gain of function mutations in MEF2B, a positive regulator, and or by inactivation of F-box protein 11 (FBXO11), responsible for ubiquitination and degradation of BCL-6. The cell surface receptor major histocompatibility complex class II (MHC II) is not expressed on the cell surface, which prevents the recognition by cytotoxic T lymphocytes and the natural killer cell mediated immune recognition [10].

The GCB B-cell subtype of diffuse large B-cell lymphoma is associated with inactivation of Gα13 signaling pathway resulting in hindrance of cell migration and phosphoinositide-3-kinase (PI3K) pathway. Often, chromosomal translocations of *B-Cell lymphoma 2 (BCL-2)* and *MYC* - in 40% and 10% of cases – are additionally involved in the GCB subtype, whereby translocation in both genes results in a poor prognosis. *Enhancer of zeste homologue 2* (*EZH2*), involved in histone modification [10], is mutated in about 21% of all cases and its activation with BCL-6 leads to promotion of epigenetic changes (gain of function). In contrast, in ABC-DLBCL the NF-KB-pathway is involved in different multiple genetic events causing a constitutive activation on the basis of gene expression. Cluster of differentiation 79 (CD79), encoding components of the BCR complex, caspase recruitment domain-containing protein 11 (CARD11) and as well myeloid differentiation primary response protein 88 (MYD88) can be affected by mutations. *CD79A/B* – in 20% of cases and *CARD11* – in 10% of cases - are activated in ABC DLBCL. Mutations in activated *MYD88* promote cell survival by activating NF-KB. Tumor necrosis factor inducible protein A20 (TNFAIP3) is inactivated in 30% of cases [10]. PRDM1 is constitutively repressed caused by the dysregulation of BCL-6 in ABC-DLBCL, whereby BLIMP1 is negatively regulated to block the differentiation [14].

1.2.2. Burkitt lymphoma

Burkitt lymphomas (BL) derived from GC dark zone B-cells is the most common and aggressive type of lymphoma in children. Three subtypes, which show different clinical variants, are classified: endemic (African) BL, sporadic BL (non-African) and AIDS-associated BL. Histological analysis is similar between the subtypes. EBV (Epstein–Barr virus) is involved in all three subtypes and shows differences in association. EBV is involved in nearly all cases of endemic BL, but patients affected by sporadic and AIDS-associated subtype are EBV-positive in 30% of all cases. In mature B-cells, phenotypical

analysis showed an expression of CD10 (class of IgM) in almost all cases. Translocation of the proto-oncogene *MYC* (100% of all cases) has been identified as the hallmark of Burkitt lymphomas. All three subtypes are affected by *MYC* translocation. Translocation on the immunoglobulin heavy chain locus on chromosome 14 is the most common mutation, followed by the chromosomes 2 and 22 on the light chain gen [15]. Genetic mutations like constitutive expression of *MYC* cooperating with activation of PI3K pathway leads to lymphomagenesis. *Transcription factor 3 (TCF3)*, which encodes the transcriptional factor E2A, is mutated in 70% of all cases and affects its negative regulator inhibitor of DNA binding 3 (ID3). Tonic BCR signaling is promoted and PI3K signaling pathway is activated. NF-KB is devoid in Burkitt lymphomas. *Cyclin D3 (CCDN3)* is mutated in 40% of sporadic BLs. TCF3 transactivates CCDN3 – this mutation is responsible for a high proliferation of the lymphoma by regulating the G1 to S phase cell cycle transition. Additionally, BL shows a disrupted Gα13-pathway and several mutated tumor suppressors, like tp53 (protein 53), phosphatase and tensin homologue (PTEN) and cyclin-dependent kinase inhibitor 2A (CDKN2A) [10].

1.2.3. Follicular lymphoma

Follicular lymphomas (FLs) originate from clonal expansion of multiple follicles consisting of intact GCs with an active somatic hypermutation activity. Depending on the grading, follicular lymphoma can be classified in 3 categories (grades 1-3). Grades are subdivided by the number of centroblasts (0,5-5 = I, 6-15 = II, >15 = III). Additionally, grade 3 is split in subtypes A (centrocytes are still present) and B (sheets of centroblast). FL is a slow growing form with a poor clinical outcome and often evolves through transformation to more aggressive DLBCL [16]. In follicular lymphomas, *BCL-2* shows a t(14;18) translocation under control of immunoglobulin heavy chain regulatory regions in more than 90% of all cases caused by RAG recombinase. *BCL-2* translocation takes place in an early stage of B-cell development and affects later stages during GC reaction. The expression of BCL-2 in an abnormal location stimulates an anti-apoptotic program and supports survival of malignant cells. A second mutated gene –in 80% of cases - is the *MLL2*, which is inactivated in an early stage of lymphoma pathogenesis. In combination with a dysregulated *BCL-2*, both promote the cancerous transformation in the GC. Inactivated CREBBP, EP300 and

activated EZH2 are implicated in alteration of chromatin remodeling processes in FLs as well as DLBCL [10].

1.3. Proto-oncogene c-MYC (*MYC*)

1.3.1. MYC in human

c-MYC, a proto-oncogene, belongs to the family of non-redundant MYC proteins, including N-MYC, L-MYC, B-MYC and S-YC. MYC is a regulator of cell proliferation, differentiation and apoptosis and is deregulated in a variety of human cancer through a number of mechanisms, and is important in the majority of B lymphoma subtypes. Mitogens are responsible for the activation of *MYC* and are repressed after contact with anti-proliferative signals. A number of *MYC*-target genes, which are involved in regulation of cell metabolism, cell cycle, signaling, cell adhesion and cell growth, have been identified. c-MYC acts as a transcription factor and represses or activates a vast number of downstream pathways. MYC contains a C-terminal region (CTD) formed of basic/helix-loop-helix/leucine zipper (b/HLZ/Z) motif on chromosome 8q24. HLZ/Z region is needed for oligomerization and allows heterodimerization with Max, a transcription factor consisting of a b/HLZ/Z region, and the basis region for recognition of CACGTG E-box sequences in the promotor of target genes. Binding of Max to GACGTG is required for transcription of target genes through MYC. Further it is needed for proliferation, malignant transformation and apoptosis. The N-terminal region (NTD) consists of the transcriptional activation domain (TAD) and other functions [17].

Mutations of *MYC* in B-cell neoplasms lead to expression of *MYC* in cells whose normal pedants do not express *MYC*. The *c-MYC* gene on chromosome 8q24 translocates to chromosome 2p11, 14q32 and 22q11 site next to the immunoglobulin heavy or light chain locus. The transcription of B lymphocytes is positively regulated by the immunoglobulin promotor and results in a constitutive activation of *MYC* [18]. MYC is overexpressed in lymphoma cells and can be used as biomarker for different types of lymphoma. Importantly, translocation of *MYC* alone is not able to initiate lymphomagenesis. Rearrangement of *MYC* and concomitant overexpression or co-rearrangement of BCL-2 and/ or BCL-6 are indicators for the prognosis of patients. MYC expression with BCL-2 overexpression, but without co-rearrangement, leads to intermediate survival and is called a “double-expressor” case. Lymphomas with BLC-2 and/or BCL-6 translocation are called “double-hit” or “triple hit” cases and have a much poorer prognosis.

These lymphomas belong to a new category - updated 2016 by WHO - and are called “High grade B-cell lymphoma (HGBL), with rearrangement of MYC and BCL-2 and/or BCL-6” [19].

1.3.2. Myc in mouse model

To imitate lymphoid tumors, the *EμMyc* transgenic mice with *Myc* translocation were developed. These transgenic mice carry the *Myc*/Ig t(8;14) translocation characteristic of Burkitt lymphomas. A normal *Myc* gene was isolated from a mouse plasmacytoma and was coupled with the immunoglobulin heavy chain enhancer (Eμ). The results were transgenic mice expressing the transgene in B-cells only and show a higher proliferation than in normal B-cells. Before birth, in mice a polyclonal pre-B-cell expansion takes place. Mice develop B-cell lymphomas with a mean latency of 12-16 weeks and 90% develop B-cell leukaemia/lymphomas in the first six months of life [20]. *EμMyc* mice need additional genetic modifications to develop malignant transformation. The second mutation, called “second hit”, comprises the loss of function of p53 or an overexpression of Bcl-2. *EμMyc* mice contain a dysregulated p19Arf-Mdm2-p53 pathway or anti-apoptotic Bcl-2 or Bcl-XL are overexpressed. Mice with dysregulated p53 have a poorer prognosis than mice with a Bcl-2 overexpression. Pro-apoptotic proteins like Bim, Bcl-2 modifying factor (Bmf) and p53 up-regulated modulator of apoptosis (Puma) act as suppressors of *EμMyc*-induced lymhomagenesis [21]. In *EμMyc* mice with *Myc*-induced lymphomagenesis p19arf or p53 are inactivated in most tumors caused by an inactive p19Arf-Mdm2-p53 pathway. Deletion of *p19arf* and a *p53* mutation result in formation of malignant cells [22]. It is known, that Myc intercommunicates with a variety of cell cycle proteins like p53, p19 alternative reading frame protein (p19Arf) and murine double minute 2 (Mdm2). The p19Arf-Mdm2-p53 pathway is a key regulator in proliferation and apoptosis triggered by Myc. Deregulated *Myc* triggers overexpression of p19Arf, which counteracts to Mdm2 and activates p53 for regulation of target genes involved in apoptosis and growth arrest. The protein p19Arf is negatively regulated by p53 which influences the transcription of MDM2. The protein p19Arf can bind directly to Myc to inhibit its transactivation.

The expression of anti-apoptotic proteins Bcl-2 and B-cell lymphoma-extra large (Bcl-XL) is suppressed by Myc. The balance between pro- and anti-apoptotic proteins is regulated by these mechanism [23]. Overexpression of Bcl-2 or Bcl-XL and Mcl-1 leads to tumor development in transgenic mice with

enhanced *Myc*-expression. In *Myc*-driven lymphomagenesis BCL-XL is an important factor for the survival of pre-leukemic cells and lymphoma development. The expression of BCL-XL is restricted to pre-B-cells during clonal selection. [24]. Additionally, expression of Bcl-2 and Bcl-XL is suppressed by c-*Myc*. Bim is a suppressor of the *EμMyc*-induced lymphomagenesis [25, 26]. In *EμMyc*-mice with loss of BIM the lymphoma development is accelerated. Bim act as an tumor suppressor in B lymphoid cells [25, 26].

1.4. Cell cycle proteins involved in lymphomagenesis

1.4.1. p19Arf - MDM2 - p53 pathway

p53 is a critical tumor suppressor gene, which is located on chromosome 17 and is described as “guardian of the genome”. *p53* acts as a transcription factor against unregulated cell growth and prevents tumor development. It triggers apoptosis, cell cycle arrest, differentiation and senescence. In human tumors, *p53* is mutated in approximately 50% of cases. Mutations occur in the DNA-binding domain of *p53* based on single amino acid substitutions. Activation of p53 occurs in response to cellular stress and consists of three basic steps. p53 is stabilized and binds to specific DNA sequences resulting in activation of the transcription of target genes. Protein p53 is phosphorylated in the amino terminus at special amino acids by other kinases or p19Arf. This mechanism inhibits the binding of Mdm2 and stabilizes p53. In tumorigenesis the response is mediated through p19Arf – Mdm2 - p53 pathway. Mdm2 is an important regulator of p53 and p53 levels are kept low under normal conditions. Stabilization of p53 occurs by interfering with the interaction between Mdm2 and p53. Mdm2 functions as ubiquitin E3 ligase and binds to p53 which is ubiquitinated by Mdm2 and leads to degradation by the proteasome. The function of p53 as a positive transcription factor is restrained. Mdm2 and p53 form an auto regulatory feedback-loop. Tp53 enhances transcription of *Mdm2* gene and Mdm2 regulates the activity of p53. In absence of p19Arf, Mdm2 acts as a negative regulator and mediates a degradation of p53 through ubiquitination. Tumor suppressor p14ARF (p19Arf in mice) binds to MDM2 and inhibits the ubiquitination effect of p53 by MDM2. The tumor suppressor is activated and stabilized and transcription of target genes like p21 or BCL-2 associated X protein (BAX) is turned on [27]. *Myc* activation leads to high levels of p19Arf and p53.

1.4.2. BCL-2 family

About 15 different BCL-2 family proteins are known and they include pro- and anti-apoptotic proteins, either promoting or inhibiting apoptosis. The mitochondrial pathway of apoptosis is regulated by proteins of the BCL-2 family to control the permeabilization of the outer mitochondrial membrane, and thus is important in maintenance and regulation of normal hematopoietic homeostasis. BLC-2 family proteins consist of up to four conserved BCL-2 homology domains (BH1, BH2, BH3 and BH4), which are important for heterodimerization among proteins of the BCL-2 family. Mammalian anti-apoptotic proteins, which possess all domains, are BCL-2, BCL-XL, BCL-W, Bcl-2-related protein A1 (BFL-1) and myeloid cell leukemia sequence 1 (MCL-1). BAX, BCL-2 antagonist/killer 1 (BAK) and BCL-XS are categorized to the group of pro-apoptotic proteins and are similar to BCL-2 in their structure and sequence. BH3-only proteins like BIM, BCL-2 associated agonist of cell death (BAD), BH3 interacting domain death agonist (BID), PUMA, BMF and immediate-early-response protein APR (NOXA) show one single BH domain (BH3) only. Pro-apoptotic and anti-apoptotic proteins interact through binding of the BH3 domain. Pro-apoptotic proteins (BAX/BAK or BH3 only), containing the BH3 domain, are able to bind into the large hydrophobic groove on the pro-survival protein [28].

Anti-apoptotic proteins like BCL-2, BCL-XL and MCL-1 are located in different regions. BCL-2 is found in the intracellular membrane only, including the outer mitochondrial membrane and the nuclear envelope. BCL-XL is either located in the cytosol and translocate to the mitochondria during apoptosis, or located in the intracellular membrane. Both are able to bind to BAK and BAK and protect against apoptosis by preventing the activation and homo-oligomerization [29].

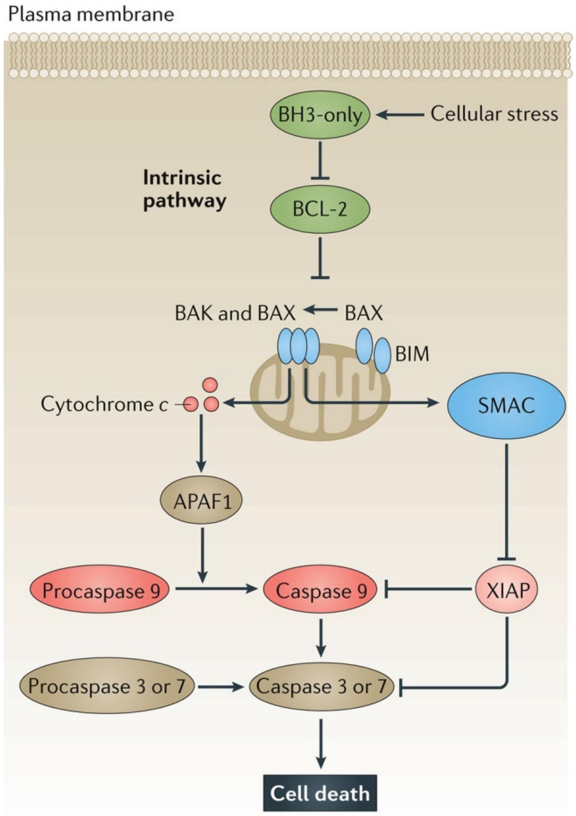

Figure 5: Intrinsic apoptosis pathway.
By cellular stress, the intrinsic pathway is activated. Pro-apoptotic BH3-only proteins inhibit BCL-2, BCL-XL and MCL-1. BAK and BAX are activated and are able to oligomerize and form pores on the outer membrane of the mitochondria. This results in permeabilization of the membrane and cytochrome c and SMAC is released. Cytochrome c interacts with a cytosolic adapter protein Apaf-1 and is able to recruit caspase-9 to activate caspase-3, resulting in apoptosis. – adapted from Ashkenazi, 2017 [30].

However, in follicular lymphomas a t(14;18) chromosomal translocation of BCL-2 on chromosome 18 and the immunoglobulin heavy chain on chromosome 14 is regularly observed. Translocation is a result of errors in VDJ recombination in the heavy chain. The rearrangement is responsible for an overexpression of BCL-2 protein. In DLBCL a rearrangement of BCL-2 is identified and leads to an elevated transcription of BCL-2 [31].

Anti-apoptotic BCL-2, an integral protein in the membrane of mitochondria, is involved in mitochondrial apoptotic (intrinsic) pathway and in regulation of apoptosis through inhibition of the release of pro-apotogenic factors from the mitochondria [32] . The responsibility of BCL-2 is to prevent or delay apoptosis in lymphoid cells. BCL-2 is expressed during B-cell development. In germinal centers BCL-2 functions as a survival signal for positive selection of B-cells. In addition, BCL-2 is down-regulated in pre-B-cells, but shows an expression in pro-B-cells and mature B-cells. BCL-X, one of the closest relatives to BCL-2,

can be spliced in shorter forms and belongs to the anti-apoptotic proteins. In humans 2 forms of BCL-X mRNAs are available: BCL-XL and BCL-XS. These proteins are responsible for different biological functions. BCL-XL is a protein, which is found in intracellular membranes as well as in a soluble form in the cytoplasm. BCL-XL is expressed in embryonic and postnatal tissues and also in primary lymphoid organs. BCL-XL is translocated to the mitochondria and perinuclear envelope and is able to inhibit apoptosis in hematopoietic cell lines. Additionally, BCL-XL is expressed in a high concentration in early B-cell lineage cells and is needed for their maintenance [33]. BCL-XL shows an overexpression in various solid tumors and in hematopoietic tumors [34].

MCL-1 is an anti-apoptotic BCL-2 family member, but it is more divergent than BCL-2 and BCL-XL. MCL-1 is also located in the mitochondria and interacts with pro-apoptotic proteins. Its gene is an early response gene in ML-1 human myeloid leukemia cells and is induced by differentiation with tetradecanoylphorbol acetate (TPA). MCL-1 inhibits, like BCL-2, apoptosis. MCL-1 is expressed at specific stages in response to defined growth and differentiation signals during hemato-lymphoid cell differentiation [35]. Mice expressing a *Mcl-1* transgene develop a diversity of B-cell lymphomas [36].

BIM is a pro-apoptotic protein, which can be found mainly in the hematopoietic system and is considered to be an antagonist of BCL-2, which mediates apoptosis. BIM belongs to BH3-only proteins and the BH3 region interacts with BCL-2 [25]. BIM is localized in intracytoplasmic membranes and three isoforms are known: BIM_{EL}, BIM_L and BIM_S, respectively. These are generated through alternating splicing. Isoforms are differentially expressed in various tissues or development stages. The shortest isoform BIM_S is the most cytotoxic one and temporary expressed during apoptosis [37]. BIM_{EL} and BIM_L are located to the microtubule-associated dynein motor complex. During apoptosis, they are released and translocate to the mitochondria, where BIM can interact with BCL-2, BCL-XL and MCL-1 and induce apoptosis [38]. BH3-only proteins are activated by cellular stress like DNA damage, activation of oncogene c-Myc and initiate the apoptotic cascade. They engage BAX/BAK directly or they engage anti-apoptotic proteins like BIM, Bad or Bid to release BAK/BAK, which are already in an active conformation [39]. BAK is located on the outer mitochondrial membrane, while BAX is a cytosolic protein. Activated BAX/BAK or BH3-only proteins bind to anti-apoptotic proteins and neutralize them. BAX and BAK change their conformation and form pores on the outer membrane and so cytochrome C is released. This interacts with a cytosolic

adapter protein Apaf-1 and is able to recruit caspase-9 to activate caspase-3 [32]. Likewise, overexpression of BCL-2, BCL-XL or MCL-1 or loss of pro-apoptotic BCL-2 family members like BIM or PUMA lead to tumor development - most in combination with c-*MYC* expression [24].

1.4.3. PARP

poly(ADP-ribose)polymerase (PARP) is an enzyme, which is activated by DNA strand breaks and promotes DNA repair, but is also involved in a caspase-independent form of apoptosis [40]. PARP is involved in a variety of cellular processes, such as DNA replication and repair, cell proliferation, cell death, as well as in carcinogenesis. 17 genes have been identified by now, which encode for different PARP proteins in mammalians. They have diverse functions in the cell and are essential for cellular homeostasis. PARP-1 is the best-known protein. PARP-1 is activated by DNA damage the activity is regulated by posttranslational modifications and different transduction pathways. [41] Active PARP transfers ADP-ribose subunits from NAD^+ to the target proteins and form negative charged polymers of ADP-ribose. This process counteracts the activity of a PAR glycohydrolase (PARG). PARG eliminates the ADP-ribose from target proteins. Poly(ADP-ribos)ylation (PARylation) and/or posttranslational modification of proteins, are/is important for molecular and cellular processes and is a prompt reaction in DNA damage. Further, it has a possible role in recombinase-mediated DNA damage in the origin of B-cell lymphomas [40]. During apoptosis, caspase 3 and caspase 7 catalyze the cleavage of PARP (116kDa) which results in separation of the PARP amino-terminal DNA binding domain (24kDa) from the carboxy-terminal catalytic domain (89kDa) [42]. VDJ recombination can also lead to PARP activation through the required nicking and joining of DNA. Further, the activation may affect the VDJ recombination and the development of B-cells [43].

1.4.4. IRF-4

IRF-4 acts as transcription factor for interferons and regulate various functions in the immune system and in tumorigenesis. The interferon regulatory factors family involves nine mammalian members (IRF-1 - IRF-9). The expression of IRF-4 is limited to T and B lymphocytes, macrophages and dendritic cells. Further, IRF-4 is important in regulation of differentiation and is needed during the immune response for lymphocyte activation and the generation of plasma

cells. Logically, a dysregulated IRF-4 is related with multiple lymphoid malignancies and acts either as tumor suppressor or oncogene [44]. In B-cells, IRF-4 and IRF-8 are involved in various stages of differentiation, their function and transformation. IRF-4 and IRF-8, both are critical key factors in regulating early B-cell development. IRF-4 expression is regulated by the NF-KB pathway. Absence of IRF-4 and IRF-8 leads to a stop in B-cell development at the large pre-B stage [45]. IRF-4 is needed for the function of mature B-cells. IRF-4 is important for CSR by inducing AID and is overexpressed in light zone B-cells in the germinal center to repress the expression of BCL-6. In multiple myeloma cells IRF-4 induces the expression of c-Myc and is critical for survival and expansion. IRF-4 is involved during the humoral immune response for the activation of lymphocytes and is a master regulator of autoimmunity. In B-cell malignancies, the expression of IRF-4 is dysregulated. It was found to be overexpressed in many B-cell lymphomas. Taken together, the expression of IRF-4 is essential and important for B-cell development and the activity of B-cells [46].

1.5. Spermidine

Spermidine, spermine and their diamine precursor putrescine are naturally occurring polycationic polyamines and are found in all organisms. Polyamines interact with negatively charged molecules like RNA, DNA and lipids and are involved in multiple important biological processes like DNA metabolism, autophagy, inflammation, cell growth, differentiation, apoptosis and survival. For the first step of polyamines biosynthesis, ornithine, which is generated in urea cyle, is decarboxylated in the cytoplasma through ornithine decarboxylase (ODC) to produce putrescine. Spermidine is synthesized by the spermidine synthase (SRM) from putrescine as a precursor of spermine. The polyamine metabolism is often dysregulated in cancer. Known oncogenes target the polyamine pathway and inhibit polyamine synthesis [47, 48]. Intracellular levels of polyamines, especially spermidine, are very dynamic and are regulated by biosynthesis, degradation and transport. Cells in growth phase show an increased level of polyamines, but the biosynthesis is down-regulated in cells which became senescent. Supplementation of polyamines contained in food (like cheese, red meat, soybeans) or water increase the level of polyamines. Accordingly, data indicate that sustaining spermidine levels in advanced age promote longevity [49]. High-polyamine diet in mice with a short or long life expectancy showed an extended life span and a significantly reduced level of age-related oxidative damage [50, 51].

Spermidine supplemented feeding of old mice resulted in longevity and showed cardioprotective effects like lowering cardiac hypertrophy and protection of diastolic function. Spermidine possesses positive effects on cardiac autophagy, mitophagy and mitochondrial respiration. It enhances the mechano-elastical properties of cardiomyocytes in vivo. Spermidine supplementation in mice lacking the autophagy-related protein 5 (Atg5) in cardiomyocytes reverses the positive effects of cardioprotection. In human, high levels of spermidine in food correlate with a decreased blood pressure and a lower frequency of cardiovascular disease [52]. The inhibition of histone acetyltransferases (HAT) through spermidine, which prevents the hypoacetylation of histone H3, leads to suppression of oxidative stress and ageing-associated necrosis in aging yeast. The modified acetylation condition of chromatin is leading to autophagy and improves longevity. Spermidine supplementation restrains ageing in yeast, flies, worms, human cells and mice [53]. *MYC* is activated in about 70% of human cancers. Moreover, ornithine decarboxylase (ODC) is a transcriptional target of c-*MYC* oncogene and encodes the first rate-limiting enzyme in polyamine biosynthesis. The *OCD* gene contains two conversed GACGTG elements in intron 1. Dimers of Myc and Max are able to activate transcription of ODC by binding to these elements in the cell. Afterwards, ODC synthesize putrescine from ornithine, which is then further converted into spermidine and spermine. MYC overexpression in cells leads to an increased level of polyamines. MYC promotes malignant transformation and accelerates the rates of cell-cycle traverse leading to a downregulation of cyclin-dependent kinase inhibitor $p27^{Kip1}$ and $p21^{Cip1}$. These cell cycle checkpoints and the apoptotic pathway are able to trigger Myc-driven lymphomagenesis. The malfunctions in transgenic knockout mice stimulate *Myc*-driven cancers. The overexpression of ODC is a hallmark in B-cell lymphomas developed in *Eμ-Myc* transgenic mice and human BL. In normal cells $p27^{Kip1}$ associates and binds to cyclin E/CDK2 and cyclinA/CDK2 complexes leading to an inactivation in the S phase. Degradation of $p27^{Kip1}$ is achieved through the SCF^{Skp2} complex, containing $p27^{Kip1}$-binding and –specify factors S Phase kinase-associated protein 2 (SKP2) and cyclin-dependent kinase subunit 1 (CKS1), ring-box 1 (RBX1), S Phase kinase-associated protein 1 (SKP1) and Cullin 1 (CUL1). Polyamines are important for the expression of that complex (Figure 6).

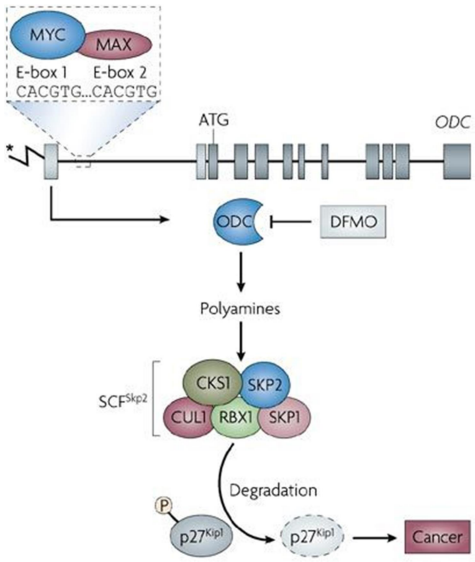

Figure 6: MYC regulation of ODC in malignant transformation
MYC promotes malignant transformation and accelerates the rates of cell-cycle traverse leading to a downregulation of cyclin-dependent kinase inhibitor $p27^{Kip1}$. CKS1 and SKP2 expression is activated by MYC to promote the degradation of $p27^{Kip1}$. OCD is required for a Myc-mediated degradation. – adapted from Casero, 2007 [47].

CKS1 and SKP2 expression is activated by MYC to promote the degradation of $p27^{Kip1}$. Interestingly, ODC is necessary for Myc-mediated degradation of $p27^{Kip1}$. Defective OCD disrupts the ability of MYC to downregulate CDK inhibitors resulting in a modified route of Myc-induced transformation. Finally, *Myc*-driven lymphomagenesis is delayed. A treatment with ODC suicide inhibitor 2-difluoromethylornitine (DFMO) or ODC heterozygosity eliminate the effects of MYC on the expression of CKS1, SKP2 and $p27^{Kip1}$ [47, 54].

Caloric restriction (CR), long-term or intermittent short term starvation, has been reported to expand the lifetime of yeast, plants, flies, worms and rodents. In humans, CR prolongs lifespan and has positive effects on cellular processes by reducing the frequency of cancer, metabolic diseases, arteriosclerosis and neurodegeneration [55]. In the absence of nutrients, autophagy is activated by depletion of intracellular acetyl coenzyme A (acetyl-CoA) leading to deacetylation of cellular proteins. Moreover, caloric restriction mimetics (CRMs) are natural components that act as acetyl-CoA reducing agents by reducing cytosolic acetyl-CoA, acetlytransferase inhibitors or deacetylase activators. All CR mimetics leading to several physiological changes, stimulate autophagy and reduce aging-associated defects [56]. Resveratrol, rapamycin, and metformin are three best studied CR mimetics

[57]. Another important CR mimetic is Spermidine, which induces the deacetylation of proteins and enhances autophagy in vivo in mice or in cultured human cells. CRM and CR influence the same molecular pathways involved in induction of autophagy. Both can be useful in therapeutic indications [56]. Fasten has a positive effect during chemotherapy through sensitization of tumors protecting against toxic side effects. Fasten-mimicking diet (FDH) in combination with chemotherapy showed an increase of common lymphoid progenitor cells in bone marrow and cytotoxic $CD8^+$ tumor-infiltrating lymphocytes (TILs) leading to hesitation of tumor progression. Stimulation of the hematopoietic system and enhancement of $CD8^+$ dependent tumor cytotoxicity by FHD combined with chemotherapy is able to increase T-cell-dependent targeted killing of cancer cells [58]. Fasting is able to improve the efficiency of anticancer chemotherapy by inducing autophagy in malignant cells. CR mimetics with spermidine and hydroxycitrate showed also an improvement of the efficacy of chemotherapy and provoked an autophagy-dependent anticancer immune response. Hydroxycitrate significantly reduced the tumor growth caused by inhibition of regulatory T cells. Short-term fasting or the treatment with CR mimetics is leading to an inhibition of tumor growth by chemotherapy in vivo [59].

1.6. MicroRNA (miRNA)

MicroRNAs (miRNAs) are small non-coding single-stranded RNA molecules (19-24 nucleotides) that downregulate gene expression at post-transcriptional level by binding to their complementary target mRNA, leading to degradation or repression of transcription. MicroRNAs function as negative gene regulators and control a wide range of biological functions. MicroRNAs are transcribed by RNA polymerase II as long primary transcripts, called pri-mRNAs, from their own genes or from genes within other introns. Pri-mRNAs contain a 5'cap and poly-A tail. In the nucleus the pri-mRNAs are cleaved to pre-miRNA by Drosha, a nuclease of the RNAse III family, and Pasha/DGCR8 (partner of Drosha), a double-strand-RNA-binding protein. The resulting pre-miRNAs consist of about 70 nucleotides and are folded in a hairpin-structure. Exportin-5 in presence of Ran-GTP complex is responsible for the transport of the pre-miRNA from the nucleus to the cytoplasm [60–62]. Once in the cytoplasm, the pre-miRNA is processed via cutting of the stem-loop by Dicer, a second RNAse III enzyme, into mature miRNA. Double-stranded RNAs consisting of two complementary short RNA molecules are formed. The double-stranded

RNA unwinds and only the functional strand is integrated into the RNA-induced silencing complex (RISC). RISC is a ribonucleoprotein complex containing argonaute proteins, which have endonuclease activity directed against mRNA strands that are complementary to their bound miRNA fragment. After integration, RISC complex guides the miRNA to complementary sites within the 3'untranslated regions (UTR) on their mRNA target. After binding of miRNA to mRNA a double-stranded RNA is formed leading to degradation of mRNA, inhibition of protein translation, or both [63, 64].

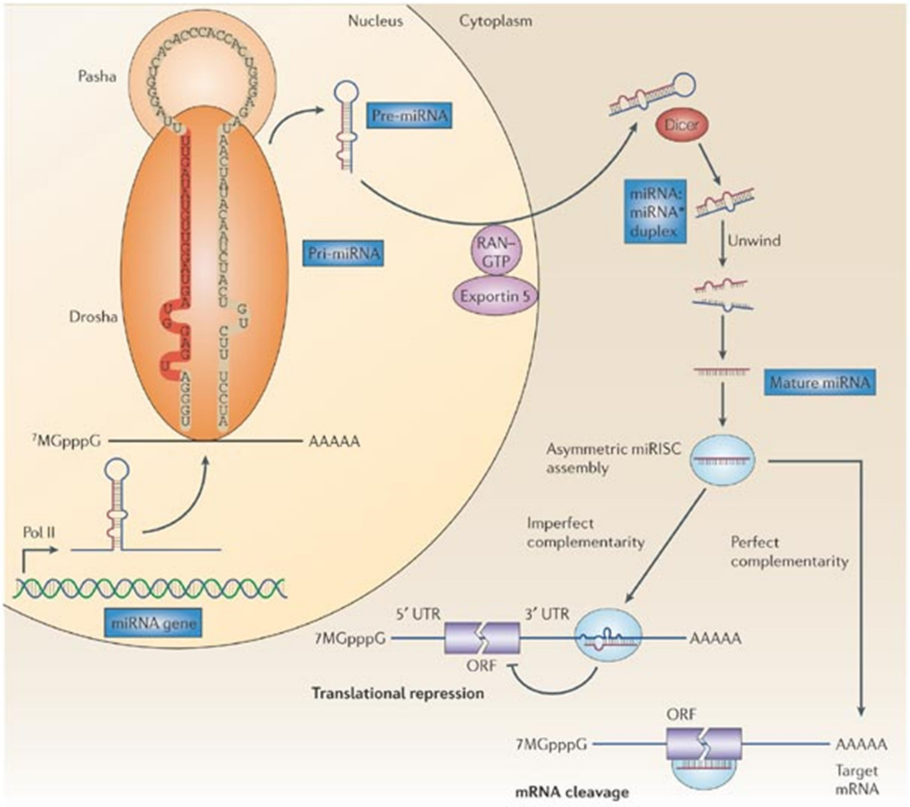

Figure 7: MicroRNA biogenesis and posttranslational silencing mechanism
MicroRNAs are transcripted by RNA polymerase II as long primary transcripts, called pri-mRNAs. In the nucleus the pri-mRNAs are cleaved to pre-miRNA by Drosha, and Pasha/DGCR8. Exportin-5 in presence of Ran-GTP complex is responsible for the transport of the pre-miRNA to from the nucleus to the cytoplasm. The pre-miRNA is processed via cutting of the stem-loop by a Dicer into mature miRNA. A double-stranded RNA consisting of two complementary short RNA molecules are formed. The double-stranded RNA unwinds and only the functional strand is integrated into the RNA-induced silencing complex (RISC). After integration, RICS complex guides the miRNA to complementary sites within the 3'untranslated regions (UTR) on their mRNA target. Binding of miRNA to mRNA leads to degradation of mRNA, inhibition of protein translation, or both. – adapted from Esquela-Kerscher, 2006 [65].

A significant discovery in recent years was to understand the role of miRNA in normal cells and cancer cells. Depending on their target genes, miRNAs can act as oncogenes (oncomiRs) or tumor suppressors. A single miRNA is able to target the mRNAs of multiple genes and plays a crucial role in different

biological entities like development, differentiation, proliferation, apoptosis as well as in cancer. An altered expression of miRNAs is shown in various cancers. In cancers, genes coding for the miRNAs are often located at fragile sites and genomic regions, typically associated with cancers [66]. On chromosome 13q14 miR-15 and miR-16 are located and responsible for the regulation of BCL-2. The miR-15/16 cluster is deleted and/or downregulated in about 68% of B-cell chronic lymphocytic leukemias (B-CLL), associated with increased survival. miRNAs are applied as excellent biomarkers for cancer diagnosis and prognosis [67]. Several miRNA have been predicted to target NR4A1 in different cells and tissues. In human vascular endothelial cells, miR-17 and miR-20a have been identified as targets of NR4A1-mRNA by regulating NR4A1-dependent gene expression [68]. In Brain miR-124 is the most common miRNA and the level of NR4A1 is regulated by this miRNA. Its function is to improve neuronal differentiation, control neutral stem cells and activate differentiation in glioma stem cells. Bioinformatical analysis showed that miR-124, miR-15a and miR-224 were expected to directly target *NR4A1* by binding to its seed region within the *NR4A1* 3'UTR. miR-124 directly targets *NR4A1* and *NR4A1* is upregulated in multiple pediatric cancer cells. NR4A1 can be indirectly regulated by miR-124 by targeting specificity protein 1 (Sp1)-mRNA. This results in reduced Sp1 and NR4A1 levels. Sp1 normally binds to the *NR4A1* promotor and increases the level of NR4A1. Nuclear Orphan Receptor *NR4A*

1.7. Background

The NR4A family consisting of *NR4A1(Nur77)*, *NR4A2(Nurr1)* and *NR4A3*(Nor-1) represent nuclear orphan receptors from the Nur77-family, with no known endogenous ligand yet. They function as transcription factors and belong to steroid hormone receptor superfamily. All three members show a high homology in their amino acid sequence. The N-terminal region (A/B) contains AF-1 (amino-terminal region 1), encoding for activation function 1, followed by DNA binding domain (DBD), a hinge region (D) and the ligand binding domain (LBD). C-terminal region encloses AF-2 (amino-terminal region 2), encoding for a dispensable activation function 2 domain. Regions of DBD (about 91-95%) and LBD (about 60%) show a high homology between their amino acid sequences in the NR4A subfamily, whereas AF-1 is highly divergent and mediates NR4A transactivation.

Figure 8: Schematic representation of NR4A nuclear orphan receptor
The N-terminal region (A/B) contains AF-1 (amino-terminal region 1), which encodes for activation function 1, followed by DNA binding domain (DBD), a hinge region (D) and the ligand binding domain (LBD). C-terminal region encloses AF-2 (amino-terminal region 2), which encodes for a dispensable activation function 2 domain. - adapted from Smith and Muscat, 2005 [69]

NR4A receptors are located in the nucleus since their DBD harbors a nuclear localization signal [70, 71]. DBD targets the receptor to a specific DNA sequence, where DBDs binds to activate gene expression as monomers to the consensus AAAGGTCA (NRBE, NGFI-B responsible element) or as homo-or heterodimer to AAA(G/A)(C/T)A (NurRE, Nur-response element). With RXR (retinoid X receptor) NRA1 and NR4A2 can build a heterodimer and bind to a DR5 motif [72]. Through external stimuli NR4A receptors are transcriptionally regulated. NR4As are early immediate-response genes, which can be activated through a wide range of physiological signals, like fatty acids, stress, prostaglandins, growth factors, calcium, inflammatory cytokines, peptide hormones and neurotransmitters. NR4A receptors are involved in various signaling pathways which regulate cell cycle arrest, apoptosis, inflammation, atherogenesis, metabolism, proliferation and DNA repair and are involved in tumorigenesis [71]. All three members are widely expressed in several tissues, such as skeletal muscle, adipose tissue, heart, kidney, liver, brain and T-cells, respectively. The activation of the NR4As is usually fugacious. NR4As affect cell growth, their survival and apoptosis. They have several functions in biological processes. They act as transcription factors for regulation of target genes, are involved in cell proliferation and survival as well as activation of target genes leading to apoptosis or the translocation to mitochondria resulting in trigger apoptosis [73]. In malignancies NR4A members influence apoptosis. Regulation of NR4A1 takes place at two levels: transcriptional and post-translational. Histone deacetylases are involved in negative regulation of NR4A1and act as co-repressors [70].

1.7.1. NR4As in malignancies

NR4A1 and NR4A3 are involved in multiple human diseases. NR4A1 is especially associated with inflammatory diseases, allergies and atherosclerosis. Gene expression analysis in DLBCL showed that NR4As act as tumor suppressor genes [71]. NR4A1 and NR4A3 are known to be a potent

tumor suppressor of acute myeloid leukemia (AML). The loss of *Nr4a1* and *Nr4a3* genes (*Nr4a1* -/- and *Nr4a3* -/-) in mice leads to a rapid development of murine AML and double knockout mice are likely to die after 3-4 weeks. In human AML *NR4A1* and *NR4A3* were shown to have a reduced expression. Hypoallelic mice (*Nr4a1 +/-* and *Nr4a3 -/-*, *Nr4a1 -/-* and *Nr4a3 +/-*) with a reduced gene dosage develop a chronic myeloid malignancy which leads to myelodysplastic/myeloproliferative neoplasms (MDS/MPNs) with progression to AML in rare cases [74].

NR4A1 is down-regulated in aggressive lymphomas and an over expression of *NR4A1* lymphoma cells results in induction of apoptosis. Apoptotic signals (Bim, Trail and Puma) were detected by reduced NR4A1 and NR4A3 occurrence [75]. The expression of *NR4A1* is highly reduced in chronic lymphocytic B-cell leukemia (71%), in follicular lymphoma (70%) and diffuse large B-cell lymphoma (74%). A low expression in aggressive lymphomas (DLBCL and FL grade 3) was significantly associated with a non-germinal center B-cell subtype with a poor overall survival. Over-expression of *NR4A1* caused apoptosis in lymphoma cell lines and suppressed lymphoma formation in vivo [70, 76].

1.7.2. Loss of Nr4a1 accelerated Myc-driven lymphomagenesis

Mice lacking Nr4a1 were crossed with *Eμ-Myc* transgenic mice to investigate the function of Nr4a1 as tumor suppressor in oncogene-driven B-cell lymphoma development. They developed malignant monoclonal lymphomas with a mean latency of 12-16 weeks. In the group, a cohort of *EμMyc Nr4a1 +/+* (n=134), *EμMyc Nr4a1 -/-* (n=84) and *EμMyc Nr4a1 +/-* (n=59) was generated and observed until disease outbreak. Visible tumors were detected significantly faster in *EμMyc Nr4a1 -/-* mice compared to *EμMyc Nr4a1+/+* (median=45 days for *EμMyc Nr4a1 -/-*, 66 days for *EμMyc Nr4a1 -/-* and 107 days for *EμMyc Nr4a1 +/+;* $p<0,001$). A shorter live span was monitored in *EμMyc Nr4a1 -/-* mice (median survival = 92days) compared to *EμMyc Nr4a1 +/+* mice (median survival = 123days; $p<0,001$) and *EμMyc Nr4a1 +/-* mice (median survival=101 days; $p<0,037$). These data indicate that Nr4a1 is involved in tumor suppressive properties in a Myc-driven lymphomagenesis.

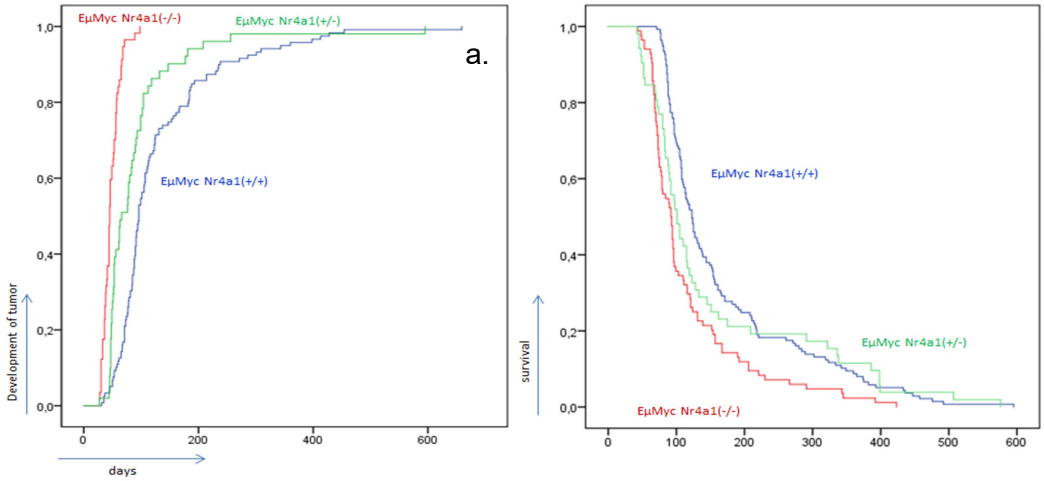

Figure 9: Tumor development and survival of *EμMyc Nr4a1 +/+, EμMyc Nr4a1 -/-* and *EμMyc Nr4a1 +/-*
a. Visible tumors was detected significantly faster in *EμMyc Nr4a1 -/-* mice compared to *EμMyc Nr4a1 +/+* (median=45 days for *EμMyc Nr4a1 -/-*, 66 days for *EμMyc Nr4a1 -/-* and 107 days for *EμMyc Nr4a1 +/+;* p<0,001). b. A shorter live span was monitored in *EμMyc Nr4a1 -/-* mice (median survival = 92days) compared to *EμMyc Nr4a1 +/+* mice (median survival = 123days; p<0,001) and *EμMyc Nr4a1 +/-* mice (median survival=101 days; p<0,037).

Developing tumors in *EμMyc* transgenic mice show an immature B-cell lymphoma immunophenotype (pro-B-cell, pre-B-cell or an immature B-cell phenotype). Isolated tumor cells from *EμMyc Nr4a1 +/+* (n=73), *EμMyc Nr4a1 -/-* (n=59) and *EμMyc Nr4a1 +/-* (n=17) were analyzed them by fluorescence-activated cell sorting (FACS) to investigate phenotypic differences. Antibodies against B-cells, T cells and myeloid cell markers were used. Regarding the immunophenotype, there were no significant differences detected between these three groups.

Furthermore, cells from bone marrow (BM) and spleen (SPL) from *EμMyc Nr4a1 +/+* mice (n=17), *EμMyc Nr4a1 -/-* mice (n=18) and wild type mice (n=4) were analyzed by FACS using antibodies against B-cells, T cells and myeloid cell markers. In the group of *EμMyc Nr4a1 -/-* mice, in bone marrow the ratio of $GR1^+$ cells to $B220^+$ cells was lower compared to *EμMyc Nr4a1 +/+* mice (p=0,025) and wild type mice (p=0,009). In the spleen the ratio of $B220^+$ to T cell receptor (TCR) was higher in E*μMyc Nr4a1 -/-* mice compared to *EμMyc Nr4a1 +/+* mice (p=0,006) and wild type mice (p<0,007). Additionally, the ratio of GR1+ cells to $B220^+$ cells was lower E*μMyc Nr4a1 -/-* mice (p=0,025) and *EμMyc Nr4a1 +/+* (p=0,089). Approximately 95% of $B220^+$ cells isolated from bone marrow and spleen of *EμMyc Nr4a1 +/+* mice and EμMyc *Nr4a1 -/-* mice displayed the same immunophenotype as lymphoma cells. These results indicate that *EμMyc Nr4a1 +/+* and EμMyc *Nr4a1 -/-* mice lymphoma cells infiltrate in bone marrow and spleen. The extent of infiltration in EμMyc *Nr4a1*

-/- is more pronounced. These data suggest that lacking Nr4a1 boosts the dissemination potential of *EμMyc* lymphoma cells.

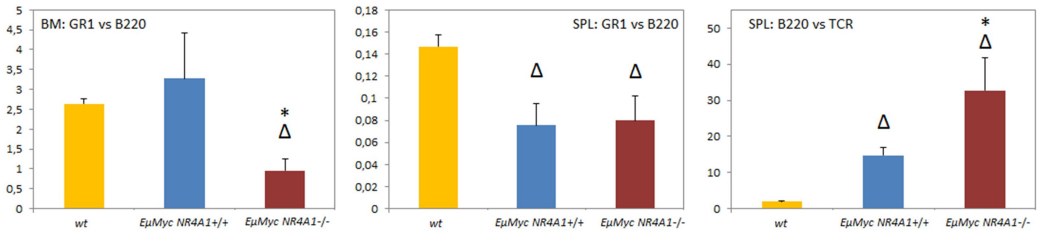

Figure 10: Comparison of the ratio of GR1$^+$ cells to B220$^+$ cells in bone marrow and spleen and the comparison of B220$^+$ cells to TCR$^+$ cells in spleen of EμMyc *Nr4a1 -/-*, EμMyc *Nr4a1 +/+* and *wild type* mice
In the group of *EμMyc Nr4a1 -/-* mice, in bone marrow the ratio of GR1$^+$ cells to B220$^+$ cells was lower compared to *EμMyc Nr4a1 +/+* mice (p=0,025) and wild type mice (p=0,009). In spleen there was detected that the ratio of B220$^+$ to TCR$^+$ (T cell receptor) was higher in *EμMyc Nr4a1 -/-* mice related to *EμMyc Nr4a1 +/+* mice (p=0,006) and wild type mice (p<0,007). The ratio of GR1$^+$ cells to B220$^+$ cells was lower *EμMyc Nr4a1 -/-* mice (p=0,025) and *EμMyc Nr4a1 +/+* (p=0,089). Triangle stands for p<0,05 compared to wild type mice and the asterisk stands for p<0,05 compared to *EμMyc Nr4a1 +/+* mice.

1.7.3. Nr4a1 loss causes resistance of non-malignant B-cells to B-cell receptor-induced apoptosis

For investigation of Nr4a1 in normal B-cells, splenic B-cells were purified through CD43$^-$, CD3$^-$ and Terr119-depletion from *Nr4a1 +/+* mice (n=5, 11 weeks old) and *Nr4a1 -/- mice* (n=6, 11 weeks old). Splenic B-cells were cultured with antibodies against CD40, interleukin-4 (CD40/IL-4), LPS (lipidpolysaccharid) and Fab fragments against IgM (BCR ligation). The expression levels of *Nr4a1* and *Nr4a3* were valuated. Annexin V staining and cell cycle analyses were done. The *Nr4a1* induction was highest in *Nr4a1 +/+* mice (more than 18 fold after 4h and 8h) at the time of BCR ligation. *Nr4a3* shows a moderate induction in both genotypes. Induction of apoptosis of *Nr4a1 +/+* splenic B-cells was induced by BCR ligation, which was shown by a higher percentage of annexin V staining and cells display SubG1 peak. The rate of apoptosis remained unchanged at the time of BCR ligation in splenic B-cells of *Nr4a1 -/-* mice. Induction of *Nr4a1* and *Nr4a3* expression was achieved by CD40/IL-4 and LPS-treatment. No differences were observed after CD40/IL-4, or LPS-treatment, annexin V staining and cell cycle analyses by comparing *EμMyc Nr4a1 +/+* mice and EμMyc *Nr4a1 -/- mice*. These data show that Nr4a1 is associated in the apoptotic effect of BCR ligation and play a fundamental role in the negative selection of B-cells.

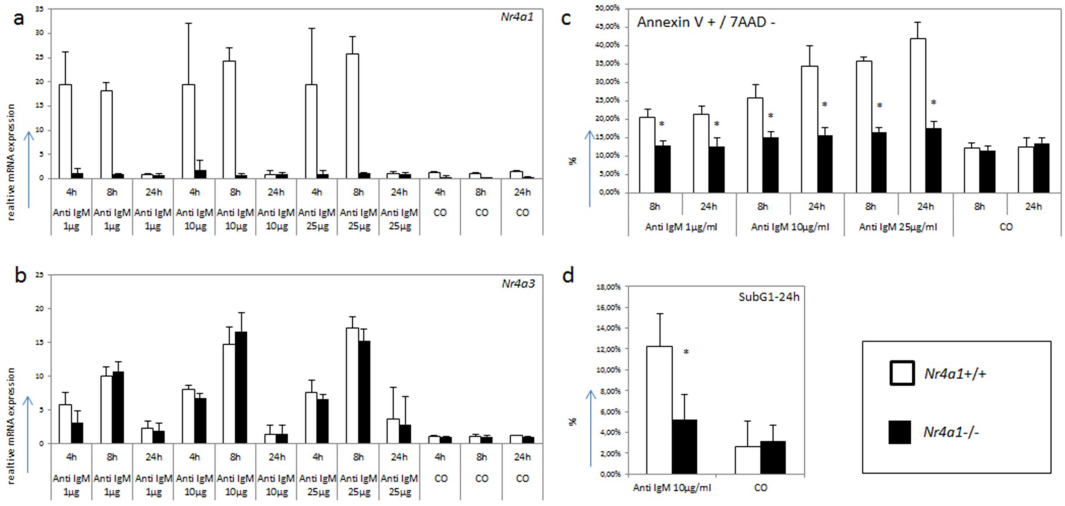

Figure 11: BCR ligation purified splenic B-cells from *Nr4a1 -/-* and *Nr4a1 +/+* mice
a. and b. Expression analysis of anti-IgM-treated B-cells from *Nr4a1 -/-* and *Nr4a1 +/+* mice show that the *Nr4a1* induction was highest in *Nr4a1 +/+* mice (more than 18 fold after 4h and 8h) at the time of BCR ligation. *Nr4a3* shows an induction in both genotypes but in moderation c. and d. Induction of apoptosis of *Nr4a1 +/+* splenic B-cells was resulted by BCR ligation, which was shown by a higher percentage of annexin V staining and cells display SubG1 peak. The rate of apoptosis remains unchanged at the time of BCR ligation in splenic B-cells of *Nr4a1 -/-* mice. Induction of *Nr4a1* and *Nr4a4* expression was achieved by CD40/IL-4 and LPS-treatment.

Additionally, a cohort of mice of *Nr4a1 -/-* (n=115) and *Nr4a1 +/+* (n=26) aged 12-16 weeks, 30-35 weeks and 52-62 weeks were generated and mice were sacrificed. Phenotypical analysis showed that *Nr4a1 -/-* mice develop significantly increased spleen weights (p<0, 05) compared to *Nr4a1 +/+* mice at all age groups, especially in older *Nr4a1 -/-* mice. Histological analysis showed that in *Nr4a1 -/-* the enlarged spleen is caused by follicular hyperplasia. This could not be detected in *Nr4a1 +/+* spleens.

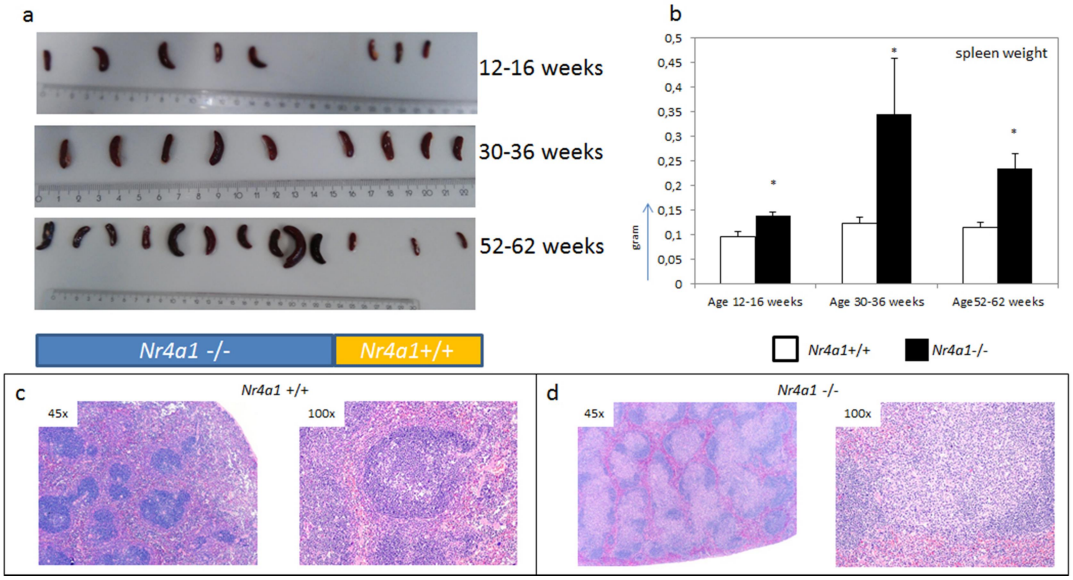

Figure 12: Phenotypic and histological analysis of *Nr4a1 -/-* and *Nr4a1 +/+*
a. and b. Phenotypical analysis showed that *Nr4a1 -/-* mice develop significantly increased spleen weights compared to *Nr4a1 +/+* mice at all age groups, especially in older *Nr4a1 -/-* mice. c. and d. Histological analysis showed that in *Nr4a1 -/-* the enlarged spleen is caused by follicular hyperplasia. This could not be detected in *Nr4a1 +/+* spleens. Asterisk stands for $p<0,05$ compared to wild type.

These data indicate that Nr4a1 plays an essential role in B-cell receptor selection. Resistance to apoptosis mediated by BCR ligation is caused by the lacking Nr4a1.

1.8. Aim

The aim of my master thesis was to investigate the role of the nuclear orphan receptor *Nr4a1* in *Myc*-driven lymphomagenesis and in normal B-cell development:

1.8.1. Aim 1

First, we investigated the requirement of *Nr4a1* and *Nr4a3* in different stages of the B-cell development and the effects in *EμMyc*-driven lymphomagenesis. A gene expression analysis was performed under non-malignant conditions comparing IgM^+ and IgM^- B-cells in *Nr4a1 -/-* and *Nr4a1 +/+* mice versus premalignant *EμMyc Nr4a1 -/-* and *EμMyc Nr4a1 +/+* mice. These data were compared with preliminary data of *Myc*-induced lymphomas derived from *EμMyc Nr4a1 -/-* and *EμMyc Nr4a1 +/+* mice.
Second, tumors with different phenotypes (IgM^+/IgM^-) in *EμMyc Nr4a1 -/-* mice were compared to *EμMyc Nr4a1 +/+* mice to clarify whether a dysregulated p19Arf-Mdm2-p53 pathway and/or overexpression of proteins involved in mitochondrial pathway like Bcl-2, Bim, Bcl-xl and Mcl-1. Additionally, Irf-4 and

Parp were investigated by Westen blot analysis to determine the influence of *Nr4a1* loss on NF-κB signaling and activation of apoptosis.
A further point was to perform a comprehensive study in human aggressive B-cells lymphomas sub classified into GCB-DLBCL, non-GCB-DLBCL as well as follicular lymphoma grade 3 (FLIII) to investigate the expression of six miRNAs at the mRNA level by real-time PCR whether they target NRA1 and NRA3.

1.8.2. Aim 2

Second, the aim of this project was to investigate the function of *Nr4a1* in gene regulation as transcription factor under non-malignant conditions in *Nr4a1 -/-* and *Nr4a1 +/+* mice. We performed expression analysis by using qPCR of 34 genes, which correlated to *NR4A1* expression in a public available gene expression dataset of DLBCL patients to *NR4A1* [77], and were significantly deregulated in tumors derived in *EμMyc Nr4a1 -/-* mice in comparison to *EμMyc Nr4a1 +/+* tumors. These genes were mainly implicated in immune regulation, immune cell migration and in NF-κB pathway. The differential expression was determined by quantitative Real-Time PCR (qPCR) and compared between the two groups

1.8.3. Aim 3

Nr4a1 deficient mice show enhanced inflammation [78]. Nr4a1 plays an important role as transcriptional mediator for inflammatory signals and controls that process [79]. It was reported that spermidine has anti-inflammatory and anti-oxidative effects in chronic inflammation [49]. Therefore, we investigated whether spermidine influences inflammation processes in *Nr4a1 -/-* mice as well the effects of spermidine in normal B-cell development in bone marrow, spleen and thymus.

2. Material and Methods

2.1. Mouse models

EμMyc transgenic mice as well as the *Nr4a1-/-* mice were bought from Jackson Laboratories (Maine, ME, USA). *EμMyc* transgenic mice were intercrossed with *Nr4a1-/-* mice to create a cohort of *EμMyc Nr4a1-/-* and *EμMyc Nr4a1+/+* mice. The genetic background of all mice was 57BL/6J ("C57 black 6").Health status and the development of lymphomas were controlled three times a week. Mice were sacrificed immediately upon tumor formation and necropsy was performed to determine the conditions of the distinct organs.

All animal experiments were approved by the Austrian Federal Ministry of Science, Research and Economy.

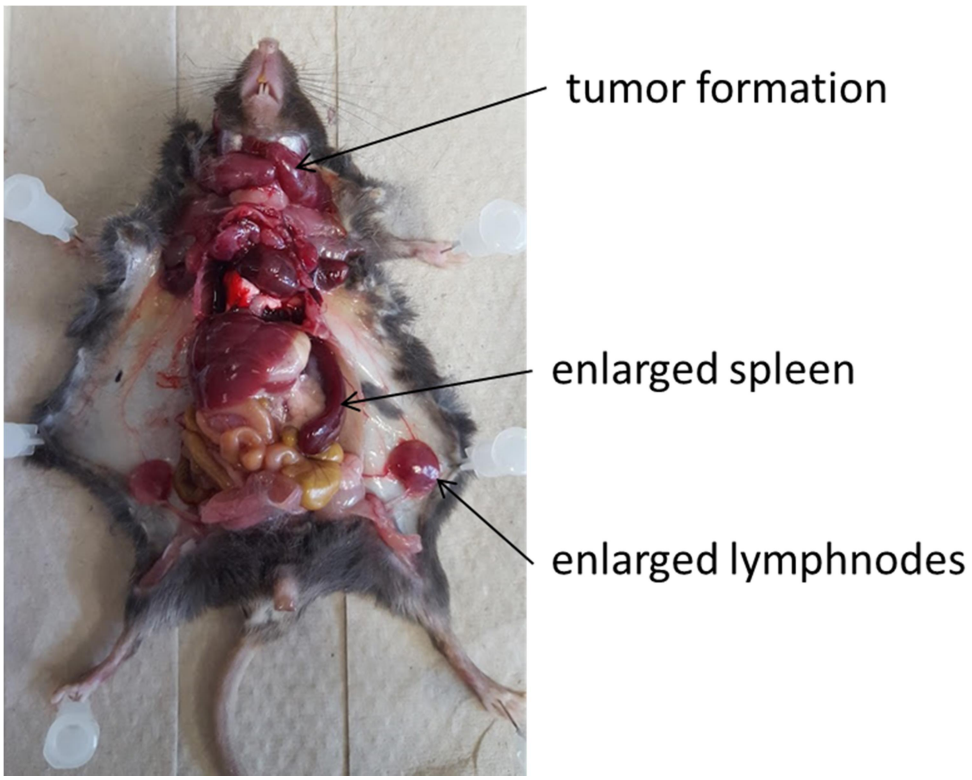

Figure 13: Scarified *EμMyc Nr4a1-/-* mouse with a tumor formation in the area of the neck, enlarged spleen and enlarged lymphnodes
The health status of the mice and signs of possible lymphoma development was controlled three times a week. Unhealthy animals were scarified. A necropsy was performed to determine the physical condition.

2.1.1. *Nr4a1 -/-* mouse

A neomycin resistance gene was integrated in the region encoding the amino-terminal domain of *Nr4a1* by homologous recombination using a targeting vector. Exon 2 was disrupted by the insertion. Homozygous mice with this

targeted mutation are viable, reproductive and do not show gross anatomical and behavioral abnormalities. [39, 80]

2.1.2. *EμMyc* transgenic mice

Transgenic *EμMyc* mice are attractive models to investigate tumor development of the B lymphocyte lineage [81]. They show an increased level of pre-B-cells in the bone marrow during their life and an increase in spontaneous pre-B and B-cell lymphomas. The tumors seem to arise at random from a population of pre-B-cells expanded by constitutive expression of the Myc transgene. 90% develop lymphomas in the first six months of life [20]. Additionally, tumors in *EμMyc* mice typically have a $CD19^+$ IgM^- pre-B-cell or an immature $CD19^+$ IgM^+ B-cell phenotype [82]

2.2. Genotyping

To determine the genotype of the bred mice, mouse tip biopsies were used. DNA was extracted by using the KAPA Express Extract Kit according to the protocol. One negative control - containing reagents only - was included.
The PCR was conducted with KAPA2G Fast Hot Start Kit (KAPA Biosystems, Wilmington) according to the manufacturer's protocol.

Table 1: Primer for the genotyping PCR of *Nr4a1* knockout mice
The oligonucleotides were synthesized by „Eurofins Genomics". Possible bands were obtained at 350bp (mutant), 350 bp and 180 bp (heterozygote) and 180bp (wildtype).

Primer for Nr4a1	Sequence 5' →3'	Primer Type
oIMR 6602	CCA CGT CTT CTT CCT CAT CC	Common
oIMR 6603	TGA GCA GGG ACT GCC ATA GT	Wild type Reverse
oIMR 2060	CAC GAG ACT AGT GAG ACG TG	Mutant

Table 2: Primer for internal positive control
The oligonucleotides were synthesized by „Eurofins Genomics“. Bands were expected at 324bp (internal positive control).

Primer for Internal Control	Sequence 5’ →3’	Primer Type
oIMR 7338	CTA GGC CAC AGA ATT GAA AGA TCT	Internal Positive Control Forward
oIMR 7339	GTA GGT GGA AAT TCT AGC ATC ATC C	Internal Positive Control Reverse

Table 3: Primer for transgene
The oligonucleotides were synthesized by „Eurofins Genomics“.Bands were expected at 210bp (transgene).

Primer for Transgene	Sequence 5’ →3’	Primer Type
14377	TTA GAC GTC AGG TGG CAC TT	Transgene Forward
14378	TGA GCA AAA ACA GGA AGG CA	Transgene Reward

PCR was performed in a Thermal Cycler (Thermo Fisher Scientific, Waltham, MA, USA). PCR program for amplification was chosen with respect to the used primers. (Table 4, Table 5, Table 6).

Table 4: PCR program to amplify *Nr4a1*
The PCR amplification with the primers oIMR 6602, oIMR 6603, oIMR 2060 was done as follow.

Cycler Program for Nr4a1

	Time	Temperature [°C]	Amplification Cycle
Step 1 PCR initial activation step	10 min	95°C	1
Step 2 DNA denaturation	15 sec	94°C	35
Step 3 Annealing	15 sec	62°C	
Step 4 Extension	15 sec	60°C	
Step 5 Final Extension	2 min	72°C	1
Step 6 Hold	∞	4°C	1

Table 5: PCR program to amplify *Eμmyc* as internal positive control
The PCR amplification with the primers olMR 7338 and olMR 7339 was done as follow.

Cycler Program for Eμmyc (Internal Control)

	Time	Temperature [°C]	Amplification Cycle
Step 1 PCR initial activation step	10 min	95°C	1
Step 2 DNA denaturation	20 sec	94°C	10
Step 3 Annealing	15 sec	65°C	
Step 4 Extension	10 sec	68°C	
Step 5 2nd DNA denaturation	15 sec	94°C	28
Step 6 2nd Annealing	15 sec	60°C	
Step 7 2nd Extension	10 sec	72°C	
Step 8 Final Extension	2 min	72°C	1
Step 9 Hold	∞	4°C	1

Table 6: PCR program to amplify the transgene
The PCR amplification with the primers 14378 and 14378 was done as follow.

Cycler Program for Transgene

	Time	Temperature [°C]	Amplification Cycle
Step 1 PCR initial activation step	10 min	95°C	1
Step 2 DNA denaturation	20 sec	94°C	10
Step 3 Annealing	15 sec	65°C	
Step 4 Extension	10 sec	68°C	
Step 5 2nd DNA denaturation	15 sec	94°C	28
Step 6 2nd Annealing	15 sec	60°C	
Step 7 2nd Extension	10 sec	72°C	
Step 8 Final Extension	2 min	72°C	1
Step 9 Hold	∞	4°C	1

PCR products were separated on non-denaturating 3% agarose (Bioenzym, Germany) gels. Detection was done with ChemiDoc Imaging System (Bio-Rad, Hercules, CA, USA).

2.3. Malignant conditions

2.3.1. Expression analysis of *Nr4a1* and *Nr4a3* in B-cell development and lymphomagenesis

To investigate the requirement of *Nr4a1* and *Nr4a3* in different stages of the B-cell development and the effects in *EμMyc* lymphomagenesis a gene expression analysis was done. To study the mRNA expression of *Nr4a1* and *Nr4a3* of B-cell subpopulation in total 15 mice were analyzed. Bone marrow cells of *Nr4a1* -/- (n=5), *Nr4a1* +/+ (n=3), *EμMyc Nr4a1* -/- (n=3), and *EμMyc Nr4a1* +/+ (n=4) mice aged 4 weeks were used.

Cells were stained with antibodies against cell surface markers (CD19-PE, IgM-FITC, CD43-APC) and sorted in Pro-B ($CD19^+/CD43^+/IgM^-$), Pre-B ($CD19^+/CD43^-/IgM^-$) and more differentiated B ($CD19^+/IgM^+$) B-cells (Table 7). Cells were sorted using a FACSAria™ III (BD Bioscience, CA, USA).

Table 7: Panel for B-cell sorting
Cells were sorted in Pro-B ($CD19^+/CdD43^+/IgM^-$), Pre-B ($Cd19^+/Cd43^-/IgM^-$) and more differentiated B ($Cd19^+/IgM^+$) B-cells from bone marrow.

Antibody	Clone	Company	Catalog number	µl/100µl sample
CD19-PE	MB19-1	eBioscience™	12-0191-82	0,5
IgM-FITC	II/41	BD Bioscience	553437	0,5
CD43-APC	S7	BD Bioscience	560663	0,125

Total RNA was extracted by using the Maxwell® 16 LEV simply RNA Cells Kit (Promega, Madison, WI, USA) according to the manufacturer's protocol. The extractions were performed on Promega's robotics platform, AS2000 Maxwell® 16 (Promega, Madison, WI, USA).

RNA was transcribed into cDNA by using "RevertAid RT Reverse Transcription Kit" from Thermo Scientific (Thermo Fisher Scientific, Waltham, MA, USA) according to the manufacturer's instructions.

The Real-Time PCR was carried out in a Bio-Rad CFX96 Touch™ Real-Time PCR Detection System (Bio-Rad, Hercules, CA, USA). All samples were assayed in duplicates. *TATA-Box Binding Protein (TBP), hypoxanthine Phosphoribosyltransferase 1 (HPRT1)* and *peptidylprolyl Isomerase A (PPIA)* served as housekeeping genes. All primers that were used were QuantiTect Primer Assays (Qiagen, Hilden, Germany) (Table 8).

Table 8: Used Primer Assays
Different genes for expression study are listed. *Tbp*, *Hprt*, *Actb* and *Ppia* are housekeeping genes which are used as endogenous controls.

Gene	Alternative Name	Assay name	Catalog number
Tbp	TATA-Box Binding Protein	Mn_Tbp_1_SG	QT00198443
Hprt	Hypoxanthine Phosphoribosyltransferase 1	Mn_Hprt_1_SG	QT00166768
Ppia	Peptidylprolyl Isomerase A	Mn_Ppia_1_SG	QT00247709
Actb	β-Actin	Mn_Actb_1_SG	QT00095242
Nr4a1	Nuclear Receptor Subfamily 4 Group A Member 1	Mn_Nr4a1_1_SG	QT00101017
Nr4a3	Nuclear Receptor Subfamily 4 Group A Member 3	Mn_Nr4a3_1_SG	QT00145873

The following cycling protocol was used: Activation at the initial step (stage 1) at 95°C, followed by a denaturation step (stage 2) for 5 seconds at 95°C and an annealing/extension step (stage3) for 10 seconds at 60°C. The program was repeated for 34 cycles. Between these repeats the plate was read. Melt curve analysis (stage 4 and 5) was used to identify the different reaction products including nonspecific products (Table 9).

Table 9: Thermal cycler amplification program for Real-Time PCR is separated in different steps
Stage 1 activates DNA-Polymerase, followed by DNA denaturation and annealing/extension at stage 2 and 3. This is repeated for 34 cycles. The plate will be read between these steps. In addition a melt curve analysis will be performed at stage 4 and 5.

Step	**Time**	**Temperature [°C]**	**Amplification Cycle**
Stage 1 PCR initial activation step	2 min	95°C	1
Stage 2 DNA denaturation	5 sec	95°C	34
Stage 3 Combined annealing/extension	10 sec	60°C	
Stage 4 Melt curve analysis	5 sec	95°C	1
Stage 5 Melt curve analyses	5 sec	60°C	1

Differences in gene expression were calculated with the $2^{-\Delta\Delta Ct}$ method. Thereby, the expression of *Nr4a1* and *Nr4a3* was elicited by comparing the obtained expression profile with several housekeeping genes (*Tbp, Hprt, Ppia, Actb.)* The comparison of expression levels was done by using Mann-Whitney U-test.

2.3.2. 2nd hit analysis, cleavage of Parp and Irf-4 expression

For western blot analysis cryopreserved tumor tissue of a cohort of *EμMyc Nr4a1 -/-* (n=17) and *EμMyc Nr4a1 +/+* (n=20) mice displaying no IgM (IgM^-), as well as *EμMyc Nr4a1 -/-* (n=12) and *EμMyc Nr4a1 +/+* (n=17) with IgM (IgM^+) on the cell surface were processed. Hence, the expression of IgM in tumors was used as a marker according to their differentiation status. To analyze proteins through antibody detection Western blots were used. Tumors were compared to examine whether a dysregulation p19Arf-Mdm2-p53 pathway and/or overexpression of proteins involved in mitochondrial pathway like Bcl-2, Bim, Bcl-xl and Mcl-1 is needed for second hit for a malignant transformation in the *EμMyc Nr4a1-/-* mouse model. Additionally, Irf-4 and Parp were investigated by Westen blot analysis to determine the influence of Nr4a1 loss on NF-κB signaling and activation of apoptosis.

The frozen tumor tissue samples were resuspended in RIPA buffer (Sigma-Aldrich, Germany) with the addition of 1x Halt™ Protease Inhibitor Cocktail (100X; Thermo Fisher Scientific, Waltham, MA, USA). Tissue samples were frozen in liquid nitrogen and afterwards thawed. This process was repeated thrice.

Protein concentrations were determined using Lowry Protein Assay according to the protocol from Bio-Rad “Bio-Rad Protein Assay (Lowry)”. The measurement was done by using the SpectraMax device (Molecular Devices, Sunnyvale, CA, USA). Protein lysates were diluted 1:17 in 2x Laemmli Sample Buffer (Bio-Rad, Hercules, CA, USA) with 2-Mercaptoethanol (Sigma-Aldrich GmbH, Deutschland). To ensure protein denaturation samples were degraded at 95°C. For Western Blot the Mini-PROTEAN® Tetra Cell System (Bio-Rad, Hercules, CA, USA) was used. 20 µg of protein lysates per lane, along with the molecular weight marker, Precision Plus Protein Dual Color Standard (Bio-Rad, Hercules, CA, USA), were separated in 1xTGS (Bio-Rad, Hercules, CA, USA) at 90V, constant voltage for about 1 ½ hours on SDS-PAGE gel. 15% (w/v) polyacrylamide gels were used for following antibodies: Ppia, Gapdh, β-Actin, Irf-4, Bim, Mdm2, p19Arf, p53, Bcl-2. 10% (w/v) polyacrylamide gels were used for following antibodies: Bcl-XL, Parp, Gapdh.
After electrophoresis, protein were transferred to PDVF membranes (Bio-Rad, Hercules, CA, USA) at 400mA constant current for 1 ½ hours at 4°C.

To prevent unspecific binding of antibodies the membrane was incubated in 5% (w/v) non-fat dry milk with TBS (Tris-buffered saline) (Bio-Rad, Hercules, CA, USA) and 1% Tween 20 (Croda International PLC, Snaith, UK) for one hour at room temperature. Antibodies were used according to the manufacturer's instructions. The primary antibody (Table 10) was prepared in 5% bovine serum albumin (GE Healthcare, Little Chalfont, UK) or 5% non-fat dry milk powder (Bio-Rad, Hercules, CA, USA). The membranes were incubated over night at 4°C

Table 10: List of primary antibodies
Antibodies were used according to the manufacturer's instructions. The membranes were incubated over night at 4°C.

1st Antibody	Company	Catalog number	Molecular Weight	5% BSA or nonfat dry milk	Dilution	2nd Antibody
β-Actin (13E5)	Cell Signaling Technology	#4970	45 kDa	BSA	1:1000	Anti-rabbit
Cyclophilin A (D2Y4M)	Cell Signaling Technology	#51418	18 kDa	BSA	1:1000	Anti-rabbit
GAPDH (14C10)	Cell Signaling Technology	#2118	37 kDa	BSA	1:1000	Anti-rabbit
p53 (1C12)	Cell Signaling Technology	#2524	52 kDa	nonfat dry milk	1:1000	Anti-mouse
Mcl-1 (D2W9E)	Cell Signaling Technology	#94296	35 kDa	BSA	1:1000	Anti-rabbit
PARP Antibody	Cell Signaling Technology	#9542	89, 116 kDa	nonfat dry milk	1:1000	Anti-rabbit
Bcl-2 (D17C4)	Cell Signaling Technology	#3498	26 kDa	BSA	1:1000	Anti-rabbit
Bim (C34C5)	Cell Signaling Technology	#2933	12, 15, 23 kDa	BSA	1:1000	Anti-rabbit
Bcl-XL (54H6)	Cell Signaling Technology	#2764	30 kDa	nonfat dry milk	1:1000	Anti-rabbit
p19 ARF (5-C3-1)	Santa Cruz Biotechnology	sc-32748	19 kDa	nonfat dry milk	1:200	Anti-rat
MDM2 (SMP14)	Invitrogen	MA1-23318	90 kDa	nonfat dry milk	1:400	Anti-mouse

Signal amplification was performed by incubation with HRP-labeled secondary antibodies for one hour at room temperature. The secondary antibodies (Table 11) were diluted in TBST with 5% non-fat dry milk powder.

Table 11: List of secondary antibodies
HRP-conjugated antibodies were used according to the manufacturer's instructions. The membranes were incubated for one hour at room temperature.

2nd Antibody	Company	Catalog number	5% w/v nonfat dry milk	Dilution
Anti-rabbit	Cell Signaling Technology	#7074	nonfat dry milk	1:1000
Anti-mouse	Cell Signaling Technology	#7076	nonfat dry milk	1:100
Anti-rat	Cell Signaling Technology	#7077	nonfat dry milk	1:100

Signals were detected with fresh prepared WesternBright ECL HRP substrate (Advansta, Menlo Park, CA, USA) according to the manufacturer's instructions on a ChemiDoc Imaging System (Bio-Rad, Hercules, CA, USA). ImageJ software (Bio-Rad, Hercules, CA, USA) was used for quantification of the signals.

2.3.3. Expression analysis of miRNA in aggressive B-cell lymphomas

To investigate the expression of six miRNAs and their influence on *NR4A1* and *NR4A3,* a comprehensive study in human aggressive B-cells lymphomas with a cohort of 68 human samples sub classified into GCB-DLBCL, non-GCB-DLBCL as well as follicular lymphoma grade 3 (FLIII) (Table 12) was performed by using real-time PCR.

Table 12: Subclassification and number of aggressive human lymphoma samples used

lymphoma samples	number
non-GCB DLBCL	25
GCB-DLBCL	23
FLIII	20

Total RNA extraction from human aggressive lymphoma samples was performed according to the manufacturer's using the miRNeasy Mini Kit (Qiagen, Hilden, Germany). cDNA was reverse transcribed using "miScript II

RT Kit" from Qiagen (Qiagen, Hilden, Germany) according to manufacturer's protocol.

Real-time PCR amplification was performed in 2x GoTaq® qPCR Master Mix for Dye-Based Detection (Promega, WI, USA) in combination with QuantiTect Primer Assays (Qiagen, Hilden, Germany) (Table 13). All samples were assayed in duplicates. *RNU6B (*RNA, U6 Small Nuclear 2*)* and *SNOR68 (*small nucleolar RNA R68) were used as endogenous controls for miRNA expression. The results of the real-Time PCR were quantified via the Bio-Rad CFX96 Touch™ Real-Time PCR Detection System (Bio-Rad, Hercules, CA, USA).

Table 13: Used Primer Assays
Different genes for expression study are listed. *SNORD68 and RNU6* are housekeeping genes which are used as endogenous controls.

Gene	Assay name
SNORD68	HS_SNORD68_11
RNU6	HS_RNU6_2_11
miR-224	HS_miR_224_1
*miR-224**	HS_miR_224*_2
miR-20	HS_mirR_20a_1
miR-17	HS_miR_17_2
miR-15	HS_miR_15a_1
*miR-15**	HS_miR_15a*_2

The thermal cycling conditions were the initial step at 95°C for 2 minutes to activate the HotStartTaq DNA Polymerase, followed by 40 cycles consisting DNA denaturation at 95°C for 3 seconds, annealing of primers and extension at 60°C for 30 seconds and finally dissociation at 95°C for 5 minutes.

By using the comparative Ct method ($2^{-\Delta\Delta CT}$ method) the fold-change was calculated. The comparison of expression levels was done by using Mann-Whitney

2.4. Non-malignant conditions

2.4.1. Expression analysis of potential *Nr4a1* target genes

A cohort of *Nr4a1 -/-* mice and *Nr4a1 +/+* mice (Table 14) was generated and sacrificed to investigate the function of *Nr4a1* in gene regulation as transcription factor under non-malignant conditions. For this study the spleens of a cohort of *Nr4a1 -/-* (n=8) and *Nr4a1 +/+* (n= 2) mice, aged 12-16 weeks, of a cohort *Nr4a1 -/-* (n=5) and *Nr4a1 +/+* (n= 8) mice, aged 30-35 weeks, and *Nr4a1 -/-* (n=5) and *Nr4a1 +/+* (n= 2), aged 52-62 weeks, were used.

Table 14: Classification in age, subtype and follicular hyperplasia in mice spleens

12-16 weeks		normal	follicular hyperplasia	in total
subtype	*Nr4a1 -/-*	7	1	8
	Nr4a1 +/+	2	0	2

30-35 weeks		normal	follicular hyperplasia	in total
subtype	*Nr4a1 -/-*	1	4	5
	Nr4a1 +/+	7	1	8

52-62 weeks		normal	follicular hyperplasia	in total
subtype	*Nr4a1 -/-*	1	4	5
	Nr4a1 +/+	2	0	2

For study of thymus and splenic B-and T-cells a cohort of *Nr4a1 -/-* (n=4) and *Nr4a1 +/+* (n= 4) mice, aged 18-21 weeks, was used. Mice were sacrificed and desired tissues were removed.

Total RNA extraction from *Nr4a1 -/-* and *Nr4a1 +/+* tissue samples was done according to the manufacturer's protocol using the Qiagen "RNeasy Mini Kit".

The removal of genomic DNA from RNA preparations was done by using RNase-free DNase set from Thermo Scientific (Thermo Fisher Scientific, Waltham, MA, USA) according to the manufacturer's instructions.

Total RNA was transcript in cDNA by using "RevertAid RT Reverse Transcription Kit" from Thermo Scientific (Thermo Fisher Scientific, Waltham, MA, USA) according to the manufacturer's instructions.

The Real-Time PCR was performed according to the protocol from “QuantiNova SYBR Green PCR Handbook”. The Real-Time PCR was carried out in a Bio-Rad CFX96 Touch™ Real-Time PCR Detection System (Bio-Rad, Hercules, CA, USA). All samples were assayed in duplicates. *TATA-Box Binding Protein (TBP), hypoxanthine Phosphoribosyltransferase 1 (HPRT1)* and *peptidylprolyl Isomerase A (PPIA)* served as housekeeping genes. All primers that were used are QuantiTect Primer Assays (Qiagen, Hilden, Germany) (Table 15).

Table 15: Used Primer Assays
Different genes for expression study are listed. *Tbp*, *Hprt*, *Actb* and *Ppia* are housekeeping genes which are used as endogenous controls.

Gene	Alternative Name	Assay name	Catalog number
Tbp	TATA-Box Binding Protein	Mn_Tbp_1_SG	QT00198443
Hprt	Hypoxanthine Phosphoribosyltransferase 1	Mn_Hprt_1_SG	QT00166768
Ppia	Peptidylprolyl Isomerase A	Mn_Ppia_1_SG	QT00247709
Actb	β-Actin	Mn_Actb_1_SG	QT00095242
Cdkn2a	Cyclin-Dependent Kinase Inhibitor 2A	Mn_Cdkn2a_1_SG	QT00252595
Bcl2a1a	B-cell leukemia/lymphoma 2 related protein A1a	Mn_Bcl2a1a_1_SG	QT00142016
Bcl2a1d	B-cell leukemia/lymphoma 2 related protein A1d	Mn_Bcl2a1d_1_SG	QT00136465
Tnfsf11	Tumor Necrosis Factor Superfamily Member 11	Mn_Tnfsf11_1_SG	QT00147385
S1pr5	Sphingosine-1-Phosphate Receptor 5	Mn_S1pr5_1_SG	QT00282744
Klcr2	Killer Cell Lectin Like Receptor C2	Mn_Klrc2_1_SG	QT001781843
Klra17	Killer Cell Lectin-Like Receptor A	Mn_Klra17_1_SG	QT00137620
Cd226	CD226 Antigen	Mn_Cd226_1_SG	QT01062187
Tnfrsf8	Tumor Necrosis Factor Receptor Superfamily Member 8	Mn_Tnfrsf8_1_SG	QT00116599
Dll1	Delta-Like 1 (Drosophila)	Mn_Dll1_1_SG	QT00113239
Gata3	GATA binding protein 3	Mn_Gata3_1_SG	QT00170828
Ccl22	C-C Motif Chemokine Ligand 22	Mn_Ccl22_1_SG	QT00108031
Il12b	Interleukin 12B	Mn_Il12b_1_SG	QT00153643
Ptgs2	prostaglandin-endoperoxide synthase 2 (COX2)	Mn_Ptgs2_1_SG	QT00165347
S100a4	S100 Calcium Binding Protein A4	Mn_S100a_1_SG	QT00107632
Tnfaip3	Tumor Necrosis Factor, Alpha-Induced Protein 3	Mn_Tnfaip3_1_SG	QT00134064
Cflar	CASP8 And FADD Like Apoptosis Regulator	Mn_Cflar_1_SG	QT00171738

Bcl2	B-Cell CLL/Lymphoma 2	Mn_Bcl2_1_SG	QT00156282
Ccnd1	Cyclin D1	Mn_Ccnd1_1_SG	QT00154595
IRF-4	Interferon Regulatory Factor 4	Mn_IRF-4_1_SG	QT00109984
Ccr7	C-C Motif Chemokine Receptor 7	Mn_Ccr7_1_SG	QT00240975
Cd96	CD96 Molecule	Mn_Cd96_1_SG	QT00112959
Aicda	Activation Induced Cytidine Deaminase	Mm_Aicda_1_SG	QT00123676
Ccl20	C-C Motif Chemokine Ligand 20	Mn_Icos_1_SG	QT00261898
Icos	Inducible T-Cell Costimulator	Mn_Icos_1_SG	QT00131579
Cd27	CD27 Molecule	Mm_Cd27_1_SG	QT01077608
Sox2	SRY-Box 2	Mm_Sox2_1_SG	QT00249347
Cda1	Cytidine Deaminase 1	Mm_Cda_1_SG	QT00263893
Havcr1	Hepatitis A Virus Cellular Receptor 1	Mn_Havcr1_1_SG	QT00112427
Havcr2	Hepatitis A Virus Cellular Receptor 2	Mm_Havcr2_1_SG	QT00112427
Il7	Interleukin 7	Mn_Il7_1_SG	QT00101318
Gcsam	Germinal Center Associated Signaling And Motility	Mn_Gcsam_1_SG	QT00113225
Pdcd1	Programmed Cell Death 1	Mm_Pdcd1_1_SG	QT00111111
Pdcd1lg2	Programmed Cell Death 1 Ligand 2	Mm_Pdcd1lg2_1_SG	QT00136640

The following cycling protocol was done: Activation at the initial step (stage 1) at 95°C, followed by a denaturation step (stage 2) for 5 seconds at 95°C and an annealing/extension step (stage3) for 10 seconds at 60°C. The program was repeated for 34 cycles. Between these repeats the plate was read. Melt curve analysis (stage 4 and 5) was used to identify the different reaction products including nonspecific products (Table 16)

Table 16: Thermal cycler amplification program for Real-Time PCR is separated in different steps
Stage 1 activates DNA-Polymerase, followed by DNA denaturation and annealing/extension at stage 2 and 3. This is repeated for 34 cycles. The plate will be read between these steps. In addition a melt curve analysis will be performed at stage 4 and 5.

Step	Time	Temperature [°C]	Amplification Cycle
Stage 1 PCR initial activation step	2 min	95°C	1
Stage 2 DNA denaturation	5 sec	95°C	34
Stage 3 Combined annealing/extension	10 sec	60°C	
Stage 4 Melt curve analysis	5 sec	95°C	1
Stage 5 Melt curve analyses	5 sec	60°C	1

The expression levels were calculated based on the $2^{-\Delta\Delta CT}$ method. After that the Mann-Whitney U-test was performed to show the statistical difference between the expressions of your genes.

2.5. Effects of spermidine in Nr4a1-/- mice and on B-cell development

A cohort of *Nr4a1 -/-* (n=5) and *Nr4a1 +/+* (n=15) mice were fed with drinking water supplemented with 3mM spermidine from 6 weeks on and sacrificed after 30 weeks. Another cohort of *Nr4a1 -/-* (n=6) and *Nr4a1 +/+* (n=4) mice were fed with normal drinking water and were sacrificed after 30 weeks.

Proinflammatory cytokines of 5 *Nr4a1 -/-* mice with spermidine administration-, 4 *Nr4a1 -/-* and 6 *Nr4a1 +/+* mice were determined by using the V-PLEX Plus Proinflammatory Panel1 Mouse Kit (Meso Scale Discovery, Rockville, Maryland, USA).

Prepared isolated cells were stained with cell surface marker antibodies. Cell suspensions from thymus, spleen and bone marrow were stained with antibody panels 1-4 (Table 17, Table 18, Table 19, Table 20). Additionally, panel 5 and 6 were done with spleen only (Table 21, Table 22).

Table 17: Panel 1
The panel was designed to identify the Pro-, Pre-, Immature, Transitional as well Early Mature und Late Mature B-cells

Antibody	Clone	Company	Catalog number	µl/100µl sample
Ly-6C (GR-1) - PE	AL-21	BD Bioscience	560592	0,033333
CD127 - PE-Cy™7	SB/199	BD Bioscience	560733	0,5
CD43 - APC	S7	BD Bioscience	560663	0,125
IgD - BV605	11-26c.2a	BD Bioscience	563003	0,1
IgM - FITC	II/41	BD Bioscience	553437	0,5
CD24 - BV421	M1/69	BD Bioscience	562563	0,025
CD45R (B220) - APC-Cy™7	RA3-6B2	BD Bioscience	552094	1
CD93 - PerCP-Cyanine5.5	AA4.1	eBioscience™	45-5892-82	2

Table 18: Panel 2
The panel was designed to identify the T1-, T2-, T3- and FO and MZ B-cells

Antibody	Clone	Company	Catalog number	µl/100µl sample
CD45R (B220) - APC-Cy™7	RA3-6B2	BD Bioscience	552094	1
CD19 - PE	MB19-1	eBioscience™	12-0191-82	0,5
CD23 - PE-Cyanine7	B3B4	eBioscience™	25-0232-82	0,2
CD24 - FITC	30-F1	eBioscience™	11-0241-85	1
CD21/CD35 - APC	7G6	BD Bioscience	558658	0,3
IgM - eFluor 450	II/41	eBioscience™	48-5790-82	0,25
IgD - BV605	11-26c.2a	BD Bioscience	563003	0,1
CD93 - PerCP-Cyanine5.5	AA4.1	eBioscience™	45-5892-82	2

Table 19: Panel 3
The panel was designed to identify $B220^+$, $B220^+$ IgM^+ and PrePro B-cells

Antibody	Clone	Company	Catalog number	µl/100µl sample
CD19 - BV510	1D3	BD Bioscience	562956	0,3
Ly-6C (GR-1) - PE	AL-21	BD Bioscience	560592	0,033333
CD127 - PE-Cy™7	SB/199	BD Bioscience	560733	0,5
CD45R (B220) - APC-Cy™7	RA3-6B2	BioLegend	103212	0,3
IgM - eFluor 450	II/41	eBioscience™	48-5790-82	0,25
CD93 - PerCP-Cyanine5.5	AA4.1	eBioscience™	45-5892-82	2

Table 20: Panel 4
The panel was designed to identify different T cells (TCR^+, $CD4^+$, $C8^+$, $CD4^-CD8^-$, $CD4^+CD8^+$).

Antibody	Clone	Company	Catalog number	µl/100µl sample
CD19 - PE	MB19-1	eBioscience™	12-0191-82	0,5
CD4 - PerCP/Cy5.5	GK1.5	BioLegend	100434	0,4
CD8a - APC	53-6,7	eBioscience™	17-0081-83	0,05
TCR - FITC	H57-597	eBioscience™	11-5961-85	0,2
IgM - eFluor 450	II/41	eBioscience™	48-5790-82	0,25
IgD - BV605	11-26c.2a	BD Bioscience	563003	0,1
CD45R (B220) - APC-Cy™7	RA3-6B2	BD Bioscience	552094	1

Table 21: Panel 5
The panel was designed to identify B-1a and T1/B1-b B-cells.

Antibody	Clone	Company	Catalog number	µl/100µl sample
CD19 - PE	MB19-1	eBioscience™	12-0191-82	0,5
IgM - eFluor 450	II/41	eBioscience™	48-5790-82	0,25
IgD - BV605	11-26c.2a	BD Bioscience	563003	0,1
CD45R/B220 - APC	RA3-6B2	BioLegend	103212	0,3
CD5 - PE-Cyanine7	53-7,3	eBioscience™	25-0051-81	0,075
Ly-6A/E (Sca-1) - FITC	E13-161.7	BioLegend	122506	0,075

Table 22: Panel 6
The panel was designed to identify GC and PC B-cells.

Antibody	Clone	Company	Catalog number	µl/100µl sample
CD45R (B220) - APC-Cy™7	RA3-6B2	BD Bioscience	552094	1
CD19 - PE	MB19-1	eBioscience™	12-0191-82	0,5
CD38 - BV421	90/CD38	BD Bioscience	562768	0,05
CD138 - APC	281-2	BD Bioscience	558626	0,5
CD95 (Fas) - FITC	Jo2 (RUO)	BD Bioscience	554257	6

FACS analyses were performed on CytoFLEX S (Beckman Coulter, Krefeld, Germany) and data analysis was done with Kaluza Software. After that the Student's T-test was performed to show the statistical difference.

2.6. Statistical analysis

All statistical analyses were performed using IBM Statistical Package of Social Sciences (SPSS) 21.0 (SPPS Inc, IL, USA). A p-value ≤ 0.05 was considered to indicate a significant difference. All estimated values are presented as mean values and error bars represent the standard error of the mean. "*" indicates p<0,05.

3. Results

3.1. Nr4a1 in lymphomagenesis

3.1.1. Expression analysis of *Nr4a1* and *Nr4a3* in B-cell development and lymphomagenesis

To investigate the function of *Nr4a1* and *Nr4a3* in B-cell development and in *EμMyc*-driven lymphomagenesis, we determined the expression levels in FACS-sorted IgM^- - immature B-cells consisting of Pro- and Pre-B-cells - and IgM^+ - mature- B-cells - isolated from the bone marrow of 6 weeks old *Nr4a1 -/-* and *Nr4a1 +/+* mice and *EμMyc Nr4a1 -/-* and *EμMyc Nr4a1 +/+* mice at the premalignant stage by using semiquantitive Real-time PCR. Furthermore, *Nr4a1* and *Nr4a3* expression pattern of these non-malignant or premalignant cells were compared to those of *Myc*-induced lymphomas derived from *EμMyc Nr4a1 -/-* and *EμMyc Nr4a1 +/+* mice.

In *Nr4a1 +/+* and in premalignant *EμMyc Nr4a1 +/+* mice, *Nr4a1* was equally expressed in IgM^+ and IgM^- B-cells. No difference was detected in the comparison of *Nr4a1+/+* and premalignant *EμMyc Nr4a1 +/+* mice in both B-cell subtypes (Figure 14). As expected *Nr4a1* mRNA levels were significantly lower expressed in IgM- and IgM+ B-cells of *Nr4a1 -/-* and premalignant *EμMyc Nr4a1 -/-* mice compared to Nr4a1 +/+ and in premalignant *EμMycNr4a1 +/+* mice ($p<0,042$, Figure 14). By comparing *Nr4a1* expression levels of IgM^- lymphomas derived from *EμMyc Nr4a1 +/+* mice to their non-neoplastic controls - IgM^- B-cells isolated from *Nr4a1 +/+* mice - revealed a 3.4 fold lower expression of *Nr4a1* in tumor samples ($p=0.045$, Figure 14). Additionally, IgM^- lymphomas derived from *EμMyc Nr4a1 -/-* mice exhibited a 1,2 fold lower expression compared to IgM^- B-cell isolated from premalignant *EμMyc Nr4a1 -/-* mice ($p=0,024$,Figure 14). In IgM^+ lymphomas derived from *EμMyc Nr4a1 +/+* mice, *Nr4a1* was 6,8 fold lower expressed compared to *Nr4a1 +/+* IgM^+ B-cells ($p=0.08$, Figure 14). No difference in the expression of *Nr4a1* was detectable between IgM^+ lymphomas derived from *EμMyc Nr4a1 +/+* mice compared to IgM^+ B-cells of premalignant *EμMyc Nr4a1 +/+* mice.

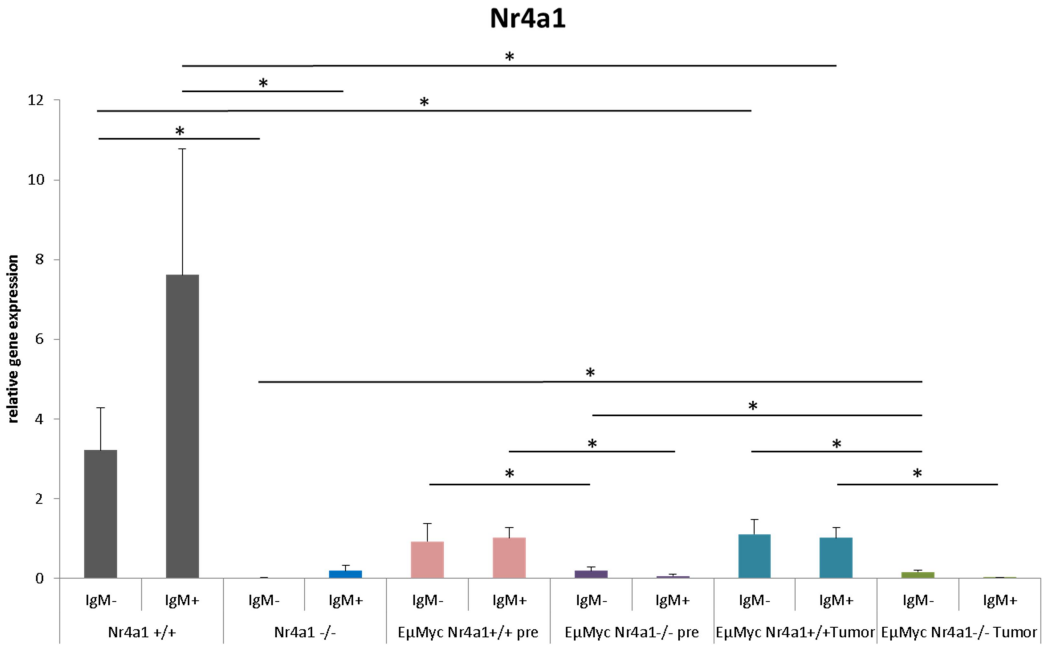

Figure 14: *Nr4a1* in IgM$^-$ and IgM$^+$ B-cells and lymphomas
Quantitative real-time PCR analysis of the expression of *Nr4a1* of cells with immunophenotypes IgM$^+$ and IgM$^-$ isolated from *Nr4a1 +/+*, *Nr4a1 -/-*, premaligne *EμMyc Nr4a1 -/-* and *EμMyc Nr4a1 +/+* mice as well of tumors derived from *EμMyc Nr4a1 -/- and EμMyc Nr4a1 +/+* mice. Each bar represents the mean values of *Nr4a1* mRNA expression levels and error bar indicates the standard error of the mean. *: p<0,05.

In *Nr4a1 +/+* and in premalignant *EμMyc Nr4a1 +/+* mice, *Nr4a3* was equally expressed in IgM$^+$ and IgM$^-$ B-cells depicted in Figure 15. Comparison of *Nr4a3* expression levels of IgM$^-$ B-cells from premalignant *EμMyc Nr4a1 +/+* mice to IgM$^-$ B-cells isolated from premalignant *EμMyc Nr4a1 -/-* mice revealed a 34 fold higher expression of *Nr4a3* in premalignant *EμMyc Nr4a1 -/-* mice (p=0.027, Figure 15). Additionally, IgM$^+$ B-cells from premalignant *EμMyc Nr4a1 +/+* mice exhibited a 3,8 fold lower expression compared to IgM$^+$ B-cell isolated from premalignant *EμMycNr4a1 -/-* mice (p=0,034, Figure 15). Comparison of *Nr4a3* expression levels of IgM$^-$ B-cells of premalignant *EμMyc Nr4a1 +/+* mice to lymphomas derived from IgM$^-$ *EμMycNr4a1 +/+* mice revealed a 10 fold lower expression of *Nr4a3* in premalignant IgM$^-$ B-cells (p=0,013, Figure 15). A trend to significance in the expression of *Nr4a3* was detectable between IgM$^+$ lymphomas derived from *EμMyc Nr4a1 +/+* mice compared to IgM$^+$ B-cells of premalignant *EμMyc Nr4a1 +/+* mice (p=0,057, Figure 15). Remarkable, the expression of *Nr4a3* was 4 fold lower in IgM$^-$ lymphomas derived from *EμMyc Nr4a1 +/+* compared to *EμMyc Nr4a1 -/-* mice (p=0,015, Figure 15). In contrast, no difference was detectable in IgM$^+$ lymphomas derived from *EμMyc Nr4a1 +/+* compared to *EμMyc Nr4a1 -/-* mice.

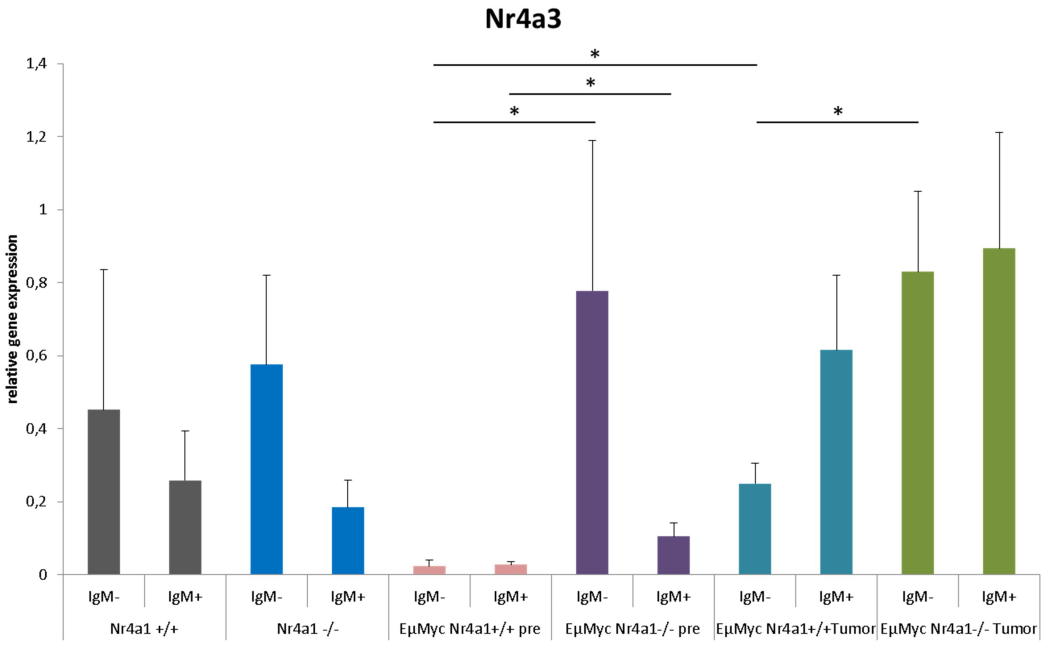

Figure 15: *Nr4a3* in IgM$^-$ and IgM$^+$ B-cells and lymphomas.
Quantitative real-time PCR analysis of the expression of *Nr4a3* of cells with immunophenotypes IgM$^+$ and IgM$^-$ isolated from *Nr4a1 +/+, Nr4a1 -/-,* premaligne *EμMyc Nr4a1 -/-* and *EμMyc Nr4a1 +/+* mice as well of tumors derived from *EμMyc Nr4a1 -/- and .EμMyc Nr4a1 +/+* mice. Each bar represents the mean values of *Nr4a1* mRNA expression levels and error bar indicates the standard error of the mean. *: p<0,05.

3.1.2. 2nd hit analysis, cleavage of Parp and IRF4 expression

In *EμMyc* transgenic mice a concomitant genetic hit - disruption of the p19ARF-MDM2-p53 pathway and/or over-expression of BCL-2, MCL-1, or BCL-xL- is needed to counteract the apoptotic effects of *Myc* [81, 83]. To investigate whether these genetic hits are needed as a second hit for a malignant transformation in the *EμMyc Nr4a1 -/-* mouse model, we performed Western blot analysis of p19Arf, p53, Bcl-2, Bim, Bcl-xl and Mcl-1 by using lymphoma tissue derived from a cohort of 17 *EμMyc Nr4a1 -/-* and 20 *EμMyc Nr4a1 +/+* mice of the IgM- phenotype, as well as 12 *EμMyc Nr4a1 -/-* and 17 *EμMyc Nr4a1 +/+* of the IgM+ phenotype.

In tumors derived from *EμMyc Nr4a1 -/-* mice p53 and p19Arf was significantly lower expressed compared to *EμMyc Nr4a1 +/+* mice (p=0,042, Figure 16a+b). Additionally, the incidence of p53 and p19Arf overexpression was significantly lower in *EμMyc Nr4a1 -/-* tumors compared to *EμMyc Nr4a1 +/+* (4 of 24 vs. 13 of 25, p=0,045).

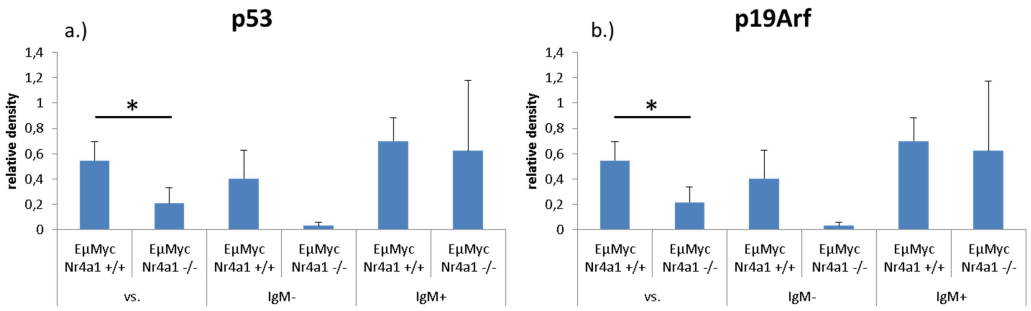

Figure 16: Relative density of p53 and p19Arf
The density was calculated using ImageJ. Data were normalized to the loading control. The bar charts show the mean and standard error of the mean. *: p<0,05.

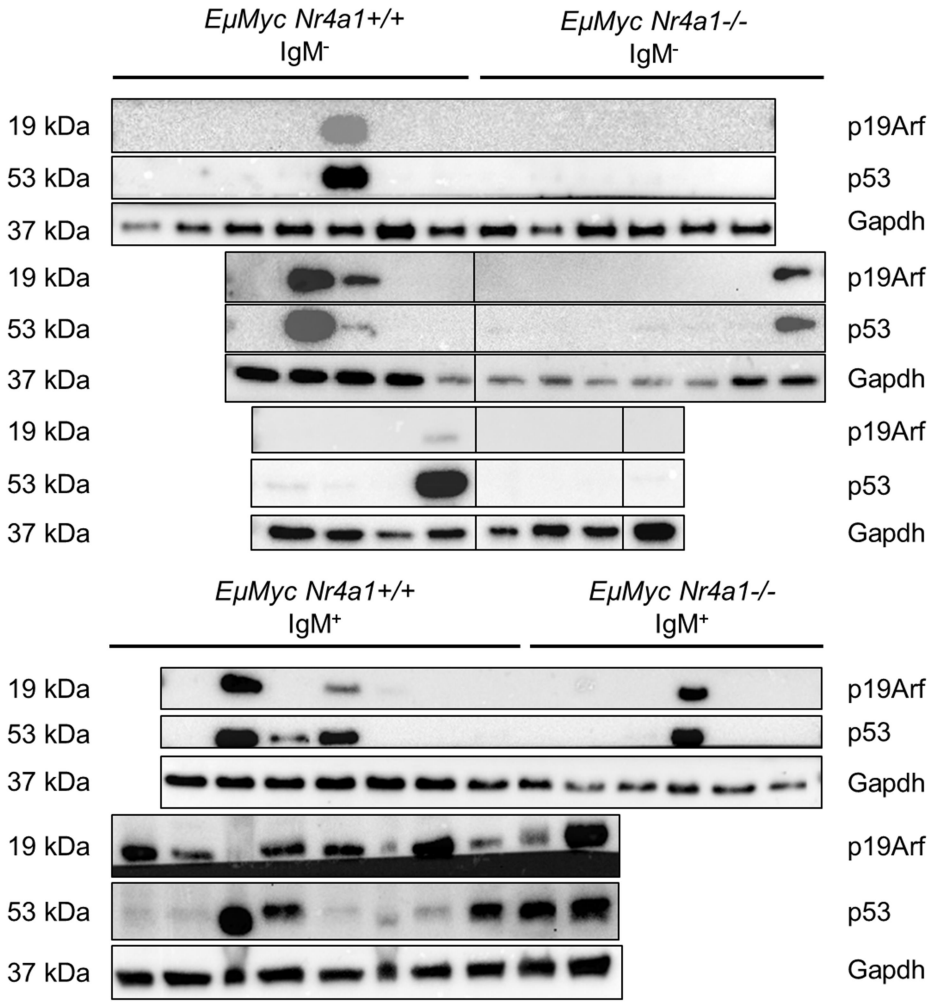

Figure 17: Western blot analysis of p19Arf and p53 expression with their loading control Gapdh
Tumors with IgM^+/IgM^- phenotype derived from *EμMyc Nr4a1 +/+* and *EμMyc Nr4a1 -/-* were analysed for p53 and p19Arf protein expression. Gapdh served as loading control.

No significant protein expressions were detectable in Bcl-2 and Bcl-XL (Figure 18 a+b). Bim_{EL} was significant lower expressed in tumors derived from *EμMyc Nr4a1 -/-* mice compared to *EμMyc Nr4a1 +/+* independent of their immunophenotype ($p<0,025$). In splicing forms Bim_L and Bim_S were no significant differences detectable (Figure 18c). Quantification of Mcl-1 protein amounts showed a lower expression of Mcl-1 protein in *EμMyc Nr4a1 -/-* mice compared to *EμMyc Nr4a1 +/+* in tumor phenotype IgM^+ ($p=0,039$). Comparison between *EμMyc Nr4a1 -/-* and EμMyc *Nr4a1 +/+* and within IgM^- phenotype showed no significant different protein expression (Figure 18d).

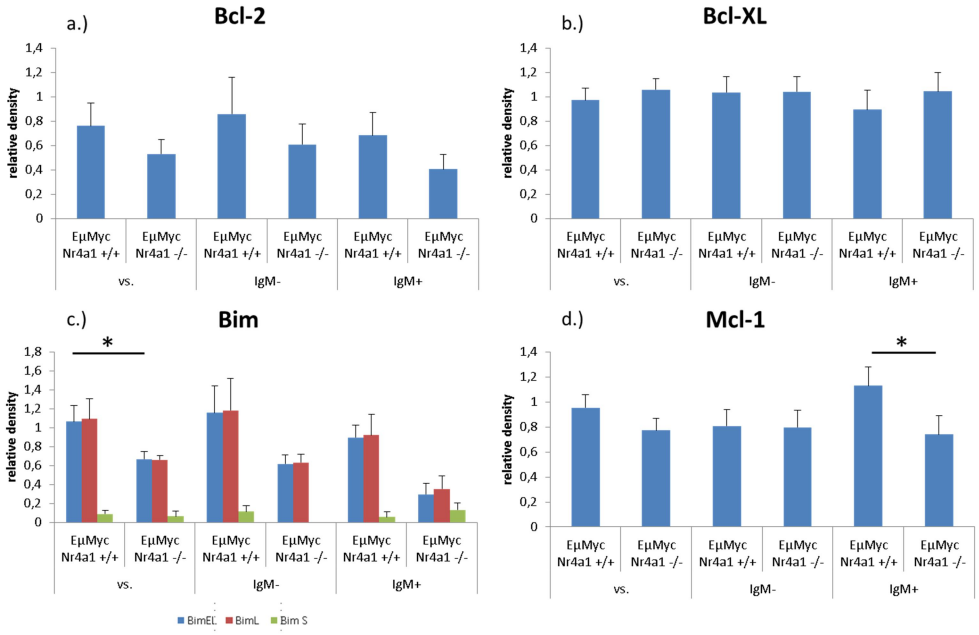

Figure 18: Relative density of Bcl-2, Bcl-XL, Bim and Mcl-1
The density was calculated using ImageJ. Data were normalized to the loading control. The barchart show the mean and standard error of the mean. *: $p<0,05$

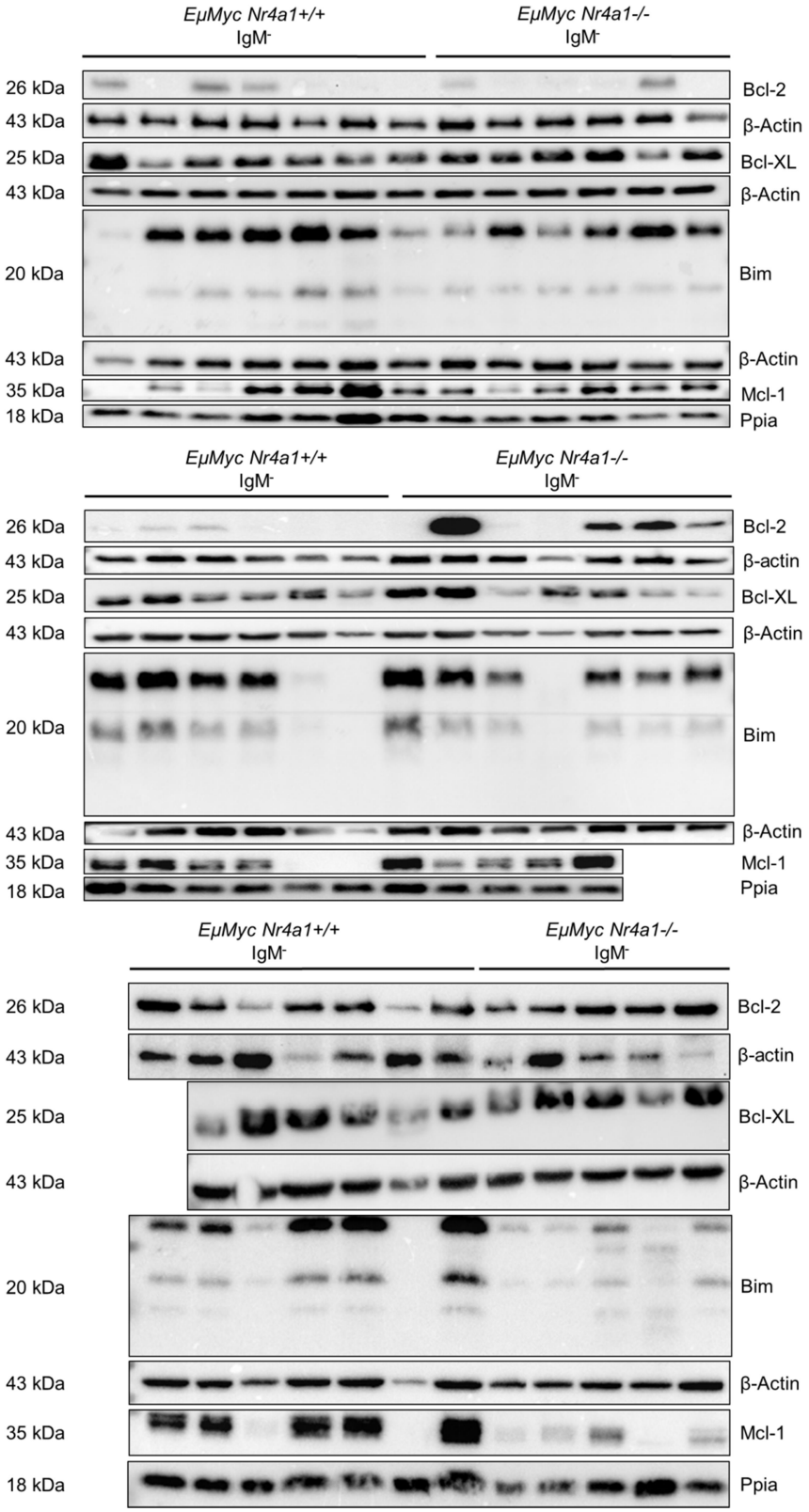

Figure 19: Western blot analysis of Bcl-2, Bcl-XL, Bim and Mcl-1 expression with their loading control β-Actin or Ppia
Tumors with IgM$^-$ phenotype derived from *EμMyc Nr4a1 +/+* and *EμMyc Nr4a1 -/-* were analysed for Bcl-2, Bcl-XL, Bim and Mcl-1 protein expression. β-Actin or Ppia served as loading control.

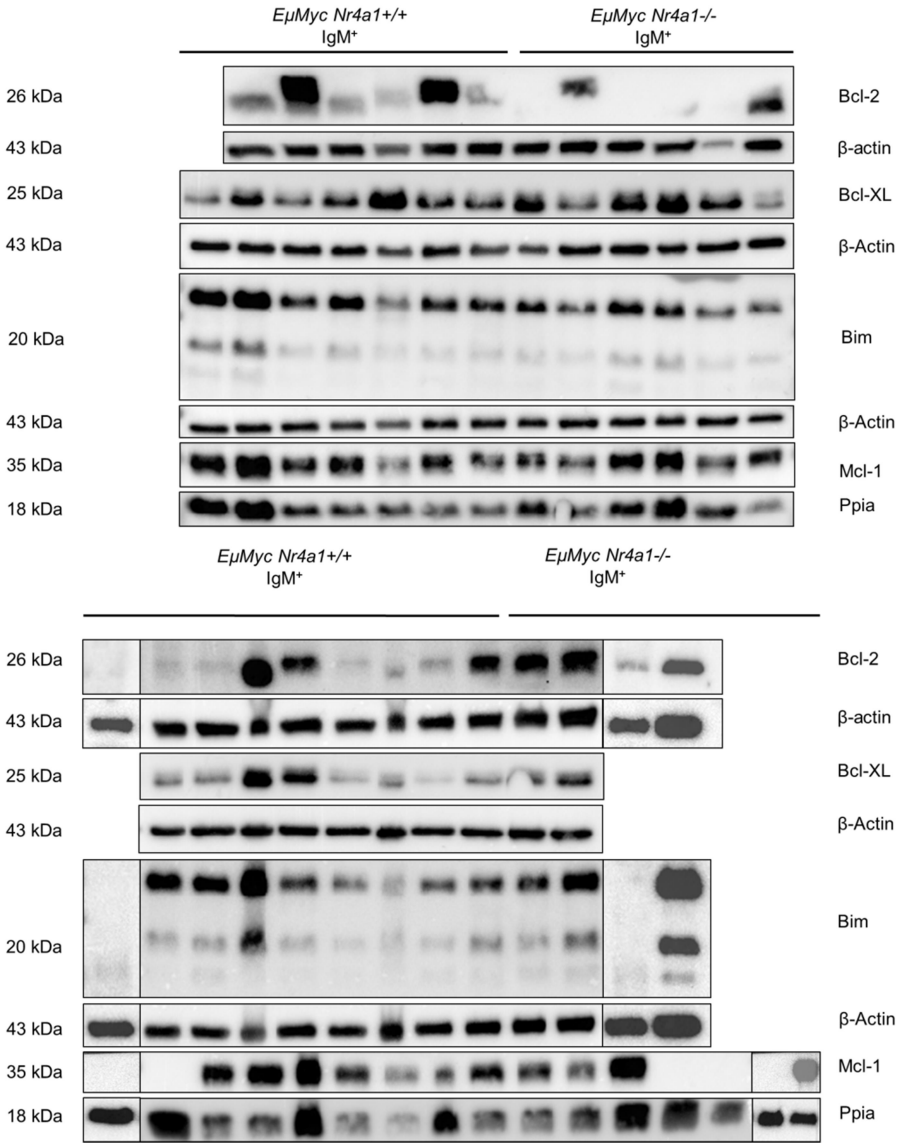

Figure 20: Western blot analysis of Bcl-2, Bcl-XL, Bim and Mcl-1 expression with their loading control β-Actin or Ppia
Tumors with IgM$^+$ phenotype derived from *EμMyc Nr4a1 +/+* and *EμMyc Nr4a1 -/-* were analysed for Bcl-2, Bcl-XL, Bim and Mcl-1 protein expression. β-Actin or Ppia served as loading control.

Since the research group previously observed that NR4A1 possesses a pro-apoptotic function in aggressive lymphoma cell lines [75] and cleavage of Parp is a marker is a marker for apoptotic processes [84, 85], we performed Western blot analysis for it. However, no significant different protein expression levels were detectable compared between *EμMyc Nr4a1 -/-* and *EμMyc Nr4a1 +/+* (Figure 21 and Figure 22).

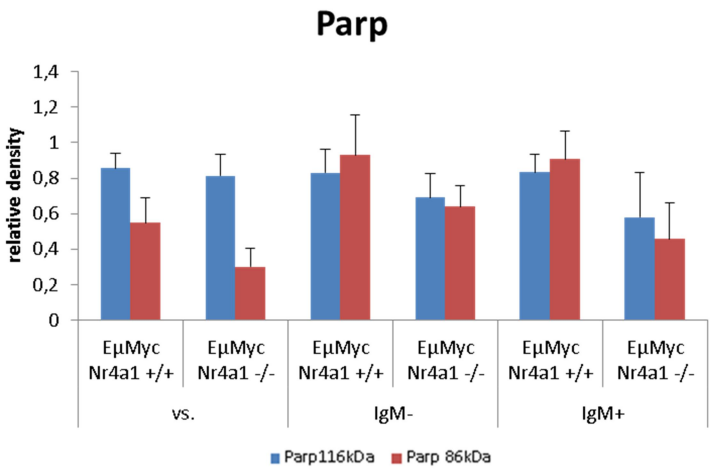

Figure 21: Relative density of Parp
The density was calculated using ImageJ. Data were normalized to the loading control. The bar chart shows the mean and standard error of the mean. *: p<0,05

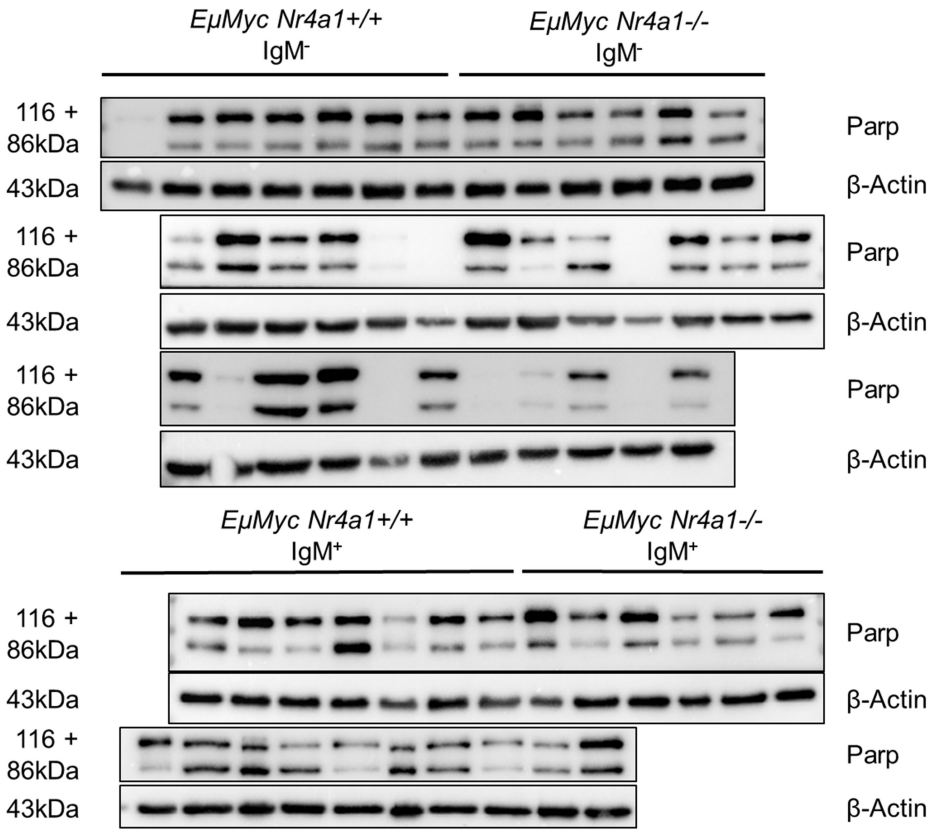

Figure 22: Western Blot of Parp with their loading control β-Actin
Tumors with IgM^-/IgM^+ phenotype derived from *EμMyc Nr4a1+/+* and *EμMyc Nr4a1-/-* were analysed for Parp protein expression. β-Actin served as loading control.

Based on the fact that enhanced NF-κB signaling is a common hallmark of many lymphoid malignancies, that Irf-4 is transcriptionally regulated by NF-κB and that NR4A1 acts as inhibitor of NF-κB [86–89], we determined the Irf-4 expression levels. Quantification of Irf-4 protein amounts showed a tendency for lower expression of Irf-4 protein in *EμMyc Nr4a1 -/-* mice compared to *EμMyc Nr4a1 +/+* in tumor of the IgM$^+$ phenotype (p=0,066, Figure 23 and Figure 24).

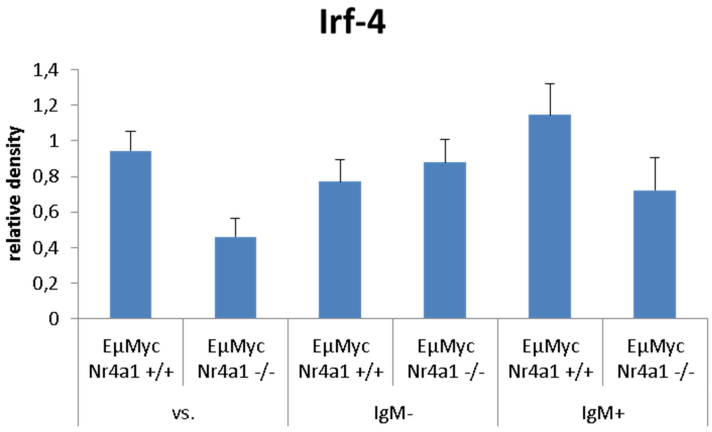

Figure 23: Relative density of Irf-4
The density was calculated using ImageJ. Data were normalized to the loading control. The bar chart shows the mean and standard error of the mean. p<0,05: *

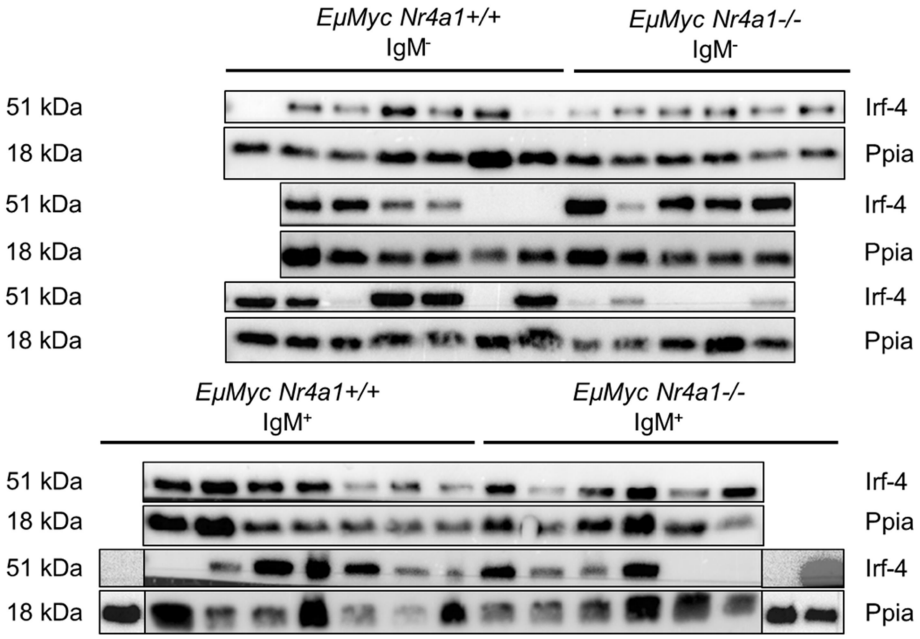

Figure 24: Western Blot of Irf-4 with their loading control β-Actin
Tumors with IgM$^+$/IgM$^-$ phenotype derived from *EμMyc Nr4a1+/+* and *EμMyc Nr4a1-/-* were analysed for Irf-4 protein expression. Ppia served as loading control.

3.1.3. Expression analysis of miRNA in aggressive B-cell lymphomas

Expression of NR4A1 and NR4A3 is significantly downregulated in aggressive B-cell lymphomas as demonstrated by our research group in previous work [70]. However, until now no event causing the down-regulation of both receptors has not been identified. Several miRNAs were discovered to target *NR4A1* and *NR4A3* expression [61, 68]. To clarify whether six miRNAs (miR-15a, miR-15a*, miR-20a, miR-224, miR-224*, miR-17) potentially cause the downregulation of *NR4A1* and *NR4A3* in aggressive lymphoma, we determined expression levels of these miRNAs in a cohort of aggressive lymphoma consisting of GCB-DLBCL, non-GCB-DLBCL as well as follicular lymphoma grade 3 (FLIII). miRNA expression levels were set in relation to *NR4A1* and *NR4A3* expression.

Interestingly, miR-15a showed a significantly negative correlation to NR4A1 protein expression determined by immunohistochemical analysis (Spearman-Rho Test = -0,371, p=0,013, Figure 25a). Furthermore, miR-15a showed at least a higher expression in non-GCB-DLBCL (p=0,07, Figure 25a), GCB-DLCBL (p=0,018, Figure 25a) and in FLIII (p=0,024, Figure 25a) compared to germinal B-cells (GC). By comparing non-GCB-DLBCL and GCB-DLCB there was a significant expression of miR-15a detectable (p=0,07, Figure 25a). Additionally, miR-15* was significantly different expressed in non-GCB-DLBCL compared to FLIII (p=0,041), as well by comparing FLIII with GCB-DLBCL (p=0,05) (supplementary Figure 39). A significant downregulation of *NR4A1* expression was determined in the vast majority of non-GCB-DLBCL (p=0,017), GCB-DLBCL (p=0,011) and FLIII (p=0,0015) compared to GC (Figure 25b) as described by Deutsch *et al*. [75]. Further, *NR4A1* mRNA expression levels were split into 2 groups (low and high NR4A1 expression) as described by Deutsch *et al*. [75] using the median of the expression. Between low and high NR4A1 expression a significant association was observed in miR-15a* (p=0,03). In the cohort of low NR4A1, miRNA-15* was significantly higher expressed compared to high NR4A1 (Figure 25e).

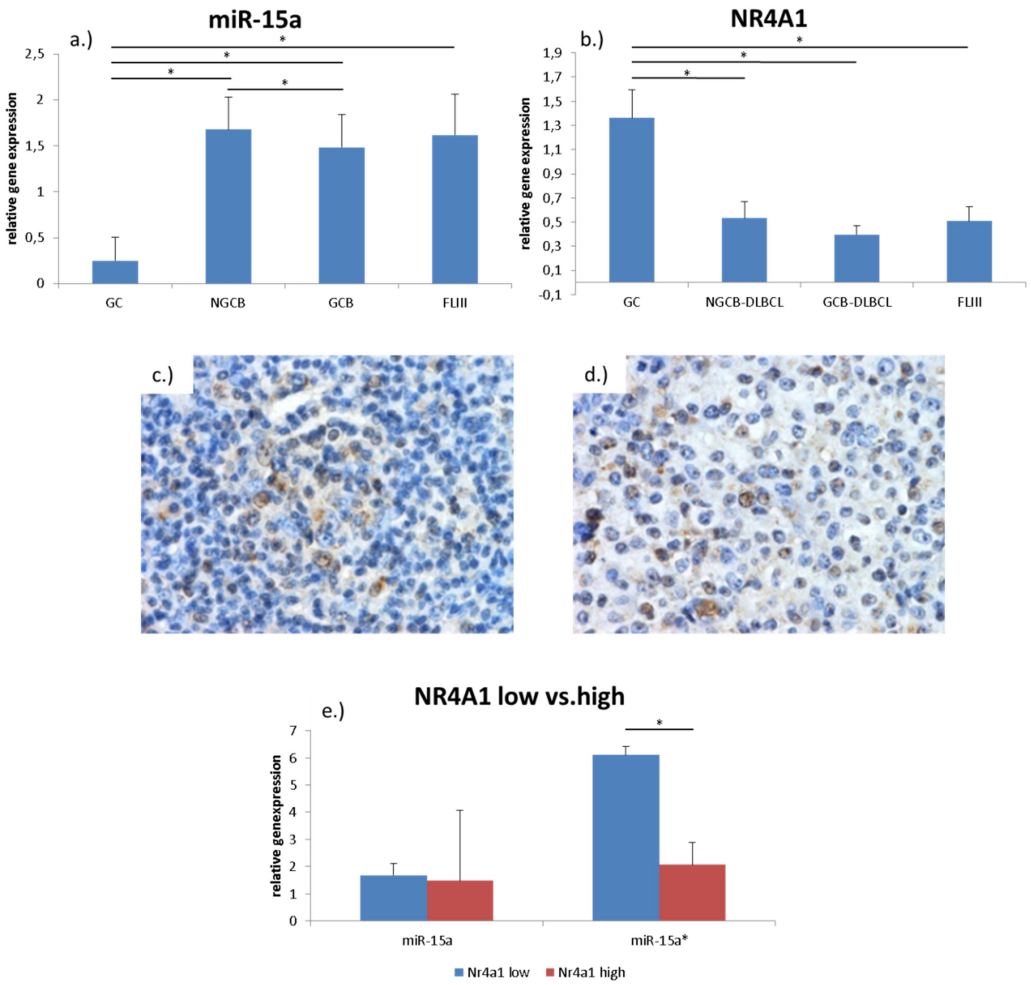

Figure 25: NR4A1, miR-15a* and miR-15a in aggressive lymphomas
The bar charts show the mean values of mRNA expression levels and standard error of the mean. a.) Relative gene expression of miR-15a in GC, NGCB, GCB and FLIII of human samples was assessed by real-time PCR b.) *NR4A1* expression in in GC, NGCB, GCB and FLIII of human samples was assessed by real-time PCR. c.) Immunohistological stain of NR4A1 in mir15a low expressing lymphoma. d.) Immunohistological staining of NR4A1 in mir15a high expressing lymphoma e.) miR-15a- and miR-15a* expression of *NR4A1* low and high expressing lymphoma. *: p<0,05:

3.2. Non-malignant conditions

3.2.1. Expression analysis of potential *Nr4a1* target genes

For the identification of biochemical pathways and/or genetic programs controlled by *Nr4a1*, mRNA sequencing derived from *EμMyc Nr4a1* -/- and *EμMyc Nr4a1* +/+ was performed. By comparing the 2 types of transgenic mice 57 genes being up-regulated and 18 genes being down-regulated were found. To confirm these data in humans the deregulated genes were analyzed in the public available gene expression data set and they were set in relation to *NR4A1* expression [77]. 39 of the 57 up-regulated genes significantly correlated in a negative manner und 8 of the 18 down-regulated genes in a positive manner compared to *NR4A1* expression (p<0,0001) indicating that these genes might be regulated by *NR4A1*. Bioinformatic analysis

demonstrated that target genes of NF-KB pathway were enriched in the expression data set of *EμMyc Nr4a1 -/-* mice. *Nr4a1* is involved in inhibition of NF-KB pathway. Nr4a1 is binding to the promoter region of the *IKBα* gene, which leads to transcriptional activation and augments *IKBα* expression. Hence, NF-KB dimers in cytoplasm get inactivated resulting in their inhibition.

Therefore, we compared *Nr4a1 -/-* vs. *Nr4a1 +/+* mouse spleens using Real-Time PCR. The assessment of two different mouse cohorts with different ages (12-16, 30-36 and 52-62 weeks) and 21 genes resulted in a wide coverage of relative expression, ranging from 0.17 to more than 3.3.

In *Nr4a1-/-* mice aged 12-16 weeks twelve genes (*Klcr2, Tnfs11, Cd226, Dll1, Il12b, S100a, Ccl22, Cd226, Tnfrsf8, Cflar1, Ccnd1* and *Ccr7*) were lower expressed than in *Nr4a1 +/+* mice at the same age. Three genes (*Cdkn2a, Bcl2a1a* and *Gata3)* showed a similar gene expression comparing these two groups. Six genes were higher expressed in *Nr4a1 -/-* mice compared to wild type. These genes were not statistically significant expressed (Figure 26).

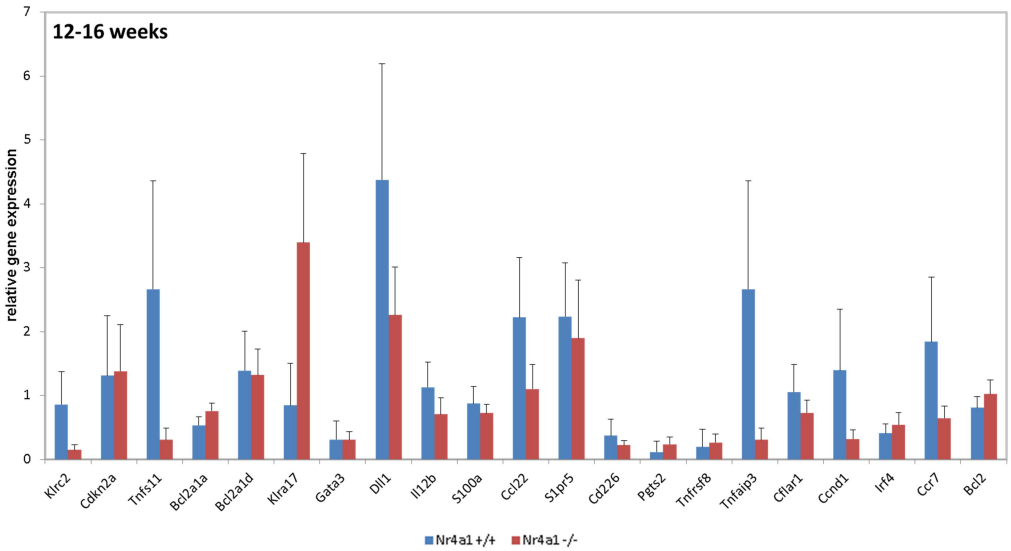

Figure 26: Relative gene expression of *Nr4a1 -/-* mice spleens compared to *Nr4a1 +/+* mice aged 12-16 weeks
21 genes of interest were assessed by real time-PCR comparing *Nr4a1 -/-* and *Nr4a1 +/+* mice in spleens. The bar charts show the mean values of mRNA expression levels and standard error of the mean. *: p<0,05

Ten out of 21 genes where found significantly (p-value <0.05) differentially expressed. *Klcr2*, *Il12b*, *Bcl2a1d*, *Gata3*, *Cd226*, *Ccdn1*, *Irf4, Tnfrsf8, S100a* and *Ccr7* were significantly lower expressed in the spleen of a cohort of *Nr4a* -/- compared to *Nr4a1* +/+ mice aged 30-36 weeks. Eight genes out of 21 genes are involved in NF-KB pathway. Four of these genes (*Bcl2a1d, Ccdn1, Irf4, Ccr7)* were significantly down-regulated in *Nr4a1* -/- mice. No difference was observed for the other genes (*Bcl2a1a, Tnfaip3, Cflar1, Bcl2, Dll1, Ccl22, S1pr5, Pgts2, Klra17, Tnfs11, Cdkn2a*) (Figure 27).

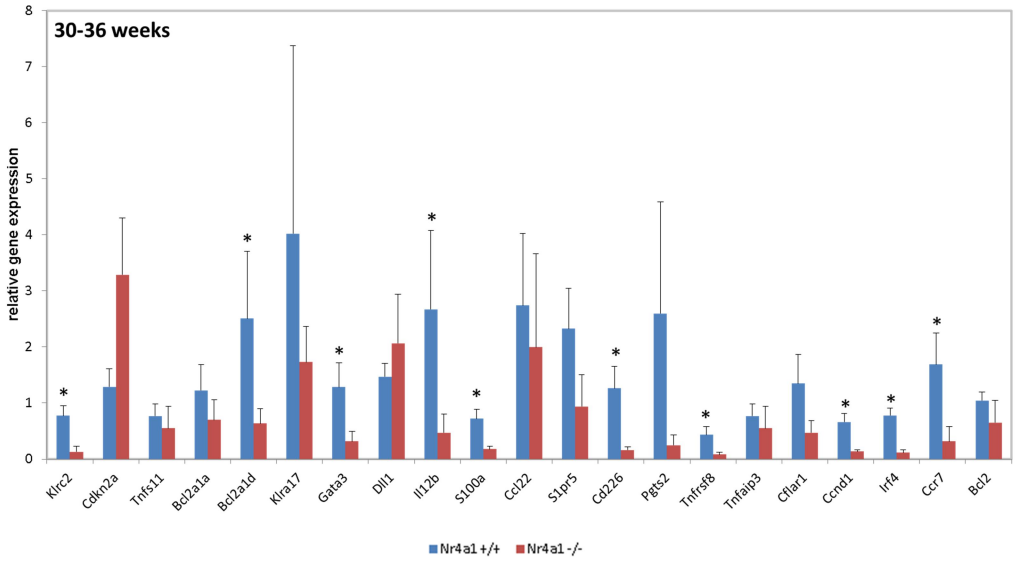

Figure 27: Relative gene expression of *Nr4a1 -/-* mice spleens compared to *Nr4a1 +/+* mice aged 30-36 weeks
21 genes of interest were assessed by real time-PCR comparing *Nr4a1 -/-* and *Nr4a1 +/+* mice in spleens. The bar charts show the mean values of mRNA expression levels and standard error of the mean. *: p<0,05

Three genes (*Bcl2a1d, Ptgs2 and Ccr7*) were expressed significantly different in *Nr4a1 -/- and Nr4a1 +/+* mice aged 52-62 weeks. Two of these genes are involved in NF-KB pathway. No difference was observed for the other genes (*Klrc2*, *Cdkn2a, Tnfs11, Bcl2a1a, Klra17, Gata3, Dll1, Il12b, S100a, Ccl22, Cd226, Tnfrsf8, Tnfaip3, S1pr5, Pgts2, Tnfrsf8, Cflar1, Ccdn1, Irf4, Bcl2*) (Figure 28).

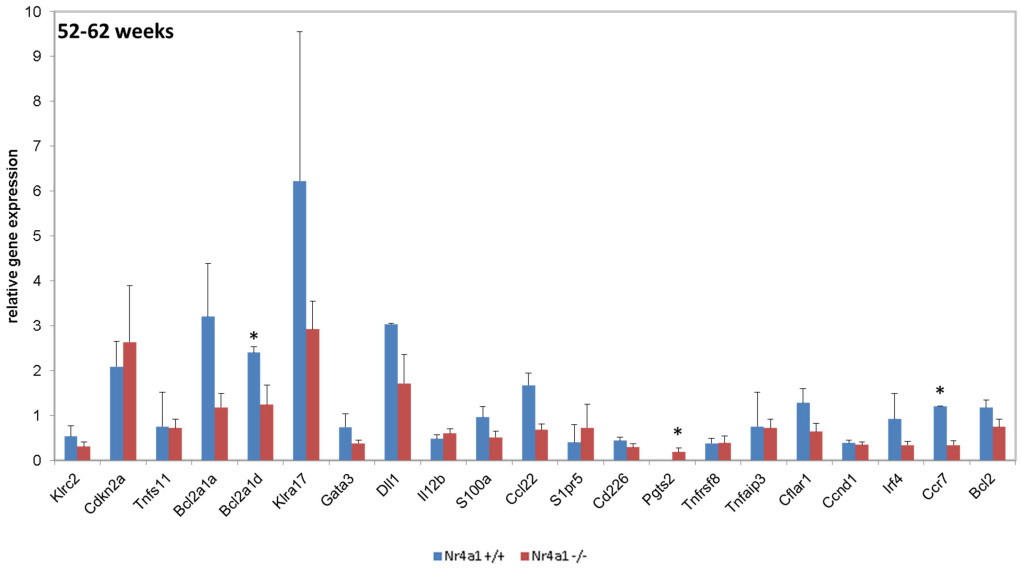

Figure 28: Relative gene expression of *Nr4a1 -/-* mice spleens compared to *Nr4a1 +/+* mice aged 52-62 weeks
21 genes of interest were assessed by real time-PCR comparing *Nr4a1 -/-* and *Nr4a1 +/+* mice in spleens The bar charts show the mean values of mRNA expression levels and standard error of the mean. *: p<0,05

Further, the relative expression levels of 34 genes of interest in thymus and splenic B-and T cells were compared between *Nr4a1 -/-* vs. *Nr4a1 +/+* mice aged 18-21 weeks using the Real-Time PCR. These genes correlate to *NR4A1* expression in a publicly available gene expression dataset of DLBCL patients [77].

We observed that in the thymus seven (*Bcl2a1a, Bcl2a1d, Ccnd1, Ccl20, Icos, Klcr2, S100a*) of the 34 investigated genes were significantly lower expressed in the *Nr4a1-/-* mice compared to *Nr4a1+/+* mice: Three NF-KB target genes (*Bcl2a1a, Bcl2a1d, Ccnd1)* were significantly lower expressed in *Nr4a1-/- mice.* 16 genes were not significantly deregulated (*Bcl2, Ccl22, Ccr7, Cd27, Cd96, Cflar1, dll1, Gata3, Gcsam, Il7, Il12b, Irf4, Ptgs2, S1pr5, Tnfaip3* and *Tnfrsf8*) (Figure 29). Eleven genes were not detectable (*Tnfsf11, Aicda, Cd226, Cdkn2a, Havcr1, Havcr2, Pdcd1, Pdcd1lg2, Sox2, Cda1, Klra17*).

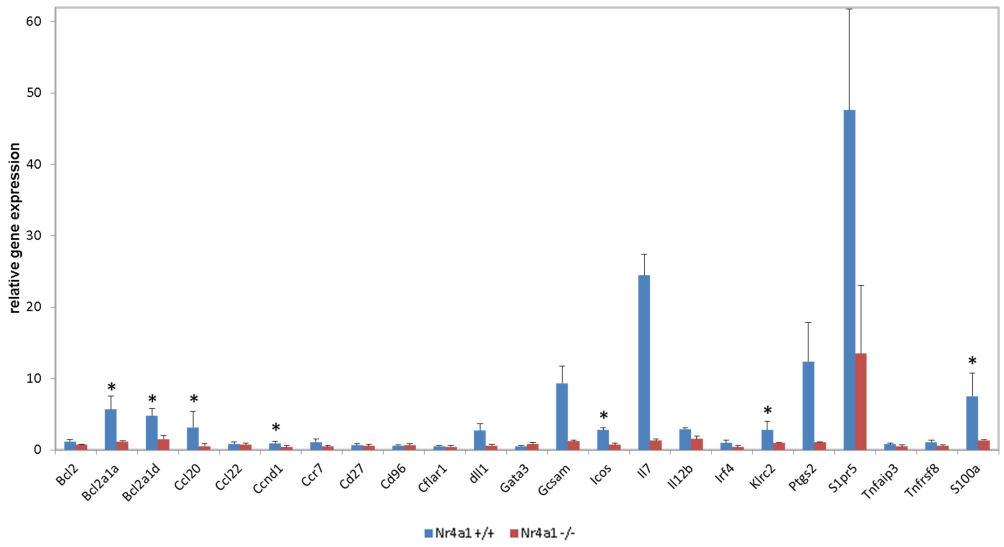

Figure 29: Relative gene expression of the thymus derived from *Nr4a1 -/-* mice compared to *Nr4a1 +/+* mice aged 18-21 weeks
34 genes of interest were assessed by real time-PCR comparing *Nr4a1 -/-* and *Nr4a1 +/+* mice. The bar charts show the mean values of mRNA expression levels and standard error of the mean. *: p<0,05.

In splenic B-cells one gene *(Bcl2a1a)* of the NF-KB pathway was significantly lower expressed. Six genes were not differentially expressed (*Bcl2, Bcl2a1d, Ccnd1, Ccr7, Tnfaip3, S100a*) (Figure 30). 27 genes were undetectable (*Tnfrsf8, Tnfsf11, Aicda, Ccl20, Cd27, Cd96, Cda1, Cd226, Cdkn2a, dll1, Gata3, Havcr1, Havcr2, Icos, Il12b, Irf4, Klrc2, Pdcd1, Pdcd1lg2, Ptgs2, Sox2, Il7, Ccl22, Cflar1, Gcsam, Klra17, S1pr5*).

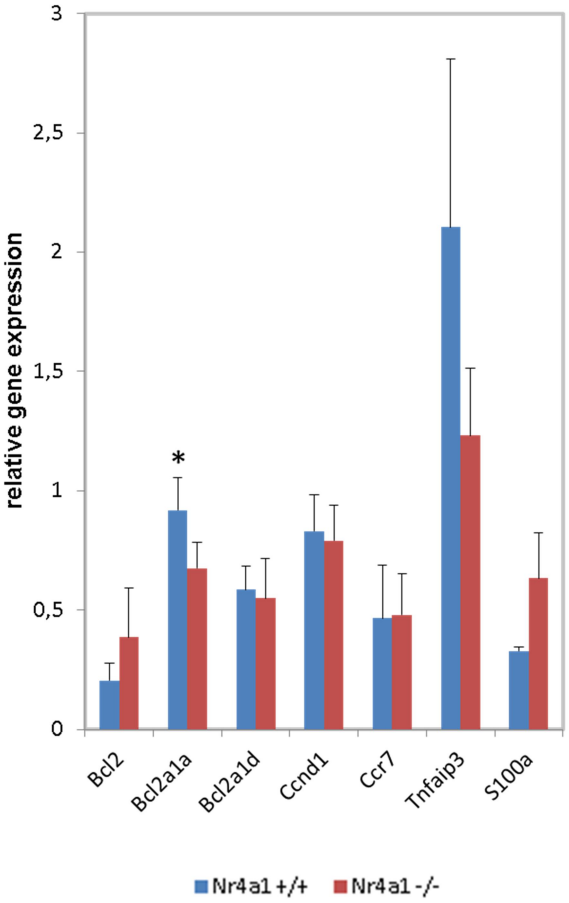

Figure 30: Relative gene expression of splenic B-cells derived from *Nr4a1 -/-* mice compared to *Nr4a1* +/+ mice aged 18-21 weeks
34 genes of interest were assessed by real time-PCR comparing *Nr4a1 -/-* and *Nr4a1* +/+ mice. The bar charts show the mean values of mRNA expression levels and standard error of the mean. *: p<0,05.

In stark contrast, eight (*Bcl2, Ccdn1, Ccr7, Cflar1, Tnfaip3, Gata3, Gcsam, Klcr2*) of the 34 investigated genes were significantly higher expressed in the splenic T-cells of Nr4a1-/- mice compared to *Nr4a1 +/+.* Five (*Bcl2, Ccdn1, Ccr7, Cflar1, Tnfaip3*) out of eight NF-KB target genes were significantly up-regulated in *Nr4a1 -/-* mice. Ten genes were not significantly expressed (*Bcl2a1a, Bcl2a1d, Ccl22, dll1, Havcr2, Irf4, Klcr2, Ptgs2, S1pr5, S100a*) (Figure 31). 16 genes were not detected (*Tnfsf11, Aicda, Ccl20, Cd27, Cda1, Cd226, Cdkn2a, Havcr1, Icos, Pdcd1, Pdcd1lg2, Sox2, Cd96, Il7, Il12b, Tnfrs8*).

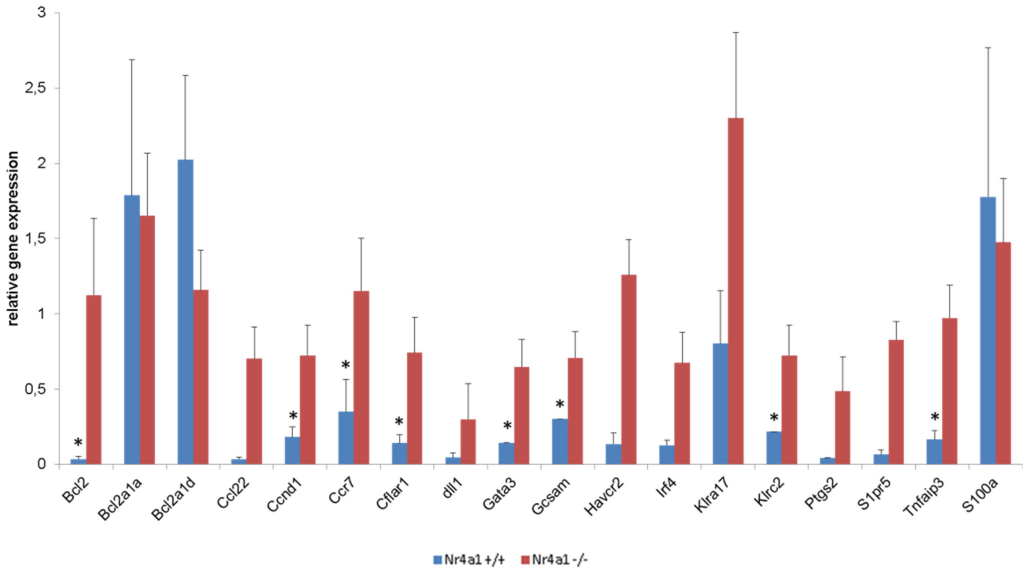

Figure 31: Relative gene expression of splenic T cells from *Nr4a1 -/-* mice compared to *Nr4a1 +/+* mice aged 18-21 weeks
34 genes of interest were assessed by real time-PCR comparing *Nr4a1 -/-* and *Nr4a1 +/+* mice. The bar charts show the mean values of mRNA expression levels and standard error of the mean. *: p<0,05

3.3. Effects of spermidine in *Nr4a1-/-* mice

Mice lacking *Nr4a1* showed at 32-month development of systemic inflammation. Additionally, an enhanced production of pro-inflammatory cytokines and immunoglobulin was observed suggesting that Nr4a1 plays an important role in inflammatory responses [90]. Besides, Nr4a1 is implicated in T cell development, T cell apoptosis and in development of subtypes of monocytes [91, 92]. Spermidine enhances T cell mediated immune responses and inhibits the tumor growth by chemotherapy *in vivo* [59]. Additionally, spermidine shows anti-inflammatory and anti-oxidative effects in chronic inflammation [49]. Therefore, we wanted to investigate whether spermidine influences inflammation processes in *Nr4a1 -/-* mice.

For this purpose, *Nr4a1 -/-* (n=5) and *Nr4a1 +/+* (n=15) mice were given spermidine via water (3mM) for 24 weeks. Mice were sacrificed for phenotypical analysis. Untreated *Nr4a1 -/-* (n=7) and *Nr4a1 +/+* mice (n=7) aged 30 weeks were included as controls. In these mice plasma levels of pro-inflammatory cytokine (TNF-α, IL-10, IL-6, IFN-γ, IL-2, IL-1β, KC/GRO and IL-5), spleen weights and the distribution of myeloid lymphoid cells in bone marrows, spleens, and thymuses were investigated.

Nr4a1 -/- SPD (Nr4a1-/- mice treated with spermidine) mice exhibited significantly evaluated level of TNF-α and IL-6 concentration compared to untreated *Nr4a1 -/-* (2.4 fold for TNF-α and 6.2 fold for IL-6, p<0,043) and untreated *Nr4a1 +/+* mice (2.7 fold for TNF-α and 6.2 fold for IL-6, p<0,027) (Figure 32a and d). IL-1β and KC/GRO levels were the highest in *Nr4a1-/-* SPD compared to *Nr4a1 +/+* (1.7 fold for IL-1β and 1.7 fold for KC/GRO, p<0.086 and *Nr4a1 -/-* mice (1.7 fold for IL-1β, p<0,086, Figure 3 g and h). *Nr4a1 -/-* mice exhibited an increased plasma levels of IL-5 compared to *Nr4a1 +/+* mice (2.3 fold, p=0,055) to *Nr4a1-/-* SPD mice (2.8 fold, Figure 32f, p=0,077). For IL-10, IFN-γ and IL-2, no differences were detectable (Figure 32b, c and e).

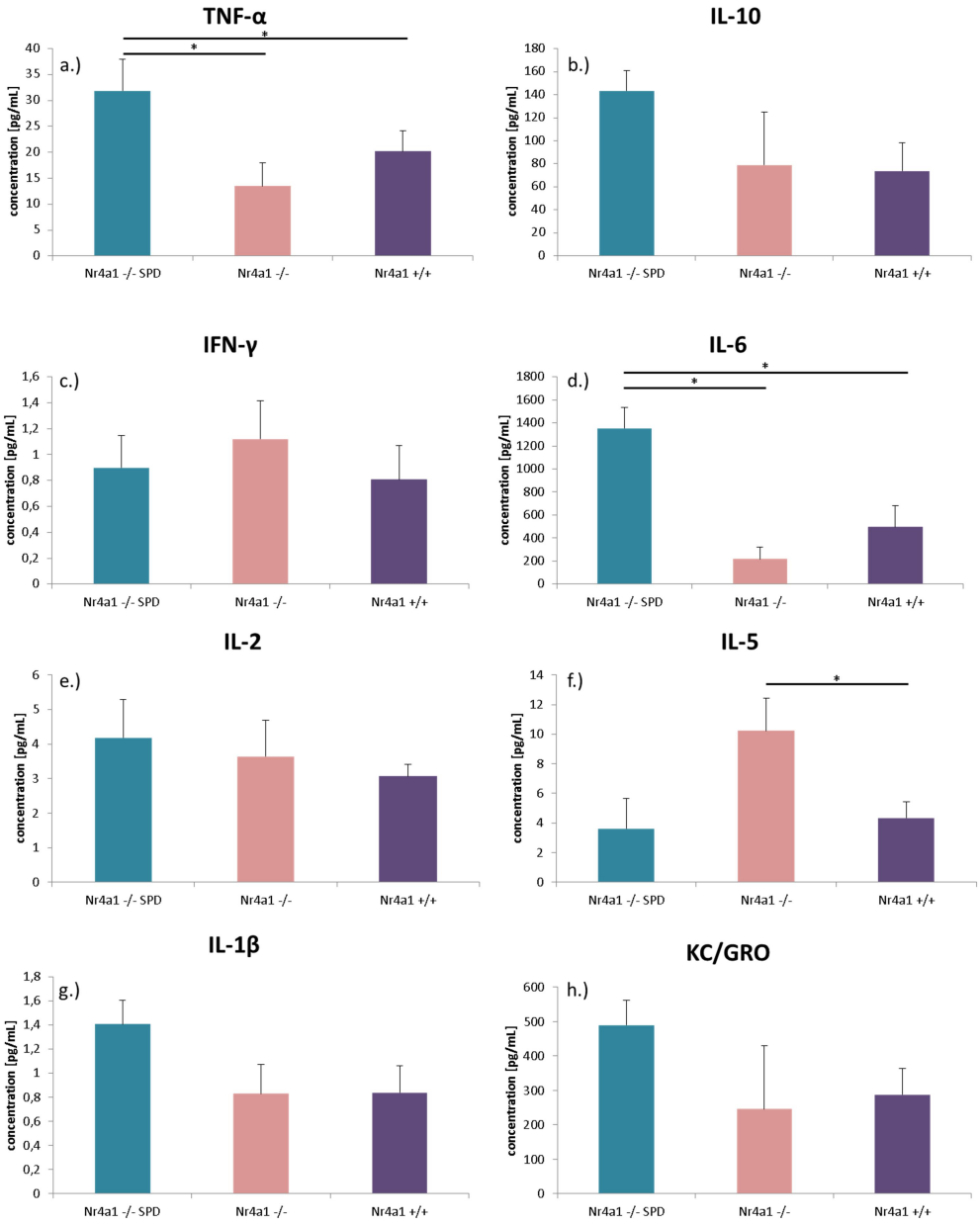

Figure 32: Multiplex measurement of inflammatory markers from *Nr4a1 -/-* SPD, *Nr4a1 -/-* and *Nr4a1 +/+* mice
The bar charts show the mean values of concentration levels in pg/ml and standard error of the mean. *: p<0,05

Nr4a1 -/- mice showed significantly enlarged spleens compared to *Nr4a1 +/+* mice, as previously described by Li et al [90] and confirmed by our group. Interestingly, SPD treatment resulted in a reduction of the spleen weight in the Nr4a1 -/- mice (p=0,016) (Figure 33).

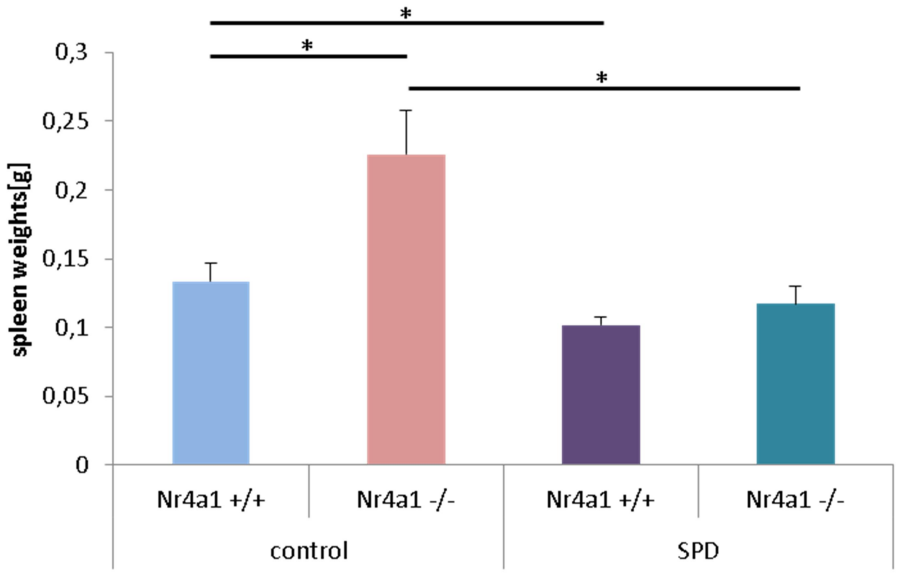

Figure 33: Phenotypical analysis of spleen from spermidine treated mice *Nr4a1 -/-* and *Nr4a1 +/+* mice and control groups without spermidine treatment
The bar charts show the mean of spleen weights and standard error of the mean. **: p<0,05*

The percentage of Gr1^{+}- myeloid cells was higher in the bone marrow of *Nr4a1 -/-* SPD and *Nr4a1 -/-* mice compared to *Nr4a1 +/+* SPD mice (71,3% vs. 66% vs.52%, p<0.015, Figure 34a)

Interestingly, the percentage of CD4^{+} T cells was higher in *Nr4a1 -/-* SPD and *Nr4a1 -/-* mice compared to *Nr4a1 +/+* SPD mice (1,86% vs. 1,38% vs. 1,06%, p<0.049, Figure 34b).

The percentage of TCR^{+} cells and CD8^{+} T cells was not altered nor by Nr4a1 loss or by SPD treatment (Figure 34b).

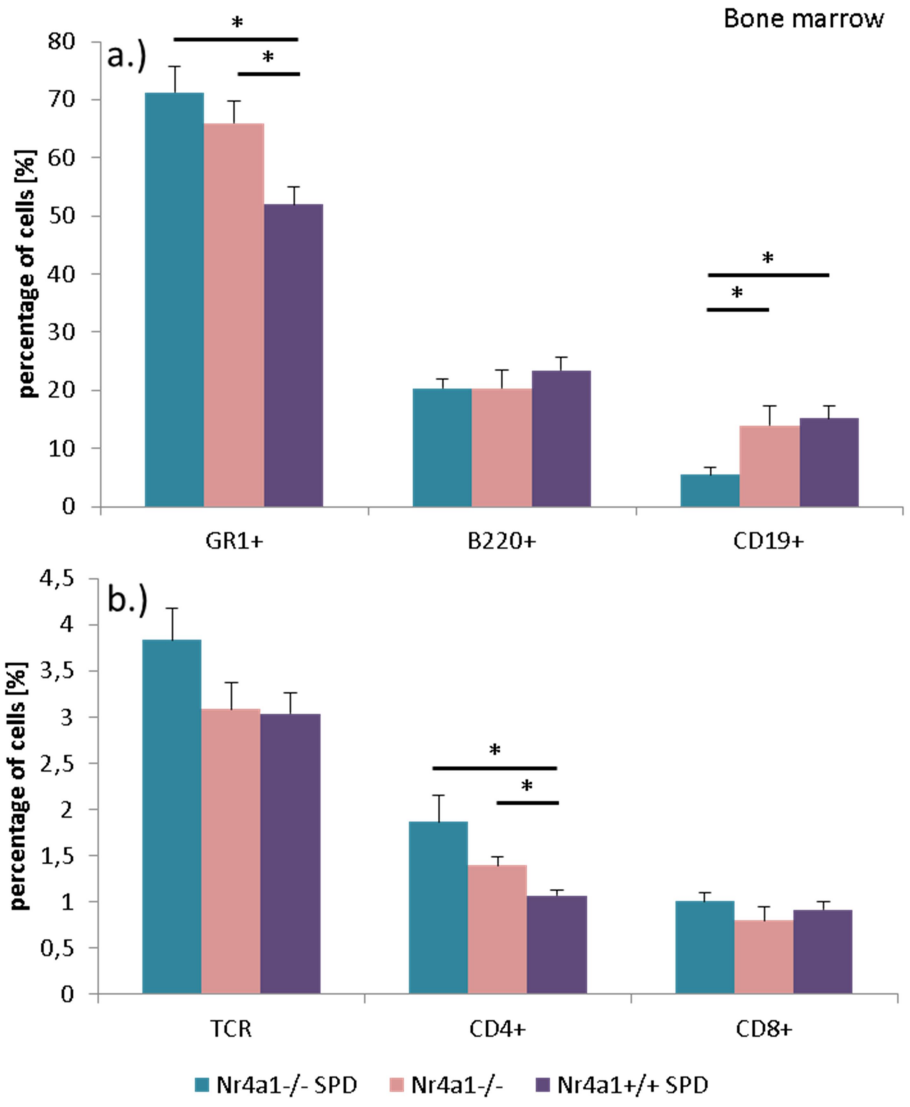

Figure 34: Comparison of Gr1^{+}, B220^{+} and CD19^{+} and T cells in bone marrow
The bar charts show the mean of percentage and standard error of the mean.
*: p<0,05

In spleen, the percentage of $Gr1^+$ myeloid cells was elevated in *Nr4a1 -/-* compared to *Nr4a1 +/+* SPD (8,64% vs. 7,57%, p=0,016, Figure 35a). In stark contrast the percentage of $B220^+$ and $B220^+CD19^+$ B-cells was dramatically reduced in *Nr4a1 -/-* SPD and *Nr4a1 -/-* mice (25,78% vs. 23,68% vs. 41,10%, p<0.014, Figure 35a) (12,85% vs.16,16% vs. 30,51%, p<0,001, Figure 35a). In spleen there was no difference in distribution of T cells in different developmental stages observable (Figure 35b).

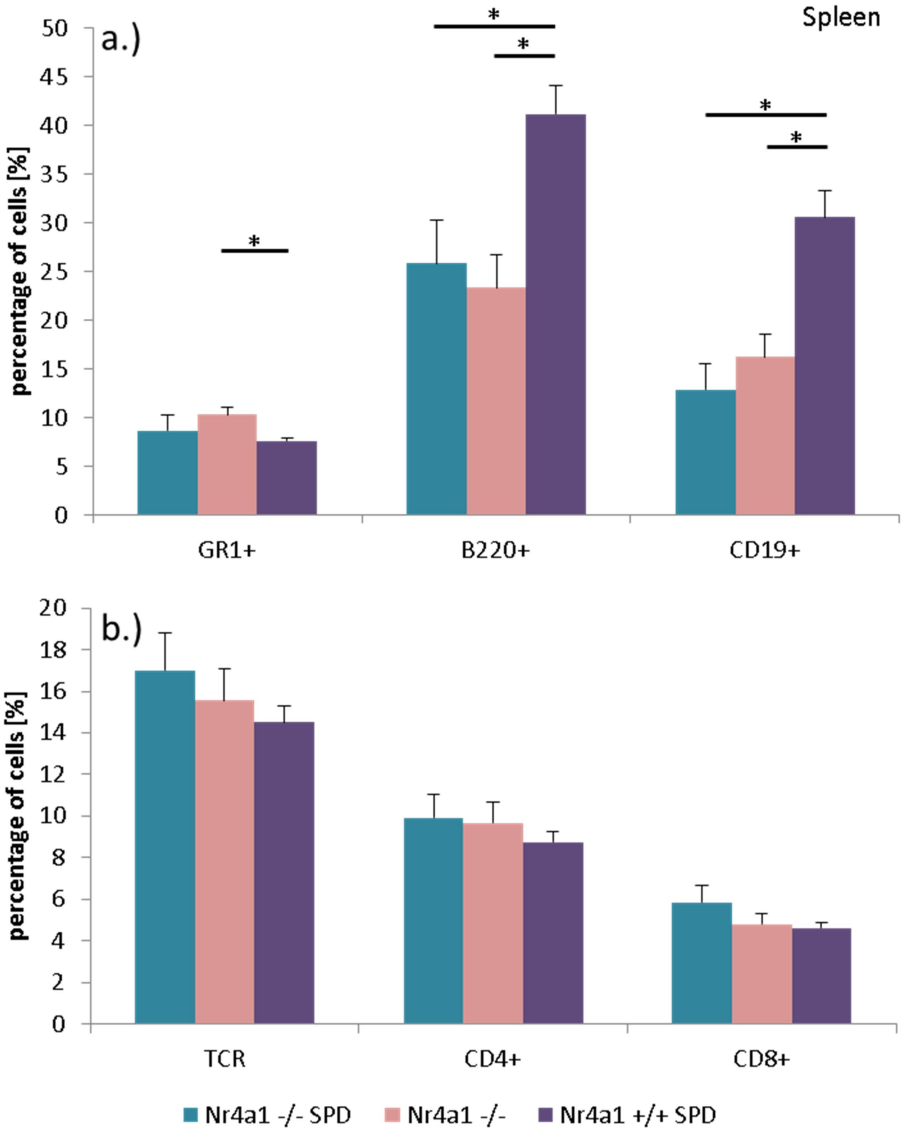

Figure 35: Comparison of $Gr1^+$, $B220^+$ and $CD19^+$ and T cells in spleen
The bar charts show the mean of percentage and standard error of the mean.
*: p<0,05

In the thymus no differences in the percentage of $Gr1^+$, $B220^+$ and $CD19^+$ was detected (Figure 36a). However, the distribution of the T-cell subsets was altered: By comparing *Nr4a1-/-* SPD to *Nr4a1* +/+ SPD mice we detected a reduced percentage for $CD8^+$ (2,21% vs. 1,34%, p<0.032, Figure 36b). Comparison of $CD4^-CD8^-$ cells showed a significant reduced percentage in *Nr4a1-/-* SPD and *Nr4a1-/-* to *Nr4a1* +/+ SPD (1,58% vs. 1,40% vs. 3,83%, p<0.024, Figure 36b). In contrast, the percentage $CD4^+CD8^+$ T cells was higher in *Nr4a1-/-* SPD mice (37,30% vs. 36,52% vs. 29,81%, p<0.022, Figure 36b).

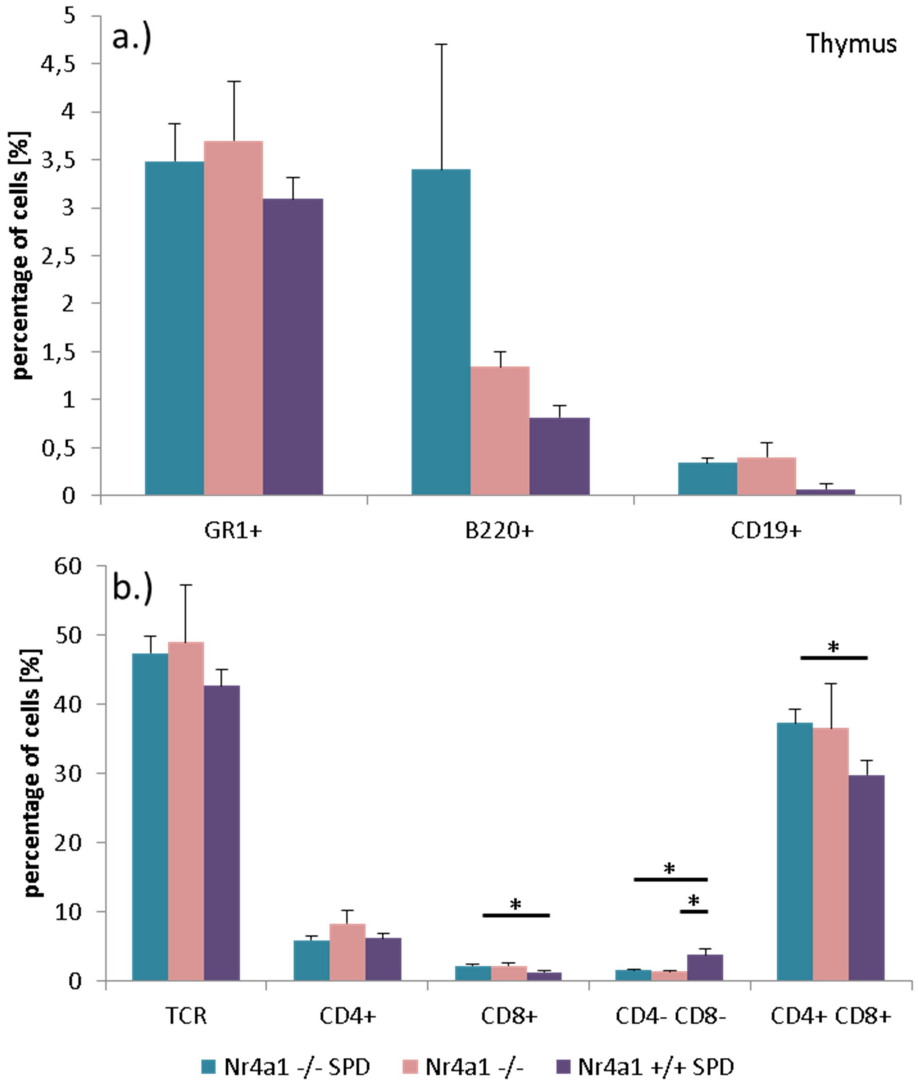

Figure 36: Comparison of $Gr1^+$, $B220^+$ and $CD19^+$ and T cells in thymus
The bar charts show the mean of percentage and standard error of the mean.
*: p<0,05

3.3.1. Effects of spermidine on B-cell development in *Nr4a1-/-* mice

Based on the fact that the *Nr4a1-/-* mice with and without spermidine administration possess a massively reduced percentage of B-cells, especially in the spleen, we analyzed B-cell development in these mice (*Nr4a1-/-* SPD, *Nr4a1-/-* and *Nr4a1* +/+ SPD) by using an antibody panel to determine Pro-, Pre-, immature, transitional (Trans B), early mature and late mature B-cells and additionally in the spleen follicular (FO), marginal zone (MZ), B1-a and T1/B1-b B-cells.

The distribution of the different subsets of the B-cell development in the bone marrow of *Nr4a1 -/-* SPD and *Nr4a1 -/-* was nearly equally, whereas stark differences were observed compared to *Nr4a1* +/+ SPD mice: The percentage of Pro B-cell was higher in *Nr4a1 -/-* SPD and *Nr4a1 -/-* (3,7% vs. 1,71%, p=0,009, Figure 37), whereas the percentage of *Nr4a1 -/-* SPD and *Nr4a1 -/-* compared to *Nr4a1* +/+ SPD of immature (1,56% vs. 1,66% vs. 3,87%, p<0,020, Figure 37), Trans B (2,4% vs. 2,26% vs. 3,66%, p<0,027, Figure 37) and late mature (1,06% vs. 0,77% vs. 2,05%, p<0,045, Figure 37) B-cells were significantly lower.

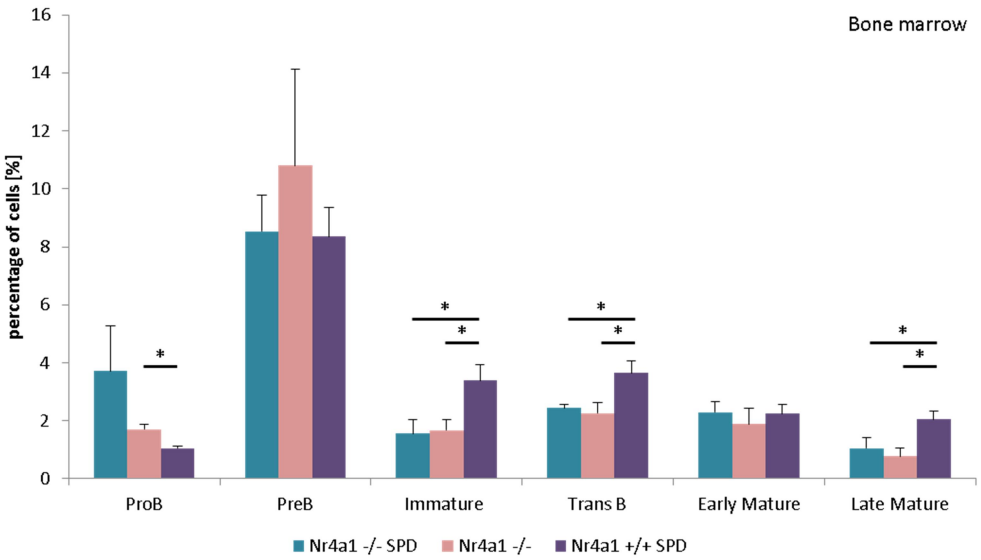

Figure 37: Relative percentage of Pro-, Pre-, immature, transitional, early and mature B-cells in bone marrow
The bar charts show the mean of percentage and standard error of the mean.
*: p<0,05

A similar distribution was observed in the spleen: Nr4a1 -/- SPD and Nr4a1 -/- exhibited a higher percentage of Pro- B-cells compared to *Nr4a1 +/+* SPD (1,17% vs. 0,22% vs.0,21%, p<0,043, Figure 38a), whereas the percentage of immature (4,54% vs. 3,86% vs. 7,07%, p<0,038, Figure 38a), transitional B-cells (3,65% vs.3,56% vs. 6,46%, p<0,0082, Figure 38a), late mature B-cells (5,4% vs. 6% vs.12,98%, p<0,082, Figure 38a) was reduced. Follicular B-cells showed a reduced percentage in *Nr4a1 -/-* SPD and in *Nr4a1 -/-* compared to *Nr4a1 +/+* SPD ((9,15% vs. 14,13% vs.25,3%, p<0,012, Figure 38b), whereas marginal zone B-cells showed a higher percentage in *Nr4a1 -/-* SPD and in *Nr4a1 -/-* mice (8,47% vs. 9,74% vs. 6,29%, p<0,02, Figure 38b). T1/B-1b B-cells were reduced in *Nr4a1 -/-* SPD and in *Nr4a1 -/-* mice (1,20% vs. 1,98% vs.2,81%, p<0,0001, Figure 38c).

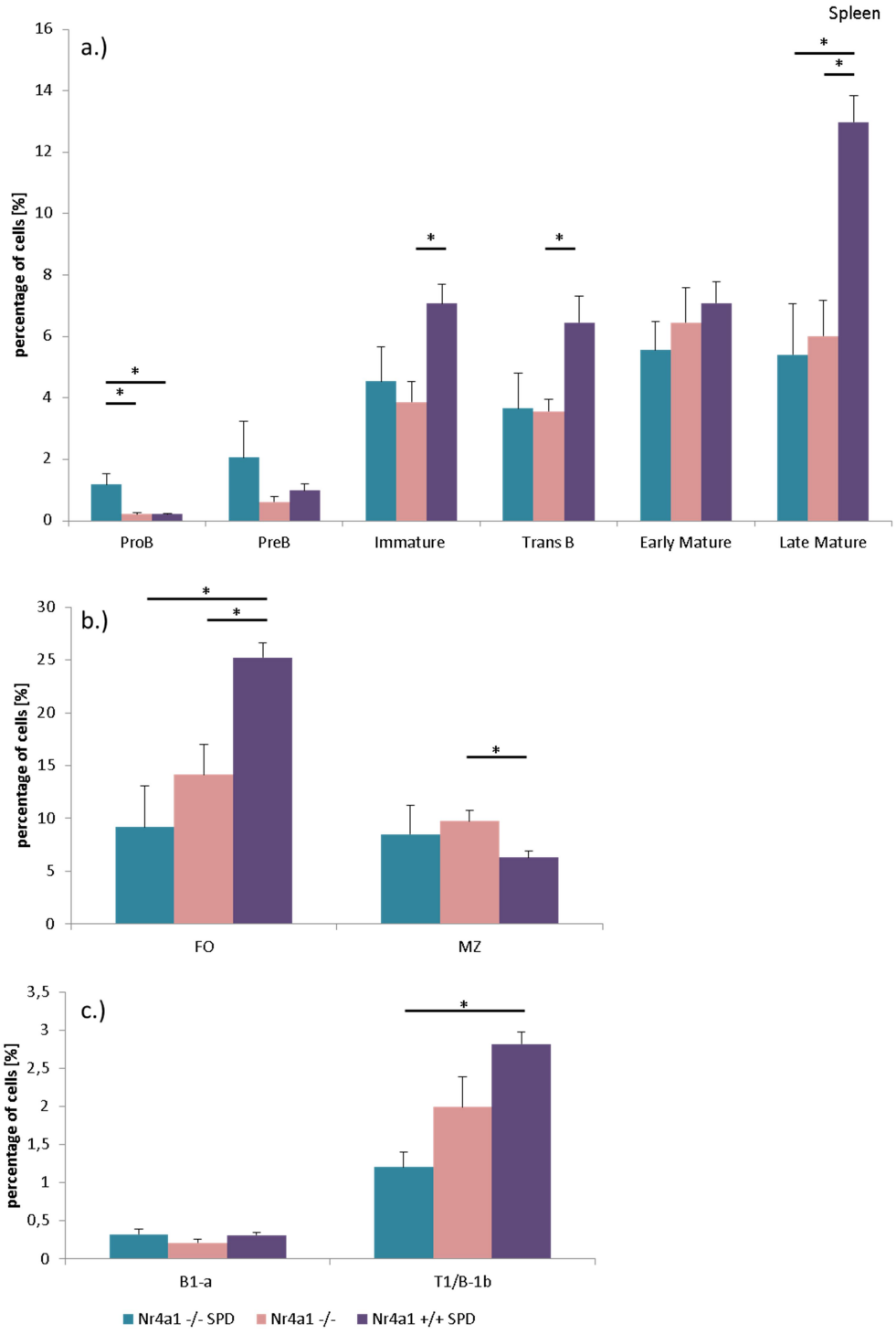

Figure 38: Relative percentage of Pro-, Pre-, immature, transitional, early and mature as well follicular, marginal zone, B1-a and T1/B1 B-cells in bone marrow
The bar charts show the mean of percentage and standard error of the mean. *: p<0,05

4. Discussion

The aim of the master thesis was to investigate the function of the nuclear orphan receptor *Nr4a1* in *Myc*-driven lymphomagenesis and in normal B-cell development.

Therefore, we determined the expression of *Nr4a1* and *Nr4a3* in B-cell development and in *EμMyc* lymphomagenesis. In IgM^+ lymphomas derived from *EμMyc Nr4a1* +/+ mice, *Nr4a1* was lower expressed compared to non-neoplastic *Nr4a1* +/+ IgM^+ B-cells, whereas *Nr4a3* was higher expressed in IgM^- and IgM^+ B-cells of premalignant *EμMyc Nr4a1* -/- mice as well in tumors derived from *EμMyc Nr4a1* -/- mice in both B-cell subtypes compared to premalignant *EμMyc Nr4a1* +/+ mice and tumors derived from *EμMyc Nr4a1* +/+ mice. However, no difference was detected for both receptors in IgM- and IgM^+ B-cells of *Nr4a1* +/+ mice. Our group has reported that in humans a reduced expression of *NR4A1* is common in aggressive lymphomas and is related with a poor survival [75]. Additionally, it was shown that NR4A3 possesses a redundant function at least in T cell apoptosis and as tumor suppressor in aggressive lymphomas like NR4A1 as demonstrated by my group [76, 93] Taking all together, these data indicate that *Nr4a1* is downregulated during malignant transformation. Additionally, it seems that *Nr4a3* is able to compensate the loss of *Nr4a1* in *Myc*-driven lymphomagenesis. Based on the fact that *Nr4a3* was higher expressed in premalignant IgM- and IgM^+ B and in lymphoma cells in *EμMyc Nr4a1* -/- mice compared to *EμMyc Nr4a1* +/+ and *Nr4a1* +/+ mice it seems that *Nr4a3* is a putative target gene of *Myc*.

In *EμMyc* transgenic mice, for malignant transformation, disruption of the p19ARF-MDM2-p53 pathway and/or over-expression of BCL-2, MCL-1, or BCL-xL- is needed to counteract the apoptotic effects of *Myc* [20, 22]. In lymphomas derived from *EμMyc Nr4a1* -/- mice the expression levels and incidence of p53 and p19Arf overexpression was significantly lower compared to *EμMyc Nr4a1* +/+ mice. Therefore, it might be speculated that malignant transformation in *EμMyc Nr4a1* -/- might be less dependent on the inactivation p53.

Further, we also observed a lower expression of Bim_{EL}, the most abundant Bim splice variant, and Mcl-1 in *EμMyc Nr4a1* -/- compared to *EμMyc Nr4a1*

+/+ mice. Bim is a pro-apoptotic member of the Bcl-2 family and mediates apoptosis whereas Mcl-1 shows anti-apoptotic effects. [32] Our group already demonstrated that ectopic overexpression of *NR4A1* results in induction of BIM in aggressive lymphoma cells [75, 76] suggesting that BIM might be a target of NR4A1. However, we were not be able to detect any differences in the apoptosis rates by comparing cleavage of Parp - a maker for apoptosis [94]- between lymphomas derived from *EμMyc Nr4a1 -/-* and *EμMyc Nr4a1 +/+* mice suggesting that the reduced pro-apoptotic signal of Bim might be compensated by the reduced anti-apoptotic signals of Mcl-1.
We also observed that miR-15a- and mir15a*-expression were associated with down-regulation of *NR4A1* in primary lymphoma sample. To the best of your knowledge Tenga *et al* showed that miR15a directly binds the 3'UTR of NR4A1 [61] and our bioinformatic analysis demonstrated that *NR4A1* possess a seed match for miR15a and miR15a*. Therefore, it might be speculated that over-expression of mir15a and mir15a* cause downregulation of *NR4A1* in aggressive lymphomas. However, with our attempt we were not able to identify the event causing *NR4A1* downregulation.

Our preliminary analysis showed that 39 genes were higher and eight genes were lower expressed in tumors derived from the *EμMyc Nr4a1 -/-* mice compared to *EμMyc Nr4a1 +/+* mice. Hence, the relative expression levels of genes of interest in spleen, thymus and splenic B-and T cells were compared between *Nr4a1 -/-* vs. *Nr4a1 +/+* mice using the Real-Time PCR. Gene expression profiling in spleens of different age groups revealed that genes being implicated in immune regulation, immune cell migration and in NF-KB pathway were significantly lower expressed in *Nr4a1 -/-* mice, especially in older mice. Moreover, NR4A1 modulates the NF-KB pathway to regulate the function of immune cells is able to repress or enhance target genes leading to an altered inflammatory effect [95]. Remarkable, by comparing the expression of the investigated genes in splenic B-cell and T cells between *Nr4a1 -/-* and *Nr4a1 +/+* mice demonstrated that most of the genes were significantly higher expressed in splenic T cells of *Nr4a1 -/-* mice. Our data suggest that Nr4a1 is involved in gene regulation in a context specific manner and its regulatory function might be influenced by interaction with other transcription factors.

We treated *Nr4a1 -/-* with spermidine for 24 weeks and determined pro-inflammatory cytokines, spleen weight and the immune cell distribution in bone

marrow, spleen and thymus. Unexpectedly, pro-inflammatory cytokines TNF-α and IL-6, IL-1β and the chemokine KC/GRO (CXCL1) showed an increased concentration in spermidine treated mice compared to *Nr4a1 -/-* and *Nr4a1 +/+* suggesting that the anti-inflammatory effects decrease. Contrary to Li *et al.* [90], we did not observe any differences of IL-6 and TNF-α. These different observations might be caused by the fact that Li *et al*. determined the levels of both cytokines on mRNA levels in liver and spleen and they determined plasma concentration on protein levels [90]. Additionally, the IL-6 plasma levels of *Nr4a1 +/+* and *Nr4a1 -/-* mice determined by Li *et al* were 10 fold lower [90] compared to our data and to data of literature [96, 97], indicating a systemic error. IL-5 was the only cytokine, which was exclusively elevated in *Nr4a1 -/-* mice. IL-5 increases immunoglobulin secretion [98] and might explain the reason for the increased immunoglobulin levels in the *Nr4a1 -/-* mouse as described by *Li et. [90].* However, in spermidine treated mice the spleen weights were significantly lower compared to the untreated *Nr4a1 -/-* mice and showed a similar extend to the untreated *Nr4a1 +/+* counterpart indicating that development of splenomegaly is blocked by spermidine. Based on your proinflammatory cytokine profile it might be speculated that the splenomegaly in the *Nr4a1 -/-* mice is not caused by chronic inflammation.
Additionally, we investigated the effects of spermidine in B-cell development in bone marrow, spleen and thymus. Surprisingly, we observed no positive effects of spermidine in B-cell and T cell development, but we demonstrated that *Nr4a1 -/-* exhibited a vastly reduced percentage of B-cells in the spleen compared to *Nr4a1 +/+* mice. Interestingly, we observed that the percentage of all B-cell developmental stages after the pre B-cell stage was significantly reduced in spleen and bone marrow. Together with the fact that B-cell receptor (BCR) signaling is required throughout B-cell development [99] and that *Nr4a1* is rapidly transcriptionally upregulated in response to BCR signaling [100, 101], it might be speculated that *Nr4a1* is mandatory for B-cell development.

In conclusion, our data indicate that Nr4a1 possess a tumor suppressive function in *Myc*-driven lymphomagenesis and that the development of lymphomas is less dependent on inactivation of the p53 pathway. Additionally, we identified two miRNAs potentially targeting *NR4A1* being overexpressed in human aggressive lymphomas. Furthermore, we clearly demonstrated that Nr4a1 loss impacts genes involved in immune regulation, immune cell

migration and in NF-KB pathway in a context specific manner under non-malignant conditions. Finally, we observed that Nr4a1 is mandatory for B-cell development.

SUPPLEMENTARY

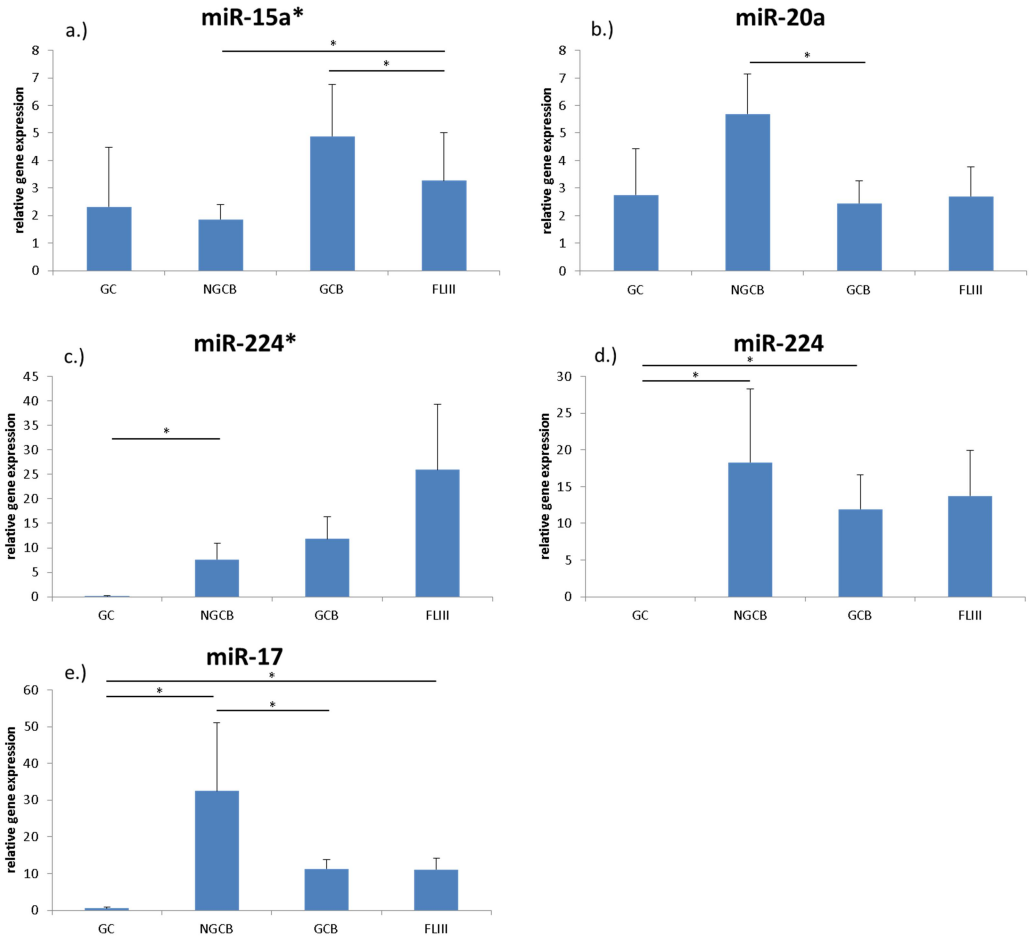

Figure 39: miRNAs in aggressive lymphomas
The bar charts show the mean values of mRNA expression levels and standard error of the mean. *:p<0,05

References

[1] A. K. Abbas, A. H. Lichtman, and S. Pillai, *Basic immunology: Functions and disorders of the immune system*. Philadelphia, Pa.: Elsevier Saunders, 2014.

[2] J. Hagman and K. Lukin, “Transcription factors drive B cell development,” (eng), *Current opinion in immunology*, vol. 18, no. 2, pp. 127–134, 2006.

[3] K. Pieper, B. Grimbacher, and H. Eibel, “B-cell biology and development,” (eng), *The Journal of allergy and clinical immunology*, vol. 131, no. 4, pp. 959–971, 2013.

[4] R. Kuppers, “Mechanisms of B-cell lymphoma pathogenesis,” (eng), *Nature reviews. Cancer*, vol. 5, no. 4, pp. 251–262, 2005.

[5] C. A. Janeway and P. Travers, *Immunobiology: The immune system in health and disease ; [CD-ROM inside ; animations, videos and figures from the book],* 6th ed. New York: Garland Science, 2005.

[6] P. Soulas-Sprauel *et al.,* “V(D)J and immunoglobulin class switch recombinations: A paradigm to study the regulation of DNA end-joining,” (eng), *Oncogene*, vol. 26, no. 56, pp. 7780–7791, 2007.

[7] B. A. Heesters, R. C. Myers, and M. C. Carroll, “Follicular dendritic cells: Dynamic antigen libraries,” (eng), *Nature reviews. Immunology*, vol. 14, no. 7, pp. 495–504, 2014.

[8] J. Stavnezer, J. E. J. Guikema, and C. E. Schrader, “Mechanism and regulation of class switch recombination,” (eng), *Annual review of immunology*, vol. 26, pp. 261–292, 2008.

[9] Y. Zhang, L. Garcia-Ibanez, and K.-M. Toellner, “Regulation of germinal center B-cell differentiation,” (eng), *Immunological reviews*, vol. 270, no. 1, pp. 8–19, 2016.

[10] K. Basso and R. Dalla-Favera, “Germinal centres and B cell lymphomagenesis,” (eng), *Nature reviews. Immunology*, vol. 15, no. 3, pp. 172–184, 2015.

[11] Z. Xu *et al.,* “DNA lesions and repair in immunoglobulin class switch recombination and somatic hypermutation,” (eng), *Annals of the New York Academy of Sciences*, vol. 1050, pp. 146–162, 2005.

[12] S. H. Swerdlow *et al.,* “The 2016 revision of the World Health Organization classification of lymphoid neoplasms,” (eng), *Blood*, vol. 127, no. 20, pp. 2375–2390, 2016.

[13] STATISTIK AUSTRIA, *Non-Hodgkin: https://www.statistik.at/web_de/statistiken/menschen_und_gesellschaft/gesundheit/krebserkrankungen/non-hodgkin/index.html*, updated 2017.

[14] L. Pasqualucci, “The genetic basis of diffuse large B-cell lymphoma,” (eng), *Current opinion in hematology*, vol. 20, no. 4, pp. 336–344, 2013.

[15] E. S. Jaffe and S. Pittaluga, “Aggressive B-cell lymphomas: A review of new and old entities in the WHO classification,” (eng), *Hematology. American Society of Hematology. Education Program*, vol. 2011, pp. 506–514, 2011.

[16] E. Campo *et al.,* “The 2008 WHO classification of lymphoid neoplasms and beyond: Evolving concepts and practical applications,” (eng), *Blood*, vol. 117, no. 19, pp. 5019–5032, 2011.

[17] M. Schuhmacher *et al.,* “The transcriptional program of a human B cell line in response to Myc,” (eng), *Nucleic acids research*, vol. 29, no. 2, pp. 397–406, 2001.

[18] L. Nguyen, P. Papenhausen, and H. Shao, “The Role of c-MYC in B-Cell Lymphomas: Diagnostic and Molecular Aspects,” (eng), *Genes*, vol. 8, no. 4, 2017.

[19] P. Korac, S. Dotlic, M. Matulic, M. Zajc Petranovic, and M. Dominis, “Role of MYC in B Cell Lymphomagenesis,” (eng), *Genes*, vol. 8, no. 4, 2017.

[20] A. W. Harris *et al.,* “The E mu-myc transgenic mouse. A model for high-incidence spontaneous lymphoma and leukemia of early B cells,” (eng), *The Journal of experimental medicine*, vol. 167, no. 2, pp. 353–371, 1988.

[21] C. Schuster *et al.,* “The cooperating mutation or "second hit" determines the immunologic visibility toward MYC-induced murine lymphomas,” (eng), *Blood*, vol. 118, no. 17, pp. 4635–4645, 2011.

[22] C. M. Eischen, J. D. Weber, M. F. Roussel, C. J. Sherr, and J. L. Cleveland, “Disruption of the ARF-Mdm2-p53 tumor suppressor pathway in Myc-induced lymphomagenesis,” (eng), *Genes & development*, vol. 13, no. 20, pp. 2658–2669, 1999.

[23] N. Meyer and L. Z. Penn, “Reflecting on 25 years with MYC,” (eng), *Nature reviews. Cancer*, vol. 8, no. 12, pp. 976–990, 2008.

[24] P. N. Kelly, S. Grabow, A. R. D. Delbridge, A. Strasser, and J. M. Adams, “Endogenous Bcl-xL is essential for Myc-driven lymphomagenesis in mice,” (eng), *Blood*, vol. 118, no. 24, pp. 6380–6386, 2011.

[25] A. Egle, A. W. Harris, P. Bouillet, and S. Cory, “Bim is a suppressor of Myc-induced mouse B cell leukemia,” (eng), *Proceedings of the National*

Academy of Sciences of the United States of America, vol. 101, no. 16, pp. 6164–6169, 2004.

[26] A. R. D. Delbridge, S. Grabow, P. Bouillet, J. M. Adams, and A. Strasser, “Functional antagonism between pro-apoptotic BIM and anti-apoptotic BCL-XL in MYC-induced lymphomagenesis,” (eng), *Oncogene*, vol. 34, no. 14, pp. 1872–1876, 2015.

[27] S. Nag, J. Qin, K. S. Srivenugopal, M. Wang, and R. Zhang, “The MDM2-p53 pathway revisited,” (eng), *Journal of biomedical research*, vol. 27, no. 4, pp. 254–271, 2013.

[28] E. F. Lee *et al.,* “The functional differences between pro-survival and pro-apoptotic B cell lymphoma 2 (Bcl-2) proteins depend on structural differences in their Bcl-2 homology 3 (BH3) domains,” (eng), *The Journal of biological chemistry*, vol. 289, no. 52, pp. 36001–36017, 2014.

[29] L. M. Dejean, S. Martinez-Caballero, S. Manon, and K. W. Kinnally, “Regulation of the mitochondrial apoptosis-induced channel, MAC, by BCL-2 family proteins,” (eng), *Biochimica et biophysica acta*, vol. 1762, no. 2, pp. 191–201, 2006.

[30] A. Ashkenazi, W. J. Fairbrother, J. D. Leverson, and A. J. Souers, “From basic apoptosis discoveries to advanced selective BCL-2 family inhibitors,” (eng), *Nature reviews. Drug discovery*, vol. 16, no. 4, pp. 273–284, 2017.

[31] A. C. Aisenberg, B. M. Wilkes, and J. O. Jacobson, “The bcl-2 gene is rearranged in many diffuse B-cell lymphomas,” (eng), *Blood*, vol. 71, no. 4, pp. 969–972, 1988.

[32] J. K. Brunelle and A. Letai, “Control of mitochondrial apoptosis by the Bcl-2 family,” (eng), *Journal of cell science*, vol. 122, no. Pt 4, pp. 437–441, 2009.

[33] D. A. Grillot, “bcl-x exhibits regulated expression during B cell development and activation and modulates lymphocyte survival in transgenic mice,” *The Journal of experimental medicine*, vol. 183, no. 2, pp. 381–391, 1996.

[34] P. J. Swanson *et al.,* “Fatal Acute Lymphoblastic Leukemia in Mice Transgenic for B Cell-Restricted bcl-xL and c-myc,” *The Journal of Immunology*, vol. 172, no. 11, pp. 6684–6691, 2004.

[35] P. Zhou *et al.,* “MCL1 transgenic mice exhibit a high incidence of B-cell lymphoma manifested as a spectrum of histologic subtypes,” (eng), *Blood*, vol. 97, no. 12, pp. 3902–3909, 2001.

[36] G. Z. Rassidakis *et al.,* “Overexpression of Mcl-1 in Anaplastic Large Cell Lymphoma Cell Lines and Tumors,” *The American Journal of Pathology*, vol. 160, no. 6, pp. 2309–2310, 2002.

[37] L. O'Connor *et al.,* “Bim: A novel member of the Bcl-2 family that promotes apoptosis,” (eng), *The EMBO journal*, vol. 17, no. 2, pp. 384–395, 1998.

[38] W. X. Zong, T. Lindsten, A. J. Ross, G. R. MacGregor, and C. B. Thompson, “BH3-only proteins that bind pro-survival Bcl-2 family members fail to induce apoptosis in the absence of Bax and Bak,” (eng), *Genes & development*, vol. 15, no. 12, pp. 1481–1486, 2001.

[39] S. L. Lee *et al.,* “Unimpaired thymic and peripheral T cell death in mice lacking the nuclear receptor NGFI-B (Nur77),” (eng), *Science (New York, N.Y.)*, vol. 269, no. 5223, pp. 532–535, 1995.

[40] S. H. Cho *et al.,* “PARP-14, a member of the B aggressive lymphoma family, transduces survival signals in primary B cells,” (eng), *Blood*, vol. 113, no. 11, pp. 2416–2425, 2009.

[41] P. Bai, “Biology of Poly(ADP-Ribose) Polymerases: The Factotums of Cell Maintenance,” (eng), *Molecular cell*, vol. 58, no. 6, pp. 947–958, 2015.

[42] B. Puig, A. Tortosa, and I. Ferrer, “Cleaved caspase-3, caspase-7 and poly (ADP-ribose) polymerase are complementarily but differentially expressed in human medulloblastomas,” (eng), *Neuroscience letters*, vol. 306, no. 1-2, pp. 85–88, 2001.

[43] H. E. Ambrose *et al.,* “Poly(ADP-ribose) polymerase-1 (Parp-1)-deficient mice demonstrate abnormal antibody responses,” (eng), *Immunology*, vol. 127, no. 2, pp. 178–186, 2009.

[44] S. Nam and J.-S. Lim, “Essential role of interferon regulatory factor 4 (IRF4) in immune cell development,” (eng), *Archives of pharmacal research*, vol. 39, no. 11, pp. 1548–1555, 2016.

[45] V. Shukla and R. Lu, “IRF4 and IRF8: Governing the virtues of B Lymphocytes,” (eng), *Frontiers in biology*, vol. 9, no. 4, pp. 269–282, 2014.

[46] S. Pathak *et al.,* “IRF4 is a suppressor of c-Myc induced B cell leukemia,” (eng), *PloS one*, vol. 6, no. 7, e22628, 2011.

[47] R. A. Casero and L. J. Marton, “Targeting polyamine metabolism and function in cancer and other hyperproliferative diseases,” (eng), *Nature reviews. Drug discovery*, vol. 6, no. 5, pp. 373–390, 2007.

[48] E. W. Gerner and F. L. Meyskens, “Polyamines and cancer: Old molecules, new understanding,” (eng), *Nature reviews. Cancer*, vol. 4, no. 10, pp. 781–792, 2004.

[49] N. Minois, “Molecular basis of the 'anti-aging' effect of spermidine and other natural polyamines - a mini-review,” (eng), *Gerontology*, vol. 60, no. 4, pp. 319–326, 2014.

[50] K. Soda, Y. Dobashi, Y. Kano, S. Tsujinaka, and F. Konishi, “Polyamine-rich food decreases age-associated pathology and mortality in aged mice,” (eng), *Experimental gerontology*, vol. 44, no. 11, pp. 727–732, 2009.

[51] K. Soda *et al.,* “Long-term oral polyamine intake increases blood polyamine concentrations,” (eng), *Journal of nutritional science and vitaminology*, vol. 55, no. 4, pp. 361–366, 2009.

[52] T. Eisenberg *et al.,* “Cardioprotection and lifespan extension by the natural polyamine spermidine,” (eng), *Nature medicine*, vol. 22, no. 12, pp. 1428–1438, 2016.

[53] T. Eisenberg *et al.,* “Induction of autophagy by spermidine promotes longevity,” (eng), *Nature cell biology*, vol. 11, no. 11, pp. 1305–1314, 2009.

[54] J. A. Nilsson *et al.,* “Targeting ornithine decarboxylase in Myc-induced lymphomagenesis prevents tumor formation,” (eng), *Cancer cell*, vol. 7, no. 5, pp. 433–444, 2005.

[55] F. Madeo, F. Pietrocola, T. Eisenberg, and G. Kroemer, “Caloric restriction mimetics: Towards a molecular definition,” (eng), *Nature reviews. Drug discovery*, vol. 13, no. 10, pp. 727–740, 2014.

[56] G. Mariño, F. Pietrocola, F. Madeo, and G. Kroemer, “Caloric restriction mimetics: Natural/physiological pharmacological autophagy inducers,” (eng), *Autophagy*, vol. 10, no. 11, pp. 1879–1882, 2014.

[57] L. Mouchiroud, L. Molin, N. Dallière, and F. Solari, “Life span extension by resveratrol, rapamycin, and metformin: The promise of dietary restriction mimetics for an healthy aging,” (eng), *BioFactors (Oxford, England)*, vol. 36, no. 5, pp. 377–382, 2010.

[58] S. Di Biase *et al.,* “Fasting-Mimicking Diet Reduces HO-1 to Promote T Cell-Mediated Tumor Cytotoxicity,” (eng), *Cancer cell*, vol. 30, no. 1, pp. 136–146, 2016.

[59] F. Pietrocola *et al.,* “Caloric Restriction Mimetics Enhance Anticancer Immunosurveillance,” (eng), *Cancer cell*, vol. 30, no. 1, pp. 147–160, 2016.

[60] R. Yi, Y. Qin, I. G. Macara, and B. R. Cullen, “Exportin-5 mediates the nuclear export of pre-microRNAs and short hairpin RNAs,” (eng), *Genes & development*, vol. 17, no. 24, pp. 3011–3016, 2003.

[61] A. Tenga, J. A. Beard, A. Takwi, Y.-M. Wang, and T. Chen, “Regulation of Nuclear Receptor Nur77 by miR-124,” (eng), *PloS one*, vol. 11, no. 2, e0148433, 2016.

[62] A. M. Denli, B. B. J. Tops, R. H. A. Plasterk, R. F. Ketting, and G. J. Hannon, “Processing of primary microRNAs by the Microprocessor complex,” (eng), *Nature*, vol. 432, no. 7014, pp. 231–235, 2004.

[63] R. S. Pillai, S. N. Bhattacharyya, and W. Filipowicz, “Repression of protein synthesis by miRNAs: How many mechanisms?,” (eng), *Trends in cell biology*, vol. 17, no. 3, pp. 118–126, 2007.

[64] Y. Cai, X. Yu, S. Hu, and J. Yu, “A Brief Review on the Mechanisms of miRNA Regulation,” *Genomics, Proteomics & Bioinformatics*, vol. 7, no. 4, pp. 147–154, 2009.

[65] A. Esquela-Kerscher and F. J. Slack, “Oncomirs - microRNAs with a role in cancer,” (eng), *Nature reviews. Cancer*, vol. 6, no. 4, pp. 259–269, 2006.

[66] G. A. Calin *et al.,* “Human microRNA genes are frequently located at fragile sites and genomic regions involved in cancers,” (eng), *Proceedings of the National Academy of Sciences of the United States of America*, vol. 101, no. 9, pp. 2999–3004, 2004.

[67] G. A. Calin and C. M. Croce, “MicroRNA signatures in human cancers,” (eng), *Nature reviews. Cancer*, vol. 6, no. 11, pp. 857–866, 2006.

[68] I. Sambri *et al.,* “miR-17 and -20a Target the Neuron-Derived Orphan Receptor-1 (NOR-1) in Vascular Endothelial Cells,” (eng), *PloS one*, vol. 10, no. 11, e0141932, 2015.

[69] A. G. Smith and G. E. O. Muscat, “Skeletal muscle and nuclear hormone receptors: Implications for cardiovascular and metabolic disease,” (eng), *The international journal of biochemistry & cell biology*, vol. 37, no. 10, pp. 2047–2063, 2005.

[70] K. Wenzl, K. Troppan, P. Neumeister, and A. J. A. Deutsch, “The nuclear orphan receptor NR4A1 and NR4A3 as tumor suppressors in hematologic neoplasms,” (eng), *Current drug targets*, vol. 16, no. 1, pp. 38–46, 2015.

[71] A. J. A. Deutsch, H. Angerer, T. E. Fuchs, and P. Neumeister, “The nuclear orphan receptors NR4A as therapeutic target in cancer therapy,” (eng), *Anti-cancer agents in medicinal chemistry*, vol. 12, no. 9, pp. 1001–1014, 2012.

[72] S. Safe *et al.,* “Nuclear receptor 4A (NR4A) family - orphans no more,” (eng), *The Journal of steroid biochemistry and molecular biology*, vol. 157, pp. 48–60, 2016.

[73] S. P. Boudreaux, A. M. Ramirez-Herrick, R. P. Duren, and O. M. Conneely, “Genome-wide profiling reveals transcriptional repression of MYC as a core component of NR4A tumor suppression in acute myeloid leukemia,” (eng), *Oncogenesis*, vol. 1, e19, 2012.

[74] S. E. Mullican *et al.,* “Abrogation of nuclear receptors Nr4a3 and Nr4a1 leads to development of acute myeloid leukemia,” (eng), *Nature medicine*, vol. 13, no. 6, pp. 730–735, 2007.

[75] A. J. A. Deutsch *et al.,* “NR4A1-mediated apoptosis suppresses lymphomagenesis and is associated with a favorable cancer-specific survival in patients with aggressive B-cell lymphomas,” (eng), *Blood*, vol. 123, no. 15, pp. 2367–2377, 2014.

[76] A. J. A. Deutsch *et al.,* “NR4A3 Suppresses Lymphomagenesis through Induction of Proapoptotic Genes,” (eng), *Cancer research*, vol. 77, no. 9, pp. 2375–2386, 2017.

[77] G. Lenz *et al.,* “Stromal gene signatures in large-B-cell lymphomas,” (eng), *The New England journal of medicine*, vol. 359, no. 22, pp. 2313–2323, 2008.

[78] A. A. J. Hamers *et al.,* “Nur77-deficiency in bone marrow-derived macrophages modulates inflammatory responses, extracellular matrix homeostasis, phagocytosis and tolerance,” (eng), *BMC genomics*, vol. 17, p. 162, 2016.

[79] J. P. McMorrow and E. P. Murphy, “Inflammation: A role for NR4A orphan nuclear receptors?,” (eng), *Biochemical Society transactions*, vol. 39, no. 2, pp. 688–693, 2011.

[80] S. L. Lee, L. C. Tourtellotte, R. L. Wesselschmidt, and J. Milbrandt, “Growth and differentiation proceeds normally in cells deficient in the immediate early gene NGFI-A,” (eng), *The Journal of biological chemistry*, vol. 270, no. 17, pp. 9971–9977, 1995.

[81] C. L. Sidman, T. M. Denial, J. D. Marshall, and J. B. Roths, “Multiple mechanisms of tumorigenesis in E mu-myc transgenic mice,” (eng), *Cancer research*, vol. 53, no. 7, pp. 1665–1669, 1993.

[82] A. Frenzel *et al.,* “Suppression of B-cell lymphomagenesis by the BH3-only proteins Bmf and Bad,” (eng), *Blood*, vol. 115, no. 5, pp. 995–1005, 2010.

[83] V. Chiarugi and M. Ruggiero, “Role of three cancer "master genes" p53, bcl2 and c-myc on the apoptotic process,” (eng), *Tumori*, vol. 82, no. 3, pp. 205–209, 1996.

[84] Y. A. Lazebnik, S. H. Kaufmann, S. Desnoyers, G. G. Poirier, and W. C. Earnshaw, “Cleavage of poly(ADP-ribose) polymerase by a proteinase with properties like ICE,” (eng), *Nature*, vol. 371, no. 6495, pp. 346–347, 1994.

[85] G. M. Cohen, “Caspases: The executioners of apoptosis,” (eng), *The Biochemical journal*, vol. 326 (Pt 1), pp. 1–16, 1997.

[86] D. Nagel, M. Vincendeau, A. C. Eitelhuber, and D. Krappmann, “Mechanisms and consequences of constitutive NF-κB activation in B-cell lymphoid malignancies,” (eng), *Oncogene*, vol. 33, no. 50, pp. 5655–5665, 2014.

[87] R. L. Boddicker *et al.,* “The oncogenic transcription factor IRF4 is regulated by a novel CD30/NF-κB positive feedback loop in peripheral T-cell lymphoma,” (eng), *Blood*, vol. 125, no. 20, pp. 3118–3127, 2015.

[88] B. You, Y.-Y. Jiang, S. Chen, G. Yan, and J. Sun, “The orphan nuclear receptor Nur77 suppresses endothelial cell activation through induction of IkappaBalpha expression,” (eng), *Circulation research*, vol. 104, no. 6, pp. 742–749, 2009.

[89] H. Harant and I. J. D. Lindley, “Negative cross-talk between the human orphan nuclear receptor Nur77/NAK-1/TR3 and nuclear factor-kappaB,” (eng), *Nucleic acids research*, vol. 32, no. 17, pp. 5280–5290, 2004.

[90] X.-M. Li *et al.,* “Nur77 deficiency leads to systemic inflammation in elderly mice,” (eng), *Journal of inflammation (London, England)*, vol. 12, p. 40, 2015.

[91] R. N. Hanna *et al.,* “The transcription factor NR4A1 (Nur77) controls bone marrow differentiation and the survival of Ly6C- monocytes,” (eng), *Nature immunology*, vol. 12, no. 8, pp. 778–785, 2011.

[92] M. S. Fassett, W. Jiang, A. M. D'Alise, D. Mathis, and C. Benoist, “Nuclear receptor Nr4a1 modulates both regulatory T-cell (Treg)

differentiation and clonal deletion," (eng), *Proceedings of the National Academy of Sciences of the United States of America*, vol. 109, no. 10, pp. 3891–3896, 2012.

[93] L. E. Cheng, F. K. Chan, D. Cado, and A. Winoto, "Functional redundancy of the Nur77 and Nor-1 orphan steroid receptors in T-cell apoptosis," (eng), *The EMBO journal*, vol. 16, no. 8, pp. 1865–1875, 1997.

[94] C. Soldani and A. I. Scovassi, "Poly(ADP-ribose) polymerase-1 cleavage during apoptosis: An update," (eng), *Apoptosis : an international journal on programmed cell death*, vol. 7, no. 4, pp. 321–328, 2002.

[95] E. P. Murphy and D. Crean, "Molecular Interactions between NR4A Orphan Nuclear Receptors and NF-κB Are Required for Appropriate Inflammatory Responses and Immune Cell Homeostasis," (eng), *Biomolecules*, vol. 5, no. 3, pp. 1302–1318, 2015.

[96] Y. Luo, Y. Su, Y. Shen, L. Zhao, and K. Li, "The levels of plasma IL-1beta, IL-6 of C57BL/6J mice treated with MPTP and brain lateralization," (eng), *Cellular & molecular immunology*, vol. 1, no. 3, pp. 219–223, 2004.

[97] B. C. R. Avraham *et al.,* "Increased plasma and optic nerve levels of IL-6, TNF-alpha, and MIP-2 following induction of ischemic optic neuropathy in mice," (eng), *Current eye research*, vol. 33, no. 4, pp. 395–401, 2008.

[98] J. S. Lee, H. D. Campbell, C. A. Kozak, and I. G. Young, "The IL-4 and IL-5 genes are closely linked and are part of a cytokine gene cluster on mouse chromosome 11," (eng), *Somatic cell and molecular genetics*, vol. 15, no. 2, pp. 143–152, 1989.

[99] L. D. Wang and M. R. Clark, "B-cell antigen-receptor signalling in lymphocyte development," (eng), *Immunology*, vol. 110, no. 4, pp. 411–420, 2003.

[100] P. R. Mittelstadt and A. L. DeFranco, "Induction of early response genes by cross-linking membrane Ig on B lymphocytes," (eng), *The Journal of Immunology*, vol. 150, no. 11, pp. 4822–4832, 1993.

[101] J. Zikherman, R. Parameswaran, and A. Weiss, "Endogenous antigen tunes the responsiveness of naive B cells but not T cells," (eng), *Nature*, vol. 489, no. 7414, pp. 160–164, 2012.